The Dissertation Committee for Xinyu Wang Certifies that this is the approved version of the following dissertation:

AMELIORATION OF OXIDATIVE STRESS IN HUMAN ENDOTHELIAL CELLS BY CAFFEIC ACID PHENETHYL ESTER (CAPE) AND FLUORINATED DERIVATIVES (FCAPES) AND PHARMACOKINETIC CHARACTERIZATION OF CAPE AND FCAPE IN RATS

Committee:

Salomon Stavchansky, Supervisor

Phillip D. Bowman

Sean M. Kerwin

Christian Whitman

Robert Williams

AMELIORATION OF OXIDATIVE STRESS IN HUMAN ENDOTHELIAL CELLS BY CAFFEIC ACID PHENETHYL ESTER (CAPE) AND FLUORINATED DERIVATIVES (FCAPES) AND PHARMACOKINETIC CHARACTERIZATION OF CAPE AND FCAPE IN RATS

by

Xinyu Wang, B.S.

Dissertation

Presented to the Faculty of the Graduate School of

The University of Texas at Austin

in Partial Fulfillment

of the Requirements

for the Degree of

Doctor of Philosophy

The University of Texas at Austin

December 2007

Dedication

I would like to dedicate this dissertation to my mom for supporting me wholeheartedly through these years. Thank you with all my love,

Xinyu

Acknowledgements

I would like to thank my supervisor, Dr. Salomon Stavchansky, for his great support, encouragement and guidance through my graduate studies. I am very grateful to Dr. Phillip Bowman for the opportunity to work together and for his generous resources, advice and encouragement. I am grateful to Dr. Sean Kerwin for his great advice, expertise and resources. I would also like to thank the other members of my dissertation committee, Dr. Christian Whitman and Dr. Robert Williams for their precious advice and review of this dissertation. In addition, my sincere appreciation goes to many people who helped me at various situations during the past several years, especially Ms. Mickie Sheppard for her endless patience and assistance to me.

AMELIORATION OF OXIDATIVE STRESS IN HUMAN ENDOTHELIAL CELLS BY CAFFEIC ACID PHENETHYL ESTER (CAPE) AND FLUORINATED DERIVATIVES (FCAPES) AND PHARMACOKINETIC CHARACTERIZATION OF CAPE AND FCAPE IN RATS

Publication No._____

Xinyu Wang, Ph.D.

The University of Texas at Austin, 2007

Supervisor: Salomon Stavchansky

Tissue ischemia is a major cause of morbidity contributing to disease processes such as cardiovascular diseases, stroke, cancer, and traumatic injury and may lead to death. Failure to quickly reestablish flow to ischemic tissue results in tissue death. However, even timely return to normal flow has a downside in that the reintroduction of oxygen to ischemic tissue results in ischemia/reperfusion (I/R) injury that produces an oxidant stress. This pathological process requires new therapeutic strategies and agents to reduce the personal, social and economic loss. One of the most generally accepted mechanisms for the pathology of I/R injury is the production of the reactive oxygen species (ROS), suggesting antioxidants may ameliorate I/R injury.

Caffeic acid phenethyl ester (CAPE), a plant derived polyphenolic compound, has been shown to protect organs from I/R induced damage *in vivo*, and this effect has been attributed to its antioxidant activity. To better understand the mechanism of CAPE protection, a model using menadione-induced oxidative stress in human endothelial cells to simulate I/R injury *in vitro* was developed. Gene expression analysis was performed with microarrays undergoing cytoprotection with CAPE. The dose-dependent cytoprotection of CAPE has been related to its induction of heme oxygenase-1 (HO-1).

With the aim of improving the beneficial effect of CAPE and understanding structure activity relationship, six new catechol ring-fluorinated CAPE derivatives were synthesized and evaluated in the menadione-endothelial cell model. The data suggest good cytoprotective effects of CAPE and some analogues and indicate important structural features for cytoprotection. Further investigation of the mechanism of cytoprotection showed that cytoprotection profiles of CAPE and derivatives correlate better to their ability to induce HO-1 in human endothelial cells than free radical scavenging activity.

One CAPE derivative (FCAPE) with cytoprotective effects similar to CAPE *in vitro* exhibited better stability in rat plasma. A validated ultra-performance liquid chromatography/tandem mass spectrometric method was developed that allowed for quantification of CAPE and FCAPE in plasma samples. Pharmacokinetic studies in male Sprague Dawley rats following intravenous bolus administration of 5, 10, and 20 mg/kg CAPE and 20 mg/kg FCAPE were performed. The results indicate that dose proportionality for CAPE does not exist in the dose range studied. Although the elimination half life was found not to be significant different between CAPE and FCAPE, significant difference was observed between the total body clearance of FCAPE and CAPE which may due to the difference in volume of distribution.

Table of Contents

List of Tables

List of Figures

Statement of Objectives and Significance of Research

This dissertation is the result of an effort directed towards drug development for ameliorating ischemia/reperfusion (I/R) injury using CAPE and its fluorinated derivatives as model drugs to establish structure cytoprotection relationships, understand the mechanism of cytoprotection, and characterize the pharmacokinetic profiles of CAPE and the most cytoprotective derivative (FCAPE) in male Sprague Dawley rats.

The following specific aims were proposed in order to:

1. Establish an *in vitro* cytoprotection assay of CAPE against oxidative stress in human umbilical vein endothelial cells that simulates I/R injury;

2. Synthesize six new CAPE derivatives fluorinated in the catechol ring;

3. Determine structure activity relationships between CAPE and its fluorinated derivatives and cytoprotection;

4. Investigate the cytoprotection mechanism of CAPE and its fluorinated derivatives: evaluate the role of heme oxygenase-1 induction and antioxidant activity;

5. Quantitatively determine CAPE and FCAPE in rat plasma using liquid chromatography with electrospray ionization tandem mass spectrometry;

6. Characterize the pharmacokinetic profiles of CAPE and FCAPE following intravenous bolus administration to male Sprague Dawley rats.

Ischemia is a restriction in blood supply, generally due to factors in blood vessels, with resultant damage or dysfunction to tissue. Restoration of blood flow after a period of ischemia can actually be more damaging than the ischemia. Reintroduction of oxygen causes a greater production of damaging free radicals, resulting in reperfusion injury. With reperfusion injury, cellular damage can be greatly accelerated. Ischemia and subsequent reperfusion injury occurs in many situation. Traumatic injury, heart disease and ultimately aging, are failures of the endothelial cell of the circulatory system to present a nonthrombogenic surface to circulating blood, leading to clot formation that may block downstream vessels leading to ischemia/ reperfusion injury. Alteplase, recombinant tissue plasminogen activator, approved by the Food and Drug Administration 1987 was a major achievement in eliminating the clot before too severe ischemia leads to tissue death. Alteplase is indicated for the treatment of acute myocardial infarction, pulmonary embolism, and acute ischemic stroke, but few other treatments are available.

There is a large body of information indicating oxidant stress accompanies ischemia reperfusion injury and that application of antioxidants before or shortly after removal of the blockage reduces the degree of injury and aids in a more rapid recovery. A significant number of studies indicate that administration of CAPE, a plant-derived antioxidant, benefits outcome of I/R injury *in vivo* as well as cytoprotective effects *in vitro*. CAPE and its fluorinated derivatives are the subjects of the current series of studies.

The hypothesis was tested that induction of heme oxygenase-1(HO-1) played a major role in the protection by CAPE and its fluorinated derivatives against oxidative injury and that selective structural modifications of CAPE could improve its pharmacological activity *in vitro* and *in vivo*. The hypothesis was based on the following observations. First, the induction of heme oxygenase-1 and its heme-catalyzing products ameliorates I/R injury in different organs *in vivo*. Second, the suppression of heme oxygenase-1 enhanced apoptosis in lung I/R injury both in vitro and *in vivo* in an organ-specific manner. Third, CAPE was shown to be a novel class of HO-1 inducers *in vitro*. A comprehensive understanding of CAPE and its structure activity relationships following derivatization with fluorine to cytoprotection, the mechanism of cytoprotection, and the *in vivo* fate after intravenous administration may facilitate developing new candidate drugs for the treatment of I/R injury.

Chapter I: Introduction and Literature Review

1.1 ISCHEMIA, REPERFUSION, AND ISCHEMIA/REPERFUSION (I/R) INJURY

1.1.1 The Definition and Significance of Ischemia, Reperfusion, and I/R Injury

Ischemia (Greek ισχαιμία, isch- restriction, hema or haema- blood) refers to the prolonged interruption of blood supply to a tissue or organ leading to a deprivation of oxygen and nutrients to the constituent cells, which may result in cell damage, and subsequent cell, tissue, or organ death. Reperfusion is required to restore oxygen and nutrients for normal metabolic function. However, the reintroduction of oxygen to ischemic tissue generates reactive oxygen species (ROS) that worsen vascular and cellular injury.

Ischemia reperfusion (I/R) injury is a potentially serious pathologic state involved in a number of cardiovascular diseases such as myocardial infarction and stroke, and also occurs following septic or circulatory shock, surgery, organ transplantations, and traumatic injury which cause great economic loss and may lead to death. The National Heart, Lung, and Blood Institute (NHLBI) has requested proposals to investigate new therapeutic strategies and agents to ameliorate I/R induced injury in cardiovascular diseases, hemostatic and thrombotic diseases [1]. Understanding I/R injury and corresponding mechanism will help achieve this goal.

1.1.2 The Mechanism of I/R Injury

A generally accepted mechanism for the pathology of I/R injury is the production of ROS such as superoxide anion ($O_2^{\bullet-}$), hydrogen peroxide (H_2O_2) and hydroxyl radical (OH•). Under normal conditions, oxygen reduction to water may go through two pathways. In the mitochondria, 95% of oxygen is tetravalently reduced to H_2O by the corresponding cytochrome oxidase without the production of any free radical intermediates. The remaining 5% of oxygen, however, is transformed by a univalent mechanism with the formation of free radicals such as superoxide anion and hydrogen peroxide. The superoxide anion is generated when one oxygen molecule accepts one electron. The protonated form is favored in acidic environments such as acidosis that occurs in ischemia and quite toxic capable of oxidative injury to fatty acids of cell membranes. Superoxide is detoxified by dismutation to form H_2O_2 mainly through superoxide dismutase (SOD). SOD is the most abundant anti-oxidant enzyme in animals, consisting of Cu/Zn-SOD in cytoplasm and Mn-SOD in mitochondria. Although hydrogen peroxide is toxic at high concentrations, the normal cell defense system converts it into water via catalase (CAT) or the glutathione system. Glutathione is a tripeptide containing cysteine, glycine, and glutamic acid, and it is the major intracellular antioxidant. Glutathione exists in reduced form (GSH) and oxidized form (GSSG). The enzyme glutathione peroxidase can neutralize hydrogen peroxide by converting two GSH into one GSSG molecules, and glutathione reductase could regenerate GSH from GSSG with NADPH as a source of hydrogen [2, 3].

During ischemia, hypoxanthine and xanthine are produced and accumulate by catabolizing large amount of ATP, and their normal metabolizing enzyme xanthine dehydrogenase is converted to xanthine oxidase activated by increased level of

intracellular Ca^{2+} and through a protease. Following reperfusion, this xanthine oxidase can use oxygen, instead of NAD^+ for xanthine dehydrogenase as the final electron acceptor to generate superoxide as a byproduct in the metabolism of hypoxanthine and xanthine to uric acid. This reaction doesn't occur until reperfusion supplies the necessary oxygen [4-6]. The well-orchestrated redox homeostasis of normal cells is upset and the most reactive and toxic radical among these three oxygen species, hydroxyl radicals, can be produced from the other two radicals through Fenton reaction and Haber-Weiss reaction with the participation of ischemia-induced iron [7-10]. Under normal physiological conditions, almost all iron ions are sequestered by various proteins such as transferrin in plasma, ferritin within cells, hemoglobin in red blood cells, and myoglobin in muscle. The amount of "free iron" is, therefore, very limited. "Free iron" refers to at least one out of six iron coordination sites open or associated with some low molecular weight compounds such as citrate and ATP. In the pathological situation like I/R, however, the overproduction of $O_2^{\bullet-}$ and H_2O_2 increases the release of "free ion" and activates the cell uptake of iron, facilitating the production of OH• [11]. These ROS, especially hydroxyl radicals attack bases in nucleic acids, amino acid side chains in proteins and double-bonds in unsaturated fatty acids, therefore, damaging DNA, protein, lipid, membrane, and eventually the whole cell [11]. The half-life of the highly reactive hydroxyl radicals is only one nanosecond, which indicates that it reacts with any molecule it first bumps into. It can cause covalent cross-linking or free-radical propagation in many biological macromolecules. The proposed mechanism of xanthine oxidase mediated free radical injury is illustrated in Figure 1.1.

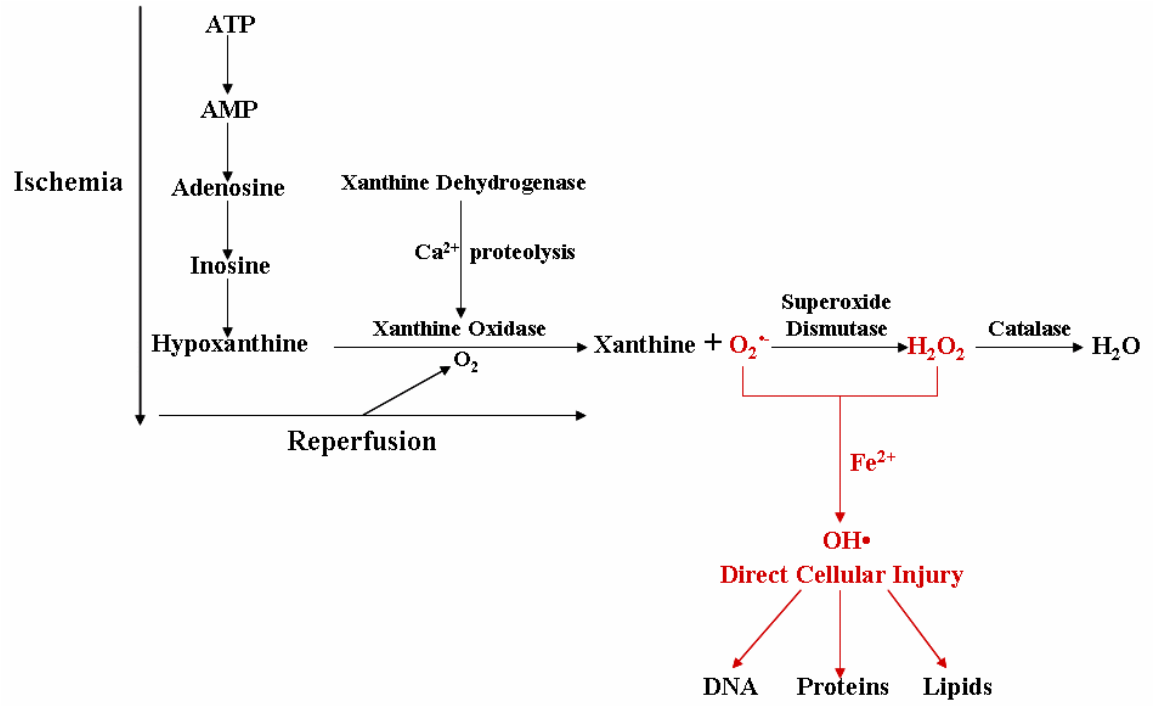

Figure 1.1: Proposed mechanism of xanthine oxidase mediated free radical injury, modified from Granger *et al.* [4]. Under the hypoxic conditions of ischemia, xanthine dehydrogenase is converted to xanthine oxidase. It utilizes oxygen reintroduced from following reperfusion producing superoxide, hydrogen peroxide, and eventually the most reactive and toxic ROS hydroxyl radicals.

1.1.3 Potential Therapeutic Antioxidants

Because ROS-induced oxidative stress plays an important role in I/R injury, compounds with antioxidant activity could be beneficial and protective. Figure 1.2 shows the process of how I/R causes tissue damage and where antioxidants could exert therapeutic effects. Tempol, a membrane-permeable radical scavenger, attenuates hepatic I/R injury in rat by reacting with free radicals to abolish their reactivity [12]. Melatonin, an antioxidant and an efficient neutralizer of hydroxyl radical, has been shown to be protective against renal I/R injury in rats [13]. N-acetylcysteine, a low molecular weight thiol antioxidant, can react with hydrogen peroxide, thereby decreasing the production of highly reactive hydroxyl radical, and increasing the cytoplasmic supply of reduced glutathione, which accounts for its beneficial effect in rat hepatic I/R injury during hemorrhagic shock [14].

Recently, plant-derived polyphenolic compounds have been shown to improve I/R-induced injury, that has been attributed to their antioxidant activity. Epigallocatechin gallate, a green tea polyphenol, reduces superoxide concentration significantly after ischemia and reperfusion in vivo, suggesting its therapeutical potential [15]. Procyanidins, a mixture of polyphenolic antioxidants, reduced the sequela of myocardial I/R damage in rats by elevating plasma antioxidant activity [16]. Other polyphenolic compounds such as curcumin, the intense yellow pigment found in turmeric, and resveratrol, a component of red wine and grapes, also exhibited cytoprotective effects against I/R-induced myocardia impairment and blood-brain barrier disruption, possibly through their free radicals scavenging abilities [17, 18].

In addition to direct interaction with free radicals, other experimental data have demonstrated that polyphenol antioxidants may benefit I/R injury indirectly by inducing

antioxidant enzymes and modulating signaling pathways. The induction of nitric oxide (NO), a signaling molecule and key biological messenger, seems to play a key role in the protection mechanism of resveratrol preconditioning [19, 20]. Epigallocatechin gallate also showed stimulation of NO through the Phosphoinositide 3-kinase (PI 3-kinase) pathway, which may explain its cardiovascular protection. The ability of epigallocatechin gallate to inhibit the NF-κB and AP-1 transcriptional pathways, may also partially explain this beneficial effect [21, 22]. Finally, it has been suggested that curcumin may be cytoprotective in I/R injury via induction of heat shock protein 70 or regulation of antioxidant enzymes like SOD and CAT [23].

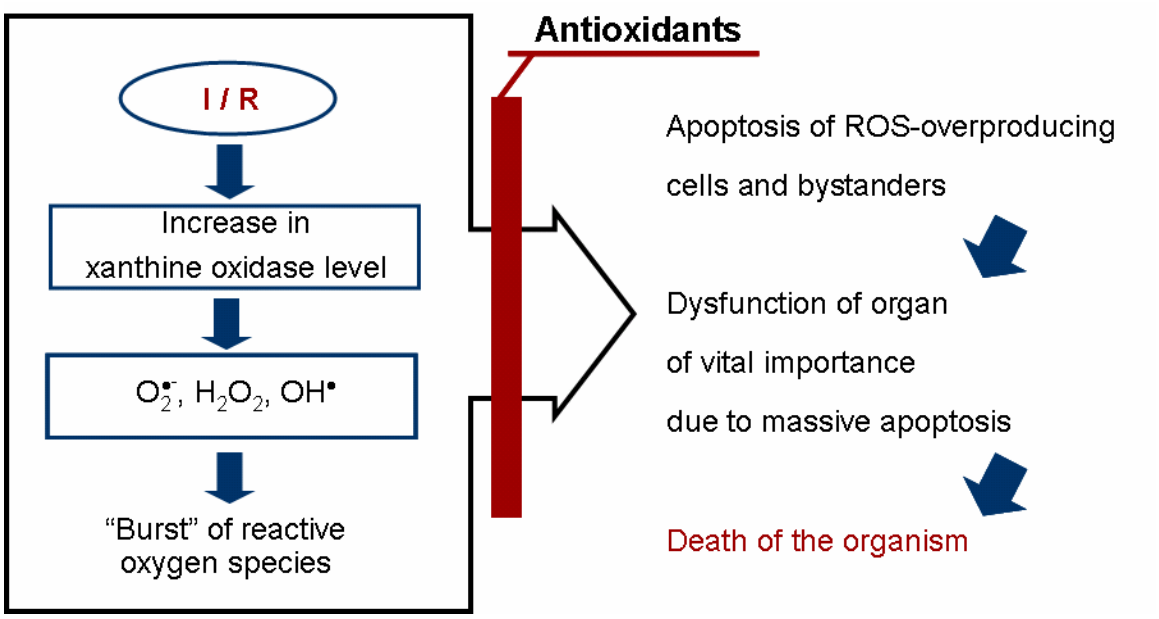

Figure 1.2: The general procedure of ROS-involved I/R injury and where antioxidants exert therapeutic effects.

1.1.4 The Beneficial Effect of Caffeic Acid Phenethyl Ester (CAPE) in I/R Injury

Numerous reports in the literature indicate that caffeic acid phenethyl ester (CAPE), a plant-derived polyphenolic compound (Figure 1.3), ameliorates I/R induced injury in various organs and tissues *in vivo*. CAPE was first reported protecting rat intestine [24] and rabbit spinal cord [25] in 1999. CAPE alleviated torsion/detorsion I/R induced injury in rat testis [26] and ovary [27]. The beneficial effect of CAPE against I/R damage has also been observed in rat skeletal muscle [28] and brain due to focal cerebral ischemia [29, 30]. The cardioprotective effect of CAPE has been documented to relieve myocardial I/R induced injuries *in vivo* by reducing apoptosis and arrhythmias [31-35]. In addition, CAPE improved myocardial I/R induced oxidative stress in rat testis and kidney [36, 37]. Compared to another antioxidant α-tocopherol (Vitamin E), CAPE showed greater activity of ameliorating I/R injury in rat brain and kidney [38, 39]. The suggested mechanism for CAPE protection in I/R injury has focused on its antioxidant activity and related anti-inflammatory and anti-apoptosis effects. The major experimental evidence cited were reduced histopathological changes and improved biochemical profile including reduced end products of lipid peroxidation malondiadehyde, increased production of antioxidant enzymes (superoxide dismutase, catalase, and glutathione reduced form GSH), and decreased level of nitric oxide and xanthine oxidase. However, the mechanisms of these beneficial effects have not been defined and further investigations into the mechanism of CAPE protection are warranted.

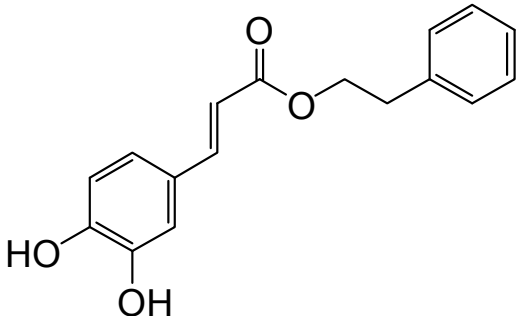

Figure 1.3: The structure of caffeic acid phenethyl ester (CAPE). CAPE is a natural polyphenolic compound, the two adjacent hydroxyl groups on the catechol ring of which contribute to its free radical scavenging ability.

1.2 CAFFEIC ACID PHENETHYL ESTER (CAPE)

1.2.1 Background

CAPE is present in relatively high amounts in honeybee propolis. Propolis is a natural resinous material collected by bees from various plant sources, and is used by bees to seal the hives, reinforce the borders of their combs, and it may protect against pathogenic microorganisms. Propolis has been used as a folk medicine since antiquity in many cultures to treat various diseases and has been demonstrated to exhibit antibacterial, antifungal, antiviral, antioxidant, anti-inflammatory, and other beneficial activities [40]. The chemical compositions and biological activities of propolis, however, vary directly from the local flora and phenology of the host plants and indirectly from the geographic regions and season of collection. CAPE has been reported to be high in propolis from European and non-tropic Asian countries such as the Netherlands, China, and Korea where there are numerous popular trees that bees have been observed to visit [41-44]. A recent study by Kumazawa et al has produced a comprehensive picture of the presence and relative quantity of CAPE in propolis from all over the world [45]. CAPE can be extracted from propolis with ethanol and their results showed that the amount of CAPE is more than 10 mg/g of propolis in extracts from Australia, China, Hungary, New Zealand, Uruguay, and Uzbekistan. Propolis from Argentina, Bulgaria, Chile, Ukraine, and the United States contained less than 10 mg/g CAPE, whereas CAPE was not detectable in ethanolic extracts of propolis from Brazil, South Africa, and Thailand. Propolis from China had the most CAPE content (up to 29 mg/g).

1.2.2 Properties

CAPE or phenethyl caffeate presents as an off-white powder with melting point 128 to 129°C. Its molecular formula is $C_{17}H_{16}O_4$ and molecular weight 284.31. CAPE is hydrophobic and dissolves in organic solvent such as DMSO, acetonitrile, methanol, acetone and ethanol. The partition coefficient LogP of CAPE determined using ChemDraw Ultra software is 3.43 compared to its much-more-hydrophilic analogue caffeic acid which is 1.15. It needs to be protected from light in order to prevent photo-oxidation due to its catechol ring during the process of storage and application. Synthetic CAPE was first made by Dr. Koji Nakanishi and Dr. Dezider Grunberger and they hold a patent on its synthesis and application as anti-inflammatory and anti-carcinogenic agents [46].

Numerous pharmacological activities have been reported for CAPE:

1) ***Anticancer/tumor:*** CAPE at a low dose of 1 μg/ml induced apoptosis in adenovirus-transformed rat fibroblasts, while the same dose of CAPE only inhibited the proliferation of untransformed fibroblasts [47]. Topical application of CAPE to mouse skin inhibited 12-o-tetradecanoylphorbol-13-acetate-induced tumor promotion. CAPE in the range of 0 to 12 μg/ml reduced the viability of mouse colon cancer cells up to 60% and ameliorated pulmonary metastasis induced in BALB/c male mice by the same tumor cell lines at the dose of 10 mg/kg/day, which may be through inhibition of matrix metalloproteinase activity and reduction of vascular endothelial growth factor level in vitro and in vivo [48]. CAPE also prevented the growth of rat C6 glioma cell line, human breast cancer MCF-7 cells, and human hepatoma HepG2 cell line and HepG2 tumor xenografts in nude mice [49-51].

2) ***Anti-inflammatory:*** CAPE decreased the cell viability of leukocytes involved in the process of inflammation by inducing apoptosis both in vitro and in a rat model of carrageenin-induced subcutaneous inflammation [52]. CAPE was shown to be cytotoxic to inflammatory-related rat macrophage and colonic epithelial cells and to ameliorate bacterial peptidoglycan polysaccharide (PG-PS)-triggered colitis in rats [53]. CAPE attenuated inflammatory stress induced by paw edema, carrageenin pleurisy, and adjuvant arthritis in rats [54], and it suppressed the interferon-γ plus lipopolysaccharide-stimulated cerebral inflammatory response in rat organotypic hippocampal cultures [55].

3) ***Antiviral:*** In 1993, CAPE was identified as a potent inhibitor of human immunodeficiency virus (HIV) integrase [56]. It selectively suppressed the integration or strand-transfer step rather than the initial neucleolytic cleavage reaction of the enzyme reaction. Furthermore, the same research group indicated CAPE not only selectively inhibited the integration step but also suppressed the dinucleotide cleavage step if preincubation of CAPE with HIV integrase was performed [57]. The relationship between CAPE structure and inhibition on HIV integrase was investigated and the results demonstrated the indispensable role of the ortho dihydroxylation for high suppressive potency of CAPE against HIV integrase [58].

4) ***Antioxidant:*** CAPE was shown to be beneficial in oxidative stress-related pathological states. CAPE was first described as a 5-lipoxygenase inhibitor by a non-competitive mechanism with free radical scavenging ability in both phorbol-12-myristate 13 acetate-activated neutrophils and cell-free superoxide-producing xanthine/xanthine oxidase enzyme system during the investigation of its anti-inflammatory activity [59]. CAPE attenuated oxidative stress-induced cyclosporine A-stimulated cardiotoxicity in rats both morphologically and chemically by reducing matrix metalloproteinase 2 expression, increasing level of its inhibitors, elevating endogenous antioxidant enzyme

cytochrome-c-oxidase activity, and decreasing cardiac level of ROS [60]. CAPE alleviated lipid peroxidation mediated cerebral vasospasm induced by experimental subarachnoidal hemorrhage, resulting in the improved basilar artery vasoconstriction and increased level of reduced glutathione and nitric oxide in rat brain [61]. CAPE ameliorated experimentally-triggered hyperthyroidism-generated oxidative stress in rat plasma and organs (liver, heart, and brain) by decreasing the level of thiobarbituric acid reactive substances which refers to the lipid peroxidation and bringing back the cellular antioxidant capacity to the hyperthyroid group [62].

Besides these major activities, CAPE has been reported to have immunomodulatory effects in vivo related to decreasing immune organ weight, increasing T lymphocyte blastogenesis and CD4(+) T cell subpopulation, and inducing the production of cytokines IL-2, IL-4 and IFN-γ at higher dose [63]. CAPE may possess neuron- and cardio-protective potential by activating TREK-1 background potassium channels [64]. CAPE was reported to exert its protective effect in variety of drugs or toxic chemicals-induced organ damage such as antibiotics amikacin [65], vancomycin [66], gentamycin [67], and doxorubicin [68, 69]-induced renal and cardiac impairment, antitumor drug methotrexate-caused neuron and cerebullar injury [70-72], antimanic medication lithium carbonate-mediated lung and kidney toxicity [72, 73], and toxic environment pollutant cadmium-induced cardiac damage [74].

1.2.3 Purported Mechanism of Action

Several mechanisms have been proposed for the beneficial effects of CAPE that depend on the test system used.

***Anticancer/tumor*:** 1). By altering redox balance in tumor or transformed cells, CAPE reduces or induces oxidative stress. The resulting effect depended on the dose of CAPE and cell type examined [47, 75]. 2). It inhibited angiogenic enzyme activity of matrix metalloproteinase-2/9 in cancer cells [50, 76]. 3). It modulated signal transduction such as inhibition of transcription factor NF-κB and activation of Fas although not through an effect on Fas ligand. Some evidence also suggests that activation of extracellular signal-regulated kinase (ERKs) and p38 mitogen-activated protein kinase (p38 MAPK) with the involvement of tumor suppressor protein p53 and down-regulation of β-catenin may be involved [49-51, 76, 77].

***Anti-inflammatory*:** 1). CAPE may exert its anti-inflammatory activity by blocking prostaglandin (PG) and leukotriene synthesis by inhibiting cyclooxygenase (COX) enzyme activity through down-regulating COX gene expression both *in vitro* and *in vivo*, which may also account for CAPE chemoprevention activity since the overproduction of PG favors malignant growth [78, 79]. 2). The involvement of nuclear factor kappa B (NF-κB) has been cited as the mechanism for CAPE anti-inflammatory effects.

NF-κB is a transcription factor discovered in the production of kappa light chain of immunoglobulins in B cells [80]. NF-κB regulates host inflammatory and immune responses by inducing the expression of proinflammatory cytokines, chemokines, adhesion molecules, matrix metalloproteinases, cyclooxygenase-2, and inducible nitric oxide synthase. Proinflammatory mediators TNF-α and IL-1β are regulated by NF-κB. TNF-α and IL-1β can also directly activate the NF-κB pathway, thus establishing a positive autoregulatory loop that can amplify the inflammatory response and increase the duration of chronic inflammation. In the cytoplasm, NF-κB exists in an inactive form associated with regulatory proteins called inhibitors of κB (IκB). Upstream activating

signal such as binding of TNF to its receptor may cause phosphorylation of IκB by IκB kinase (IKK). This triggers the degradation of IκB through the ubiquitin system, where the target molecule is tagged by a chain of ubiquitins for degradation by the 26 protesome. The free NF-κB (a heterodimer consisting of p50 and p65 proteins) can then translocate to the nucleus and activate transcription of proinflammatory genes. NF-κB activation has been found in many inflammatory diseases such as rheumatoid arthritis [81] and inflammatory bowel disease [82]. Therefore, it is considered as a novel target for treating inflammatory diseases.

In 1996, Natarajan *et al* reported that CAPE was a potent and specific inhibitor of NF-κB activation in U937 cells, providing an explanation for the anti-inflammatory effect of CAPE [83]. In this report, CAPE was shown to suppress the binding of NF-κB to its target DNA during NF-κB activation by many inflammatory agents such as TNF, phorbol ester, ceramide, hydrogen peroxide, and okadaic acids. This inhibition of CAPE was specific to NF-κB since the binding of some other transcription factors such as AP-1, TFIID, and Oct-1 to the DNA were not affected. The suppression of NF-κB activation by CAPE was also confirmed in rat macrophage, colonic epithelial cells, and PG-PS-induced colitis [53]. CAPE also modulated other transcriptional factors such as elevating anti-inflammatory factor cAMP-response element binding protein (CREB) activity in rat cerebral organotypic hippocampal slices [55], down-regulating nuclear factor of activated T-cells in stimulated Jurkat cells [84], and suppressing *Helicobacter pylori*-induced activator protein-1 expression in gastric epithelial cells [85].

***Antioxidant*:** The catechol ring configuration of CAPE may account for its free radical scavenging ability. The presence of the electron donating hydroxyl groups on the catechol ring not only stabilize oxygen free radicals by the formation of a more stable aroxyl radical through intramolecular hydrogen bonding but can also chelate of metal

ions as well [86, 87]. This may account for the cytoprotective effect of CAPE against cellular oxidative stress induced by tert-butylhydroperoxide and hydrogen peroxide in U937 cells [88]. The main evidence for CAPE antioxidant activity comes from cell-free *in vitro* assays such as the 2,2'-diphenyl-picrylhydrazyl radical (DPPH) free radical scavenging assay, peroxynitrite-scavenging assay, 2,2'-azobis(2-amidinopropane)dihydrochloride (AAPH)-induced lipid peroxidation system, Rancimat test (lipid oxidation), and corn oil-in-water emulsion system for antioxidative activity examination [89-91]. These tests, however, may not accurately reflect the oxidation-reduction environment of a live cell.

In addition to direct antioxidant activity, CAPE was recently shown to induce antioxidant or detoxifying phase II enzymes. The phase II system exerts protective effects through enzymes such as NAD(P)H: quinine oxidoreductase (NQO1) and heme oxygenase-1 [92, 93] that may be activated through transcriptional factor NF-E2 related factor-2 (Nrf2)/antioxidant-responsive element (ARE) signaling pathway [94]. Considering that CAPE may undergo extensive biotransformation and metabolism in liver and intestine such as glucuronidation, sulfation, and methylation, its true *in vivo* concentration may be much lower than what it needed to scavenge free radicals directly [95, 96]. Therefore a role for CAPE in cytoprotection mechanisms involving activation of detoxifying enzymes, modulating cell signaling, or altering gene expression at doses too low to counteract the deleterious effects of oxidative stress directly becomes more attractive.

Recent studies have identified CAPE as a novel inducer of heme oxygenase-1 (HO-1) in astrocytes, the cytoprotective component of cellular defense system protecting organs from I/R insult. This result supports the hypothesis on the mechanism of CAPE

protection involving the induction of HO-1 as a key component in CAPE protection against I/R induced oxidative stress [93, 97, 98].

1.3 HEME OXYGENASE-1 (HO-1)

1.3.1 Heme Oxygenase System

Heme oxygenase (HO) was first identified for its ability to catalyze the degradation of heme to bilirubin in hepatic microsomes by Tenhunen and Schmid in 1968 [99], and this enzymatic activity was later clarified to be independent of cytochrome P-450 [100]. The metalloporphyrins heme (Fe-protoporphyrin IX) is integral to life. It promotes most biological oxidative reactions and electron transfer processes, transports molecular oxygen to cells, and participates in mitochondrial respiration and signal transduction [101]. Heme is also a potentially toxic substance that contains iron that can lead to ROS generation and causing lipid peroxidation damaging cellular membranes and other cell structures [102]. Therefore, the metabolism of heme by the HO system plays a key role in maintaining the cellular heme homeostasis. The HO enzyme catalyzes the first and rate-limiting step in the oxidative decomposition of heme. This enzymatic reaction utilizes three moles of molecular oxygen per heme molecule degraded and requires a reducing agent to activate O_2 and reduce heme-chelating iron from Fe^{3+} to Fe^{2+}, where NADPH: cytochrome P450 reductase is applied to provide the reducing equivalents and electron transfer as well. HO specifically breaks the α-methene bridge of the heme molecule to generate the open-chain tetrapyrrole α-isomer of biliverdin. Biliverdin-IXα (BV) is then rapidly converted to bilirubin-IXα (BR) by NAD(P)H: biliverdin reductase.

The breakdown of heme releases its chelated iron in the ferrous form which is subsequently sequestered to iron-binding protein ferritin and disposing of the α-methene bridge carbon as carbon monoxide (CO). The pathway of heme catabolism by HO action is shown in Figure 1.4.

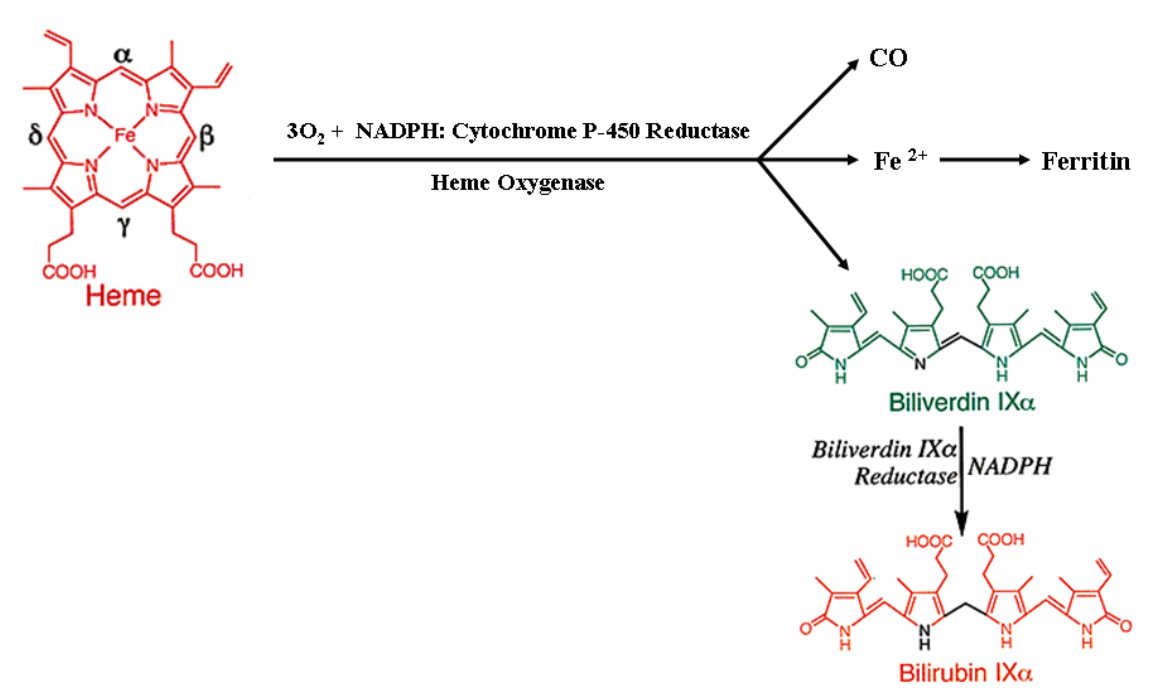

Figure 1.4: Metabolic pathway of heme by heme oxygenase.

In mammals, two different forms of HO have been characterized so far. The first isozyme HO-1 is the inducible isoform, which was identified about 3 decades ago [100]. The other form, HO-2 was initially purified from rat testes in 1986 and has been reported to exist constitutively in multiple tissues [103-106]. HO-1 is also referred to as the stress protein HSP32 [107] with the molecular weight of about 32 kDa, while HO-2 has a relatively larger molecular weight (~42 kDa). These two isozymes of HO have been defined as different gene products with differences in gene organization, structure, chromosomal localization, cell type, subcellular localization, and tissue distribution [108, 109]. Despite these differences, both enzymes catalyze the same heme-degrading reaction with similar substrate specificity and cofactor requirements.

Not too long ago, the HO system was only considered as the catabolic enzyme in the category of maintaining the internal balance of cellular heme, and its downstream products were thought to be waste or cytotoxic materials. Nowadays, the induction of HO-1 has being considered as an important component in a cell defense system mediating cellular and tissue protection against a variety of stimuli and agents resulting in oxidative stress and pathological conditions. HO-1 inducers can be subcategorized into 1). ROS or ROS inducer such as H_2O_2, peroxynitrite, menadione, and UVA radiation; 2). heavy metals like cadmium and cobalt; 3). metalloporphyrins such as heme, CoPPIX, and ZnPPIX; 4). pro-inflammatory cytokines like interleukin and tumor necrosis factor; and 5). phenolic antioxidants such as curcumin, carnosol, quercetin, resveratrol, and CAPE. Other inducers include prostaglandin family members, tumor promoter 12-O-tetradecanoylphorbol 13-acetate (TPA), hypoxia/hyperoxia, angiotensin, and non phenolic phase II enzyme inducers such as sulfurophane. Investigations of the mechanisms of HO-1 induction have revealed two major signaling pathways including

protein phosphorylation-depenent signaling transductions and redox sensitive signaling regulations [108, 109].

Activation of mitogen-activated protein kinases (MAPKs) has been implicated as participating in HO-1 induction by various physical and chemical stresses through using the chemical inhibitors for MAPKs. The MAPKs superfamily consists of three major signaling cascades: the extracellular signal regulated kinases (ERK), the c-Jun NH2-terminal kinases (JNK), and the p38 MAPKs. HO-1 activation has been reported involving one or a combination of these MAPK pathways to achieve better HO-1 gene expression. Among these MAPK pathways, p38 and ERK seems to play major roles in HO-1 activation. Additional evidence from the expression of dominant negative mutants, wild-type, and activated forms of various MAPKs further implicates MAPKs in HO-1 gene activation. Other kinases potentially contributing to induction include phosphatidylinositol 3-kinase (PI3K), protein kinases A and C, and tyrosine kinase [109].

The Nrf2/ARE pathway, a redox-sensitive signaling cascade activated by cells when faced with electrophils, oxidative toxicants, or physiological injury also has been implicated in HO-1 induction. Under normal conditions, Nrf2 is sequestered in cytoplasm by a cytoplasmic factor Keap1, which represses Nrf2 transactivation activity. During oxidative stress, electrophils and ROS can directly react with the sulfhydryl groups from two (C273 and C288) cysteine residues of Keap1, facilitating the formation of disulfide bonds and resulting in the dissociation of Nrf2/Keap1 complex. The “free” Nrf2 can then translocate to the nucleus, where it could bind to ARE to initiate the expression of antioxidant genes such as HO-1 [110]. Other transcriptional factors that have been reported to modulate HO-1 expression include Bach 1 as a repressor of HO-1 induction, heat shock factor 1, NF-κB, and AP-1 [111, 112].

The beneficial effects of HO-1 induction have been reported [113-115] and confirmed with HO-1 knockout mice [116, 117] and one human case with HO-1 deficiency [118]. In addition to degrading the prooxidant heme, the cytoprotective mechanism of HO-1 induction has been recently attributed to the end products of HO-1 action (CO and BV) and BR. CO is a colorless and odorless gas first discovered in the late 18th century and considered only a toxic air pollutant mainly from incomplete combustion of organic molecules. Its strong affinity to hemoglobin (Hb) (about 240 times more than that of oxygen) leads to its harmful effects which could result in displacement of O_2 from Hb and eventually tissue hypoxia. The major source of endogenous CO comes from the HO-catalyzed hemoglobin turnover. The protective effects of CO demonstrated so far include anti-inflammation, cell or tissue-specific suppression of apoptosis, proliferation, and vasodilation mainly through activating the soluble guanylate cyclase (sGC)/ cyclic 3',5'-guanosine monophosphate (cGMP) pathway and MAPKs signaling cascades [119]. BV and BR are primarily generated from hemoglobin degradation in vivo [120]. BV is a hydrophilic and nontoxic greenish pigment, which is rapidly converted to BR, an insoluble yellowish pigment. The endogenous BR used to be considered a toxic waste product eliminated from cells and tissues via blood and exclusively metabolized by liver UDP:glucuronyltransferases. Excessive accumulation of unconjugated BR in the blood causes neonatal jaundice and neurotoxicity [121]. The landmark studies by Stocker et al [121] first confirmed the strong antioxidant role of BV and BR at physiological micromolar concentrations, which could scavenge the chain-carrying peroxyl radical either by donating a hydrogen atom (BR) or directly react to form stable addition product. In addition, The conversion from BV to BR by BV reductase may contribute to amplifying the protective effect of BR. Baranano et al [122] indicated that 10 nM BR could protect against up to 100 μM H2O2-induced oxidative stress, which is feasible

through the powerful redox cycle of BR being oxidized to BV which is recycled back to BR. This BV-BR redox process that protects the membrane components is comparable to that of GSH-GSSG conversion to protect cytoplasmic components from ROS insult. Besides CO and BV, iron is also released by heme degradation. Since free iron could facilitate ROS production through Fenton reaction, it possesses prooxidant activity and is itself toxic. Some studies suggest that HO-1 induced cytoprotection could be linked to either exporting iron out of the cells mediated by an iron-transporting ATPase [123] or sequestering iron into ferritin, the intracellular iron-binding protein [124].

1.3.2 HO-1 and I/R Injury

The production of HO-1 stimulated either by its chemical inducer hemin [125] or by physiological stimuli such as hypoxia preconditioning [126] has been shown to directly correlate with amelioration of I/R injury in vivo. Further investigation into the protective role of HO-1 activation in I/R injury was recently confirmed by repressing HO-1 production [127] with HO-1 siRNA and showing enhanced apoptosis in endothelial cells in mouse lung during I/R injury. In addition, overexpression of HO-1 with or without the incorporation of erythropoietin hypoxia response elements regulating the HO-1 expression by a preemptive adeno-associated vector-carried HO-1 gene delivery system reduced various tissue damage triggered by I/R [128, 129]. Exogenous administration of heme-degrading end products by HO-1 enzymatic activity also provides beneficial effects in the deleterious situation of I/R through different mechanisms. Antioxidant BR and BV at micromolar level, signaling molecular CO exposure, and overexpression of heavy chain Ferritin with iron-sequestering ability protected I/R injury in vitro, ex vivo, and in vivo [130-135].

1.4 HUMAN ENDOTHELIAL CELLS

1.4.1 The Importance of Endothelial Cells in I/R Injury

Endothelial cells (EC), as an important component of the blood vessel wall, play a critical role in the preservation of normal vessel wall structure and function, and regulate vessel growth. Rather than just being a passive barrier, EC also maintain several important physiological functions such as modulating microvascular substance exchange, metabolizing circulating molecules, regulating vascular tone and blood flow, controlling leukocyte trafficking, and mediating angiogenesis [136]. I/R injury begins within EC in blood vessels. Endothelial injury at the initial site of tissue damage is inevitable and plays a key role in the tissue dysfunction and organ failure after ischemia and reperfusion.

EC have been identified as a source of oxygen free radical production when subjected to hypoxia and reoxygenation simulating ischemia and reperfusion *in vitro* [137, 138]. When confronted by oxidative stress induced by ROS generated from I/R injury, EC are activated, expressing proinflammatory properties, recruiting and accumulating neutrophils facilitated by the expression of adhesion molecules (P-selectin, E-selectin). Collateral damage can occur to endothelial cells by ROS produced by neutrophils at a site of injury. These neutrophil products damage EC directly by reacting with membrane lipids, nucleic acids, and polyunsaturated fatty acids, which result in the disruption of cellular integrity [139].

Damage to endothelial cells following I/R injury leads to delays in recovery due to poor delivery of nutrients, removal of waste products, and reduction in the ability of mononuclear cell immigration to repair injured tissue. Damage to endothelial cells can

also lead to secondary tissue injury as a consequence of diminished vascular function and more severe impairment of a variety of organs leading to multiple organ failure. Therefore, endothelial cells provide an important cell target for modeling of cytoprotectants against I/R injury *in vitro*.

1.4.2 The Human Umbilical Vein Endothelial Cells (HUVEC) Model

The umbilical cord, discarded after birth, has provided a readily available source of human endothelial cells that are probably the best characterized model of the endothelium. The isolation of HUVEC could be achieved using enzyme like collagenase to remove the cells from the internal lining of umbilical veins, which provides good yield and high purity of HUVEC. To minimize variation caused by harvesting from different individuals, HUVEC are usually pooled from several umbilical cords. During cell culture, the cells are grown to confluence for at least two days before experiments to mimic the in vivo situation where endothelial are relatively proliferatively inactive. In general, only passages from 1 to 5 were used in the experimental treatments to avoid characteristic cellular changes known to occur with long in vitro culture which may consequently affect the integrity of experimental results.

HUVEC in vitro have been used to simulate the I/R situation in vivo [140-142]. Because oxygen free radical generation play a major role in I/R injury and the burst of ROS has been identified produced from HUVEC mitochondria after hypoxia/reoxygenation, the application of menadione to induce oxidative stress in HUVEC could simulate I/R triggered oxidative injury in vitro. Menadione (MD) is one of the simplest quinones (Figure 1.5), and it belongs to the vitamin K family. It has been widely studied as a model for evaluating the cellular effects of oxidative stress in

endothelial cells (EC), including induction of apoptosis [143, 144]. The major mechanism of EC cytotoxicity caused by menadione is the stimulated production of ROS by redox cycling, where one electron reduction of O2 by the semiquinone form of menadione generates superoxide. Superoxide dismutates to form hydrogen peroxide either spontaneously or enzymatically through superoxide dismutase, which then participates in the Fenton reaction producing hydroxyl radicals. Therefore, MD has been proposed to initiate a cascade of ROS formation in EC. Note that, when treated with MD, different passages and batches of HUVEC respond differently to a given dose of menadione, therefore the dose required to reduce survival by 90% had to be determined prior to a study. The pattern of cell damage caused by MD toxicity compared to normal HUVEC morphology is shown in Figure 1.6.

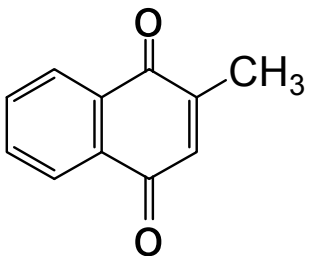

Figure 1.5: Chemical structure of menadione.

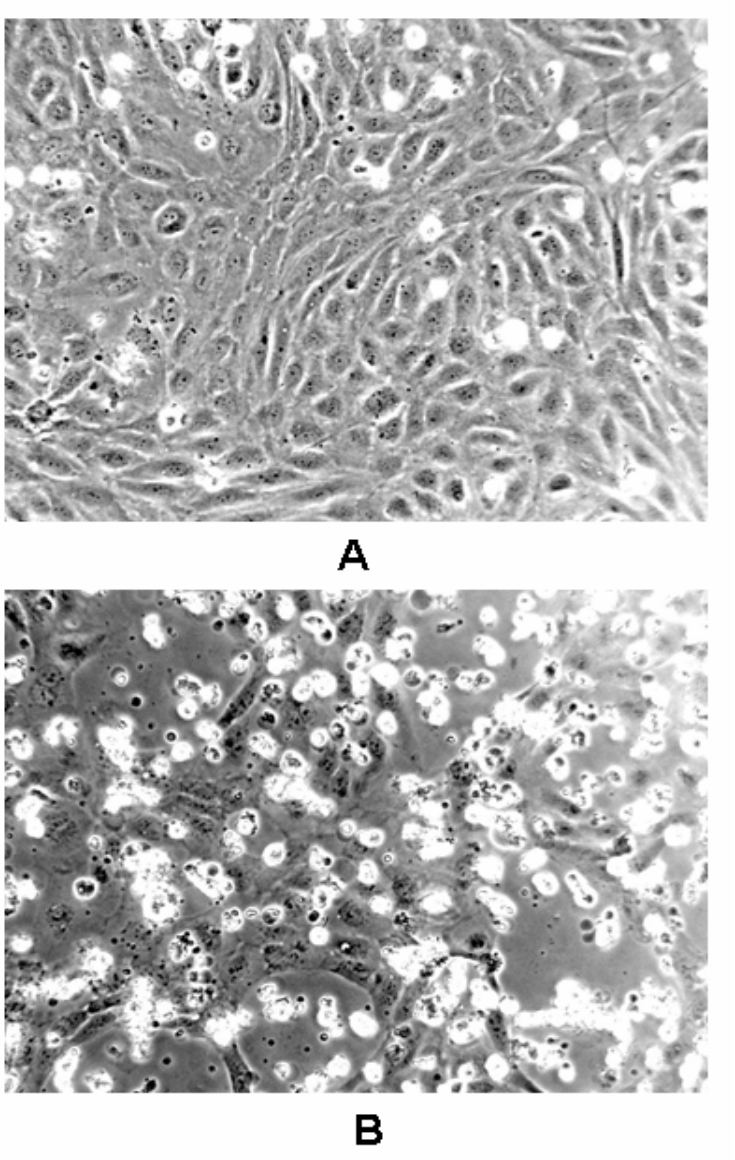

Figure 1.6: Oxidative stress-induced apoptosis and damage in HUVEC after 24-hr MD exposure. Cultured confluent HUVEC were treated with either vehicle control (A) or 25 μM MD (B). The rounded up cells in B are endothelial cells in the later stages of apoptosis.

1.5 SYNTHESIS OF CAPE FLUORINATED DERIVATIVES

Despite the wide variety of biological activities associated with CAPE, only limited structural analogs have been examined [145-147], especially those incorporating modifications to the caffeic acid catechol ring [148-150]. We are unaware of any fluorinated CAPE derivatives in the literature. Ring-fluorinated derivatives of other catechol-containing drugs may display a "fluorine-effect," in which the position of the fluorine ring substituent has a profound impact on binding or selectivity of the receptor [151, 152]. The introduction of fluorine into the catechol ring exerts a negative inductive effect, increases the electronic density in this conjugated system, strengthens the ester bond, and can diminish interactions with catechol methyltransferase [153-155].

With the aim of studying structure activity relationship of CAPE, new CAPE derivatives fluorinated in the catechol ring were synthesized through the Wittig reaction. This reaction was discovered by Georg Wittig, a German chemist who won the Nobel Prize in 1979. The Wittig reaction is an important method for the preparation of alkenes with specific introduction of carbon carbon double bond in a known location through the reaction of an aldehyde or ketone with a phosphorus ylide [156]. CAPE analogues were prepared through the reaction between various fluorinated benzaldehydes and a triphenyl phosphonium halide. The necessary fluorinated benzaldehydes were either commercially available or easily obtained through demethylation reaction with boron tribromide [157]. The Wittig reagent phosphonium salt was obtained from the reaction between triphenylphosphine and chloroacetic acid ester [148].

1.6 PHARMACOKINETICS OF CAPE AND FCAPE

Pharmacokinetics (PK) is what the body does to the drug and it is indispensable in both preclinical and clinical phases of new drug development. The ultimate purpose of studying PK and pharmacodynamics (PD), which is what the drug does to the body, and corresponding PK/PD modeling is to optimize drug dose regimen for clinical trials. Although many preclinical studies have demonstrated primary safety and biological activities of CAPE in animal and *in vitro* models, the pharmacokinetics of CAPE has not been reported in the literature. It will be useful to obtain preliminary data on pharmacokinetics of CAPE and its most cytoprotective fluorinated derivative (FCAPE) in animal model.

Prior to pharmacokinetic characterization, the integrity of target compounds in collected samples must be maintained because further degradation could confound the results. As an aryl ester, CAPE is liable to enzymatic hydrolysis *in vivo* by the action of plasma esterases. Therefore, the determination of the stability of CAPE and FCAPE in plasma was critical for evaluating their effects, understanding the protection mechanism, and studying their pharmacokinetic behavior *in vivo*. The application of the esterase inhibitor sodium fluoride and pH adjustment were investigated to avoid further hydrolysis of CAPE and FCAPE [158].

In addition, the quantitative determination of CAPE and FCAPE in biological matrix is essential for establishing their pharmacokinetic profiles. A review of the literature showed that a limited number of quantitative CAPE assays are available [159-161]. With the objective of studying pharmacokinetics of CAPE and FCAPE, a quantitative method using ultra-performance liquid chromatography with electrospray ionization tandem mass spectrometry was developed and validated for CAPE and

FCAPE. The main advantages of ultra-performance liquid chromatographic system are to provide better resolution and sensitivity, reduce analytical time, and minimize carryover effect compared to traditional HPLC system.

Finally, pharmacokinetic profiles of CAPE and FCAPE were established following intravenous administration to Sprague Dawley rats. Non-compartmental analysis and bi-exponential fit was performed to obtain preliminary pharmacokinetic parameter data.

Chapter II: Cytoprotection of Human Endothelial Cells from Menadione Cytotoxicity by Caffeic Acid Phenethyl Ester: The Role of Heme Oxygenase-1

2.1 INTRODUCTION

Caffeic acid phenethyl ester (CAPE) has been reported to ameliorate ischemia/reperfusion (I/R) injury *in vivo* [24-39]. The mechanism of cytoprotection, however, has not been determined. Without clear understanding of its mechanism of action and potential side effects, it is unlikely that it will be applied in the clinical setting. With the aim of understanding the mechanisms of action of CAPE for using CAPE as a model drug for treating I/R injury, an *in vitro* assay simulating I/R injury was established.

Menadione (MD)-induced oxidative stress in human umbilical vein endothelial cells (HUVEC) was used to simulate I/R injury *in vitro* for assessing the ability of CAPE as a cytoprotectant. Although the cytoprotective activity of CAPE has been attributed to its known antioxidant ability, CAPE has been shown to also affect transcriptional activity, which may contribute to its cytoprotective effect. Some other polyphenolic antioxidants such as curcumin and resveratrol have also been reported to effect transcriptional activity [93, 162, 163]. The results presented here indicate that cytoprotection in human endothelial cells by CAPE involved transcriptional activation of heme oxygenase-1 (HO-1).

The purpose of this study was to develop a CAPE cytoprotection model *in vitro* and investigate the mechanism of CAPE protection against ROS-mediated injury. We hypothesized that HO-1 induction is the key component in CAPE protection against oxidative stress.

2.2 MATERIALS AND METHOD

2.2.1 Materials

CAPE was purchased from Cayman Chemical (Ann Arbor, MI). Bilirubin (BR), menadione sodium bisulfite (MD), and DMSO were purchased from Sigma (Saint Louis, MO). Biliverdin hydrochloride (BV) and Sn(IV) protoporphyrin IX dichloride (SnPPIX) were purchased from Frontier Scientific (Logan, UT).

2.2.2 Cell Culture

First passage HUVEC (Cascade Biologics, Portland, OR) were cultivated on 1% gelatin-coated 75-cm^2 culture flasks (Corning Incorporated, Corning, NY) in Medium 200 supplemented with 2% fetal calf serum, penicillin (100 units/ml), streptomycin (100 units/ml), and Fungizone (0.25μg/ml) supplied by Cascade Biologics [164]. The cells were cultivated at 37 ºC in a humidified atmosphere of 95% air and 5% CO_2 with medium changes every 2 days until confluent. Prior to an experiment, HUVEC were subcultivated with Trypsin/EDTA onto 1% gelatin-coated 48- or 6-well Costar® multiplates (Corning Incorporated, Corning, NY) at 5000 cells/cm^2 and grown to confluence (3-4 days), and kept for 72 hrs to produce a quiescent cell layer. On the day before the experiment, the medium was changed. Only the second through fifth population doublings of cells were used.

2.2.3 Cell Viability Assay

Cell viability was assessed at 24 hours after initiation of treatment using Alamar Blue™ (Biosource International, Camarillo, CA), which is converted to a fluorescent compound in amounts proportional to the number of viable cells [165]. The cells were incubated for two hours at 37 °C with culture medium containing 10% Alamar Blue™. After incubation, fluorescence was measured at 545 nm excitation and 590 nm emissions using SpectraMAX® M2 microplate reader (Molecular Devices, Sunnyvale, CA). HUVEC were regularly observed under phase contrast microscopy and images were captured with a digital camera.

2.2.4 MD Cytotoxicity

MD was dissolved in phosphate buffered saline (PBS) to produce a 0.5 M solution [166] and diluted with medium before being added to the plate wells. Due to differences in responses to menadione, each group of pooled HUVEC was initially assessed for a dose of menadione which is close to its maximum toxicity producing 90% cell death. Cells were incubated in 5 to 38 μM MD depending on the sensitivity of a given set of cells for 24 hrs followed by Alamar Blue viability assay.

2.2.5 *In Vitro* Cytoprotection Assay

CAPE, BV, and BR were dissolved in DMSO and diluted 1000-fold with medium before addition of serial dilutions to 48-well culture plates. To assess protection against

oxidative stress, confluent HUVEC were initially pretreated with CAPE, BV, and BR at various concentrations for 6 hrs to allow transcriptional response to occur. The cytotoxic dose of menadione chosen from MD cytotoxicity assay was then given to the HUVEC in the presence of testing compounds. After 24 hrs incubation, cell viability was measured using the Alamar Blue assay.

2.2.6 Total RNA Isolation

Total RNA was extracted from cultured HUVEC in 6-well culture plates with TRI™ reagent according to the manufacture's instructions (Molecular Research Center, Cincinnati, OH). RNA yield was quantified using a NanoDrop® ND-1000 Spectrophotometer (NanoDrop Technologies, Wilmington, DE), and the quality was assessed by 1% agarose gel electrophoresis containing 1:1000 SYBR Gold nucleic acid stain (Invitrogen, Carlsbad, CA) in loading buffer (Figure 2.1).

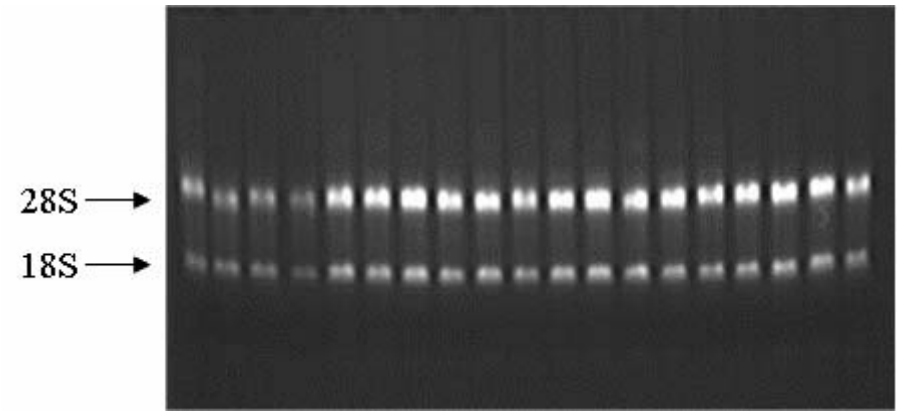

Figure 2.1: Intact total RNA on a 1% agarose gel. The quality was assured by the intensity ratio (≈2) of 28S band versus 18S band.

2.2.7 Protein Extraction

Protein was extracted from the HUVEC grown on 24-well multiplates. After incubation with 5 μg/ml (17.5 μM) of CAPE or 0.1% DMSO for 24 hrs, protein for gel electrophoresis was obtained by incubating them in 100 μl of lysis Buffer (NOVEX, San Diego, CA) containing 1% β-mercaptoethanol (Sigma) at 70°C for 10 min.

2.2.8 Gel Electrophoresis, Total Protein Determination and Western Blotting

Ten microliters, containing approximately 10 μg of protein, from each treatment were run on NuPage 4-12% Bis-Tris Gels (NOVEX) for 1 hr at 125 volts. The protein was then transferred to a PVDF membrane (NOVEX) for 5 hrs at 95 mA (Semi-Dry Blotter II, Kem En Tec, Flander, NJ). Membranes were hydrated in a 50% methanol/water solution for 10 min, then incubated three times, 15 minutes each, in a blocking solution of 0.2% I-Block (Tropix, Bedford, MA), 0.1% Tween-20 (Sigma) and 0.1% thimerosal (Sigma) in PBS (Sigma). The blots were then incubated with a rabbit anti-rat HO-1 primary antibody (1:5000 dilutions) for 2 hrs, which was purchased from Stressgen Biotechnologies Inc. (San Diego, CA). Blots were then washed another three times in blocking solution for 15 minutes each, and incubated in biotin labeled antibody against rabbit (Vector Laboratories) and 1:4,000 dilution of alkaline-phosphatase labeled secondary antibody. Finally, the blots were washed three times in PBS, 15 minutes each, before staining. Following staining for HO-1, the blots were stripped and restain with mouse anti-actin. The blots were stained in a 10% NBT-BCIP solution (Invitrogen) until the bands developed. Quantitative analysis was performed NIH Images (NIH) on blots scanned into the computer.

2.2.9 Gene Expression Analysis

Microarrays containing ~ 22,000 human genes per array were produced by spotting oligonucleotides (Qiagen/Operon Human ArrayReady Oligo Set V 2.0, Alameda, CA) onto epoxy-coated slides (Cel Associates, Pearland, TX). A GeneMachines Omni Accent Gridder (GeneMachines, San Carlos, CA) and SMP-3 pins from Telechem International were applied to print the microarrays. Microarrays were blocked with 1% BSA in 3X SSC and 0.1% SDS for 1 hr at 50 °C before use. For gene expression analysis, sample RNA was extracted from 5 μg/ml CAPE and 0.1% DMSO-treated HUVEC for 6 hrs, while reference RNA was human universal reference RNA (Stratagene, La Jolla, CA). cDNA targets were then generated with the 3DNA Array 900 kit (Genisphere Inc., Hatfield, PA) according to the manufacture's instructions. The high-resolution scans were acquired with a GenePix scanner 4000B (Axon Instruments, Inc., Union City, CA) and tabulated with GenePix pro 5.1 software. To determine intra-assay variability, each condition (3 replicates) was individually labeled and compared to a universal reference of pooled RNA that was labeled as a pool sufficient for 6 microarrays. Following washing and scanning, the microarray data analysis and statistical comparison were performed using BRB Array Tools (Biometric Research Branch, National Cancer Institute, http://linus.nci.nih.gov/BRB-ArrayTools.html).

2.2.10 Quantitative Real-Time Reverse Transcription Polymerase Chain Reaction (qRT-PCR)

One μg of total RNA from the same samples used for microarray analysis was converted to cDNA using random primers and Superscript III reverse transcriptase according to the manufacture's instruction (Invitrogen ^{TM} life Technology, Carlsbad, CA). Real-time PCR was performed on a LightCycler^{TM} thermal cycler (Idaho Technology, Salt Lake City, UT) with Roche LightCycler® TaqMan Master for HO-1 and β-actin (Roche Diagnostics, Indianapolis, IN). HO-1 and β-actin primer sets were from TaqMan® Gene Expression Assays (Applied Biosystems, Foster City, CA). HO-1 gene was normalized to the expression level of β-actin gene for each sample. Relative quantification was acquired by comparative C_T method.

2.2.11 HO-1 Inhibition with SnPPIX

HUVEC were pretreated with 5 μg/ml CAPE plus different doses (10, 20, and 30 μM) of HO-1 inhibitor SnPPIX [167], respectively, for 6 hrs before exposing to MD for 24 hrs. SnPPIX was dissolved in 0.1 M NaOH and dilute 1000-fold with medium before being added to the 48-well culture plates. Cell viability was measured using the Alamar Blue assay.

2.2.12 Carbon Monoxide (CO) Exposure

HUVEC were exposed to 1% CO and 5% CO_2 in air (Matheson-TriGas, Kyle, TX) in sealed incubator chambers (Billups-Rothenberg Inc, Del Mar, CA). Cultures identically treated but exposed to 95% air 5% CO_2 served as control. After a 10 minute purging of either CO or air, HUVEC were incubated for 2 hrs. Various concentrations of MD were then added to the culture media and the culture plates were returned to the chambers. After 10 minutes of purging with 1% CO or air, HUVEC were incubated for additional 24 hrs in sealed chambers. The cell culture chambers were humidified and maintained at 37 °C. Cell viability was measured using the Alamar Blue assay. Control cultures were identically treated but with 95% air and 5% CO_2

2.2.13 Statistical Analysis

Data are presented as the mean ± standard deviation. Differences between or among the groups were analyzed using the independent samples T test or one-way analysis of variance combined with Tukey (equal variances assumed) or Games-Howell (equal variances not assumed) test through SPSS statistical software. A difference of p value < 0.05 was considered significant. Each experiment was repeated at least 3 times and a representative experiment is presented. For microarray analysis through BRB Array Tools (http://linus.nci.nih.gov/BRB-ArrayTools.html), genes were first excluded if both intensities of red and green signals <100, spot sizes <10, and spot flag contained numeric values other than 0. Then, lowess smooth normalization was applied to balance the difference in labeling intensities of the red and green dyes. Genes considered non-informative were filtered out if less than 20 % of expression data had at least a 1.5 -fold

change in either direction from the gene's median value and percent of data missing or filtered out exceeds 50%. Two-class or multiple-class comparison was performed to identify genes that were differentially expressed using a random-variance t or F-test. Genes were considered statistically significant with p value < 0.001. The common genes significantly up-regulated were identified by intersecting genelists generated from two independent experiments.

2.3 RESULTS AND DISCUSSION

2.3.1 Protective Effects of CAPE against MD-Induced Oxidative Stress in HUVEC

I/R injury may occur in cardiovascular disease, surgical procedures and following traumatic injury. Natural polyphenolic compounds such as CAPE may provide some relief from I/R injury. To better understand the potential protective mechanism of CAPE, an in vitro model of MD-induced oxidative stress in HUVEC was developed.

MD-induced cytotoxicity in HUVEC is shown in Figure 2.2. MD induced a dose-dependent decrease in the viability of HUVEC as determined by the Alamar Blue assay. CAPE cytotoxicity was examined at 5, 10, and 15 μg/ml and is shown in Figure 2.3. Because 15 μg/ml of CAPE caused more than 10% cell death, the maximum dose of CAPE used for cytoprotection testing was 10 μg/ml. CAPE protected HUVEC against MD-induced I/R-like injury in a dose-dependent fashion (Figure 2.4). At 5 μg/ml, CAPE exhibited the maximum cytoprotective effect against MD-induced toxicity, recovering 65% HUVEC compared to about 15% HUVEC viability after MD exposure alone.

The morphology of HUVEC is shown in Figure 2.5. The control HUVEC (Figure 2.5A, 0.1% DMSO for 24 hrs) exhibited normal mitotic cells. MD-treated HUVEC (Figure 2.5B, 30 μM menadione for 24 hrs) displayed significant shrinkage and fragmentation, morphological characteristics of apoptosis. HUVEC pretreated with 5 μg/ml CAPE for 6 hrs before MD treatment exhibited relatively normal cell morphology with few cells undergoing apoptosis (Figure 2.5C).

This study demonstrated that CAPE provided dose-dependent cytoprotection of HUVEC against MD-caused oxidative injury.

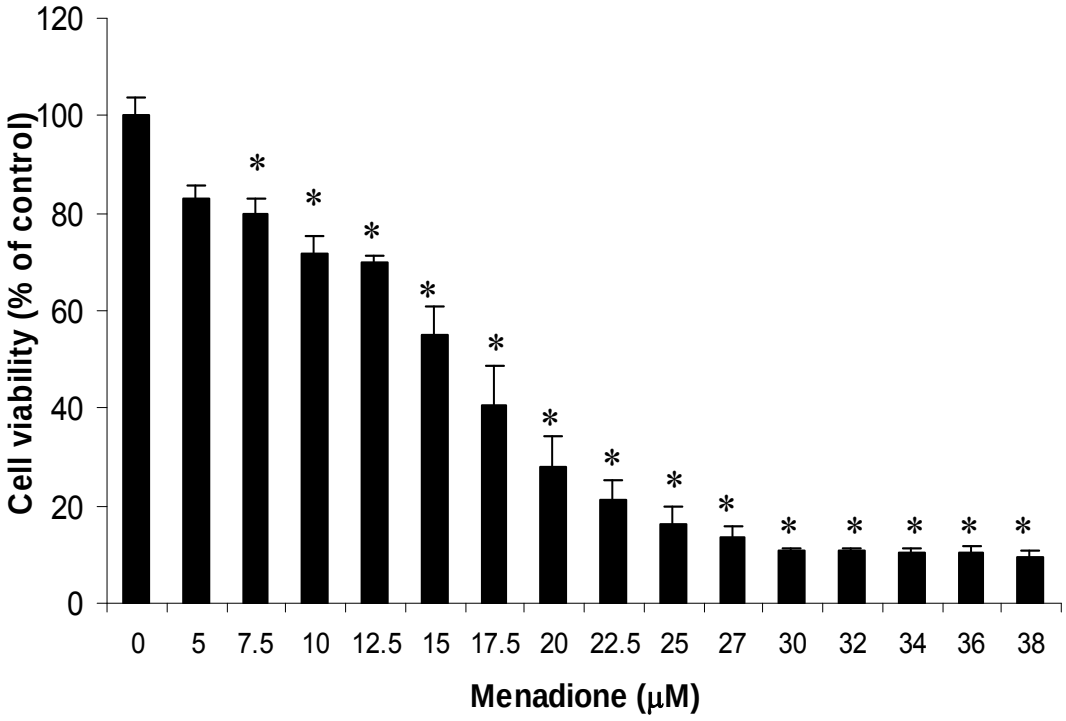

Figure 2.2: Cytotoxicity of MD to HUVEC. MD caused a dose-dependent reduction of viability in HUVEC. Values are presented as means with standard deviations (n=3). The dose of MD at 25 μM was used in CAPE cytoprotection assay. ∗: $P<0.05$ versus control (MD at 0 μM).

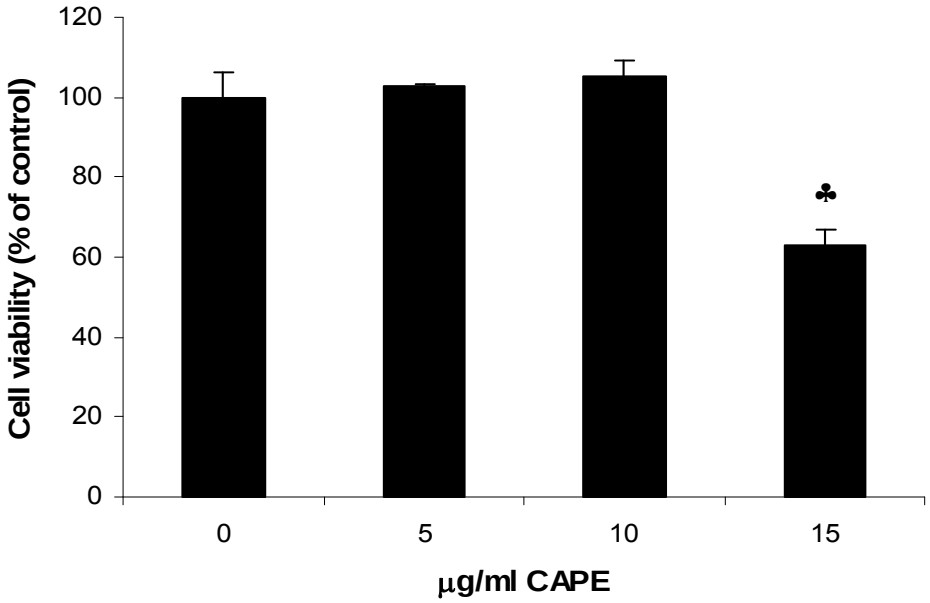

Figure 2.3: Cytotoxicity of CAPE to HUVEC. Values are presented as means with standard deviations (n=3). Cell viability is shown as percent of control, and less than 90% was considered toxic. CAPE at 15 μg/ml was considered toxic. ♣: $P<0.001$ versus vehicle control (CAPE at 0 μM).

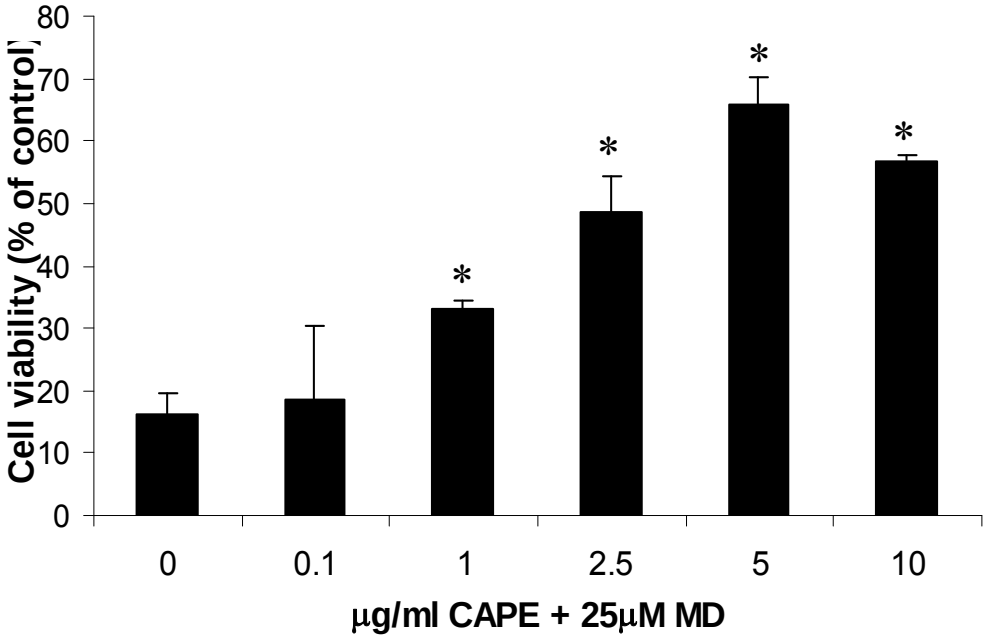

Figure 2.4: CAPE cytoprotection against MD-induced injury in HUVEC. MD was used at 25 µM. Values are presented as means with standard deviations (n=3). CAPE showed dose-dependent cytoprotection against MD. CAPE at 5 µg/ml recovered HUVEC significantly to about 65% from MD-induced injury. ∗: $P<0.05$ versus 25 µM MD alone (CAPE at 0 µg/ml).

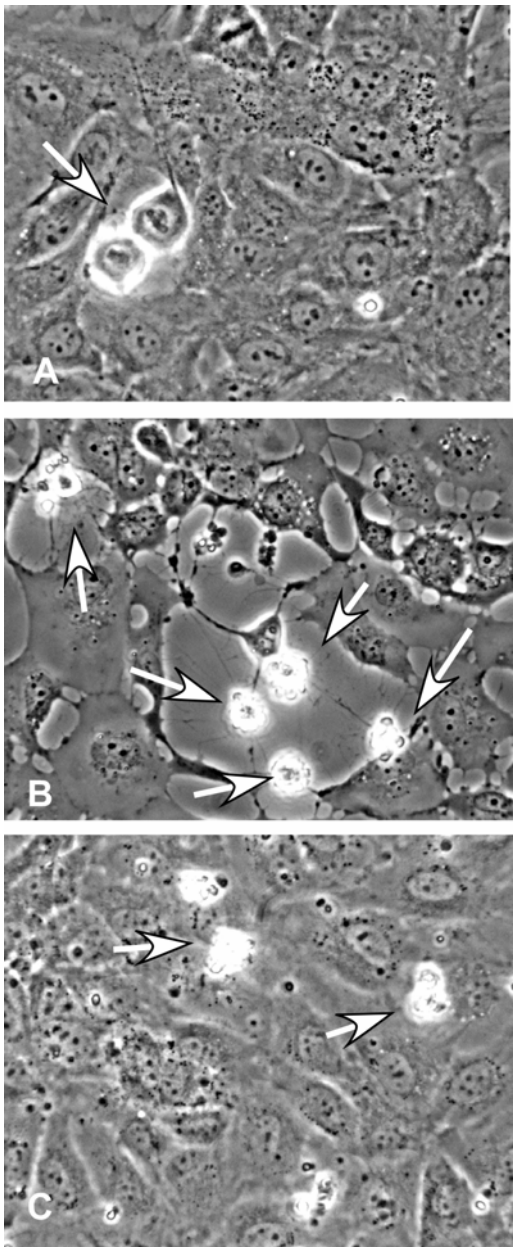

Figure 2.5: Morphology of HUVEC treated with 0.1% DMSO (A), 30 µM MD alone (B), or pretreated with 5 µg/ml CAPE for 6 hrs before incubation with 30 µM MD (C) for 24 hrs. In panel A, HUVEC undergoing normal mitosis are indicated with an arrow. In panels B and C, apoptotic cells are indicated by arrows. HUVEC were protected by CAPE pretreatment against MD toxicity, as shown by much less cell damage and fewer apoptotic cells.

2.3.2 HO-1 Induction by CAPE in HUVEC

The mechanism for the beneficial effects of CAPE has been proposed result from its free radical scavenging ability due to 3, 4-dihydroxyl configuration on its catechol ring. Several recent studies suggested polyphenolic antioxidants such as curcumin and resveratrol altered transcriptional events to exert their beneficial effects, which provides an alternative explanation to antioxidant effects. To investigate the mechanism for CAPE cytoprotection at the transcriptional level, we performed gene expression analysis using oligonucleotide microarrays. The data showed that out of the 22,000 human genes examined from two independent experiments, 23 genes were statistically significantly up-regulated early (within 6 hrs) to CAPE (Table 2.1). Among them, HO-1 was highly induced (8.25 fold) by CAPE compared to the DMSO control. To validate this microarray screening result, qRT-PCR and western blotting were performed to identify HO-1 mRNA and protein level in HUVEC after 6-hr and 24-hr preincubation with CAPE, respectively. The results confirmed that HO-1 mRNA and protein product level were elevated about 29-fold (Figure 2.6) and 6-fold (Figure 2.7), respectively.

HO-1 induction has been shown to be beneficial in I/R injury *in vivo* [125, 128]. Several mechanisms of HO-1 protection against I/R injury have been proposed: 1) metabolism of heme, the toxic cellular component from disposed heme proteins; 2) consumption of excessive O_2 during I/R injury in the process of heme degradation by HO-1; and 3) cytoprotection through heme catabolizing products such as BV/BR, ferrous iron/ferritin, and CO [168].

Table 2.1: CAPE-regulated significant alteration of gene expression in HUVEC

Gene category	Gene description	Fold change
Detoxification	**Heme oxygenase (decycling) 1**	**8.245**
Molecular chaperone	Heat shock protein 90kDa beta (Grp94), member 1	2.832
	Heat shock 70kD protein 5 (glucose-regulated protein, 78kD)	3.954
Growth factor	KIT ligand	4.727
	Prostate differentiation factor	4.625
	Endothelial cell-specific molecule 1	2.878
Transporter	Solute carrier family 3, member 2	3.187
	Solute carrier family 30 (zinc transporter), member 1	2.492
	Solute carrier family 39 (zinc transporter), member 14	2.834
	START domain containing 4, sterol regulated	2.705
	Karyopherin alpha 2 (RAG cohort 1, importin alpha 1)	0.432
Binding	Selenoprotein K (selenium binding)	3.399
	Nucleobindin 2 (calcium ion binding)	3.146
	Asp (abnormal spindle)-like (calmodulin binding)	0.285
	Phorbol-12-myristate-13-acetate-induced protein 1 (protein binding)	2.508
Transcription regulator	DNA-damage-inducible transcript 3 (P38 MAPK signaling pathway)	4.717
Apoptosis	BCL2/adenovirus E1B 19kD interacting protein 3	3.490
Cytokine	Interleukin 8	3.479
Kinase	Eukaryotic translation initiation factor 2-alpha kinase 3	2.914
Transferase	Phosphatidylinositol glycan, class A	2.942
Others	Spindle pole body component 25 homolog (S. cerevisiae)	0.313
	Transmembrane protein 50B	3.451
	CDNA FLJ14162 fis, clone NT2RM4002504	2.696

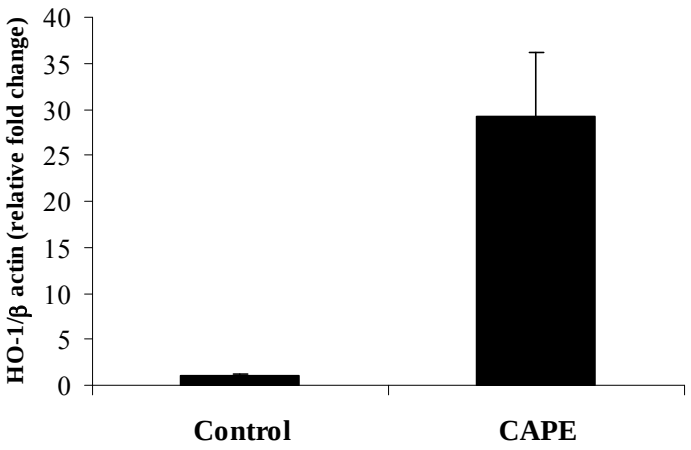

Figure 2.6: HO-1 mRNA induction by CAPE at 5 μg/ml for 6 hr in HUVEC by relative quantitative real-time RT-PCR. HO-1 expression was highly increased (29.24 fold) in CAPE group compared to DMSO control. Values are presented as means with standard deviations (n=3).

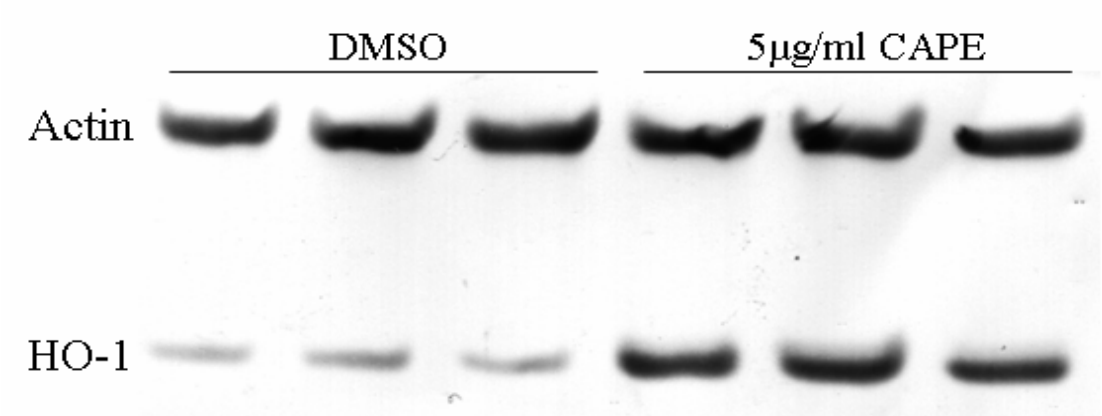

Figure 2.7: Effect of CAPE on HO-1 protein expression in HUVEC by western blotting. The induction of HO-1 protein was determined in HUVEC after incubating with 5 μg/ml CAPE and DMSO control for 24 hrs.

2.3.3 HO-1 Inhibitor SnPPIX Effects on CAPE Cytoprotection

To further elucidate the role of HO-1 induction in CAPE cytoprotection, HO-1 activity was suppressed by HO-1 enzyme competitive inhibitor SnPPIX. Coincubating with various non-toxic concentrations of SnPPIX and optimal cytoprotective dose of CAPE (5 μg/ml), the cytoprotective effect of CAPE against MD-induced cytotoxicity was abrogated in a concentration-dependent fashion (Figure 2.8). This result indicated that HO-1 induction may play an important role in CAPE cytoprotection.

2.3.4 The Effects of BV, BR, and CO

Heme degradation by HO-1 results in BV, BR, and CO production. All of them have been reported to ameliorate I/R induced injury in different organs *in vivo* [133, 169, 170]. The cytoprotective activities of BV, BR, and CO were examined in the HUVEC-MD model. BV and BR were reported as potent antioxidants against linoleic acid peroxyl radicals [171], which may contribute to the protective effect of HO-1. BR as low as 10 nM can protect cells against oxidative stress induced by 100 μM hydrogen peroxide, which seems to function through the conversion from BV to BR by the action of BV reductase [122]. Therefore, the cytoprotective effects of BV and BR ranging from 0.01 to 1 μM were tested, but no protection was observed compared to CAPE (Figure 2.9A and B), and these doses did not appear to be toxic alone in HUVEC (Figure 2.9C).

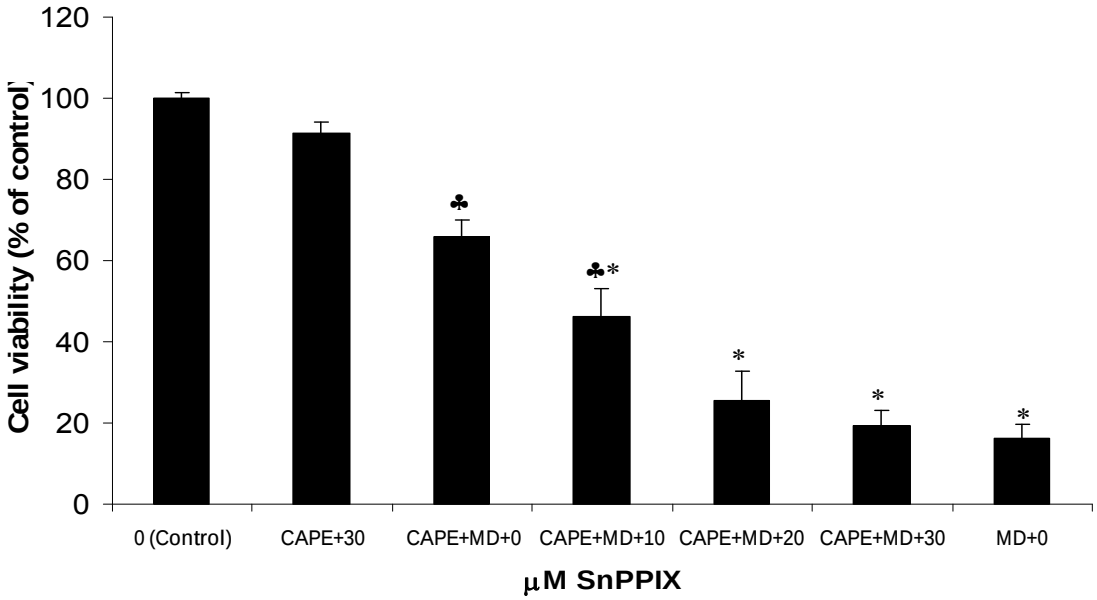

Figure 2.8: The effect of HO-1 inhibitor SnPPIX on CAPE cytoprotection against MD-mediated oxidative injury in HUVEC. Values are presented as means with standard deviations (n=3). SnPPIX exerted dose-dependent suppression on 5 μg/ml CAPE protection against 25 μM MD-induced oxidative injury. CAPE plus 30 μM SnPPIX alone was not toxic. *: $P<0.01$ versus CAPE + MD alone. ♣: $P<0.001$ versus MD alone.

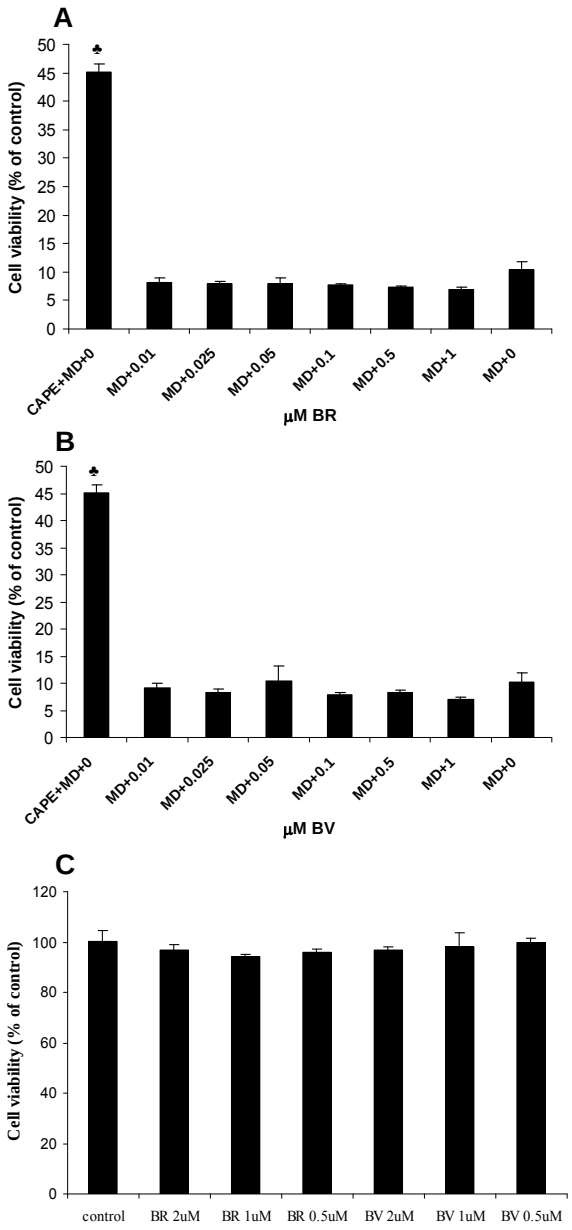

Figure 2.9: BR (A) and BV (B) cytoprotection testing compared to 5 µg/ml CAPE in HUVEC against oxidative stress induced by 30 µM MD. Values are presented as means with standard deviations (n=3). Neither BV nor BR from 0.01 µM to 1 µM showed cytoprotection. ♣: $P<0.01$ versus MD alone. BV or BR alone was not toxic up to 2 µM (C).

Brouard et al have shown that 1% CO treatment suppressed apoptosis and improved survivability of endothelial cells [172]. Mishra recently reported that CO provided cytoprotection in ischemic lungs by interrupting mitogen activated protein kinase expression of early growth response 1 genes and their downstream target genes [173]. To determine if CO could account for the cytoprotective effect of HO-1, HUVEC were exposed to various concentrations of MD in the presence or absence of 1% CO and cell viability was assessed by the Alamar Blue assay. HUVEC in the presence of CO showed better survivability at low doses of MD (5 – 10 μM) (Figure 2.10).

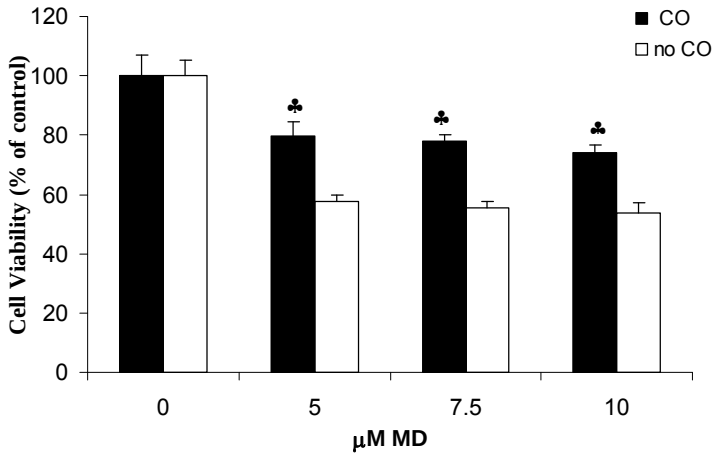

Figure 2.10: The cytoprotective effect of 1% CO against low doses of MD-induced oxidative damage in HUVEC. Values are represented as means with standard deviation (n=3). About 20% more cell viability was observed in 1% CO-treated HUVEC (black column) than control (white column). ♣: $P<0.01$ versus corresponding MD treatment without CO exposure.

The observation that 1% CO (10,000 ppm) only provided partial protection at low doses of MD challenge but not at higher doses (data not shown) plus the fact that no cytoprotective effect could be demonstrated for BR and BV suggests that further investigations to clarify the role of the products of heme oxygenase enzymatic activity are needed. One possibility is that delivering carbon monoxide to the environment in the gas phase rather than generating it intracellularly in the appropriate cellular compartment where HO-1 is located may explain the fact that complete cytoprotection was not obtained compared to CAPE. In addition, the amount of heme proteins in non-erythroid cells available as the substrate for HO-1 action, may limit the generation of heme catabolic products. Two recent studies have demonstrated that non-heme induction of HO-1 or overexpression of mutated HO-1 incapable of heme catalytic activity still provided protection against ROS-induced oxidative stress [174, 175]. Therefore CAPE may have as yet undetermined effects that have not yet to be defined.

2.4 CONCLUSIONS

An *in vitro* model simulating I/R-induced damage in endothelium was developed, where MD triggered oxidative stress in HUVEC and induced apoptosis. CAPE displayed cytoprotective ability in a dose-dependent manner increasing cell survivability up to 65% against MD toxicity at the optimal cytoprotective dose of 5 μg/ml. The alteration in HUVEC transcriptional activity especially the induction of HO-1 by CAPE provided information about the mechanism of cytoprotection. The loss of CAPE cytoprotection in the presence of HO-1 enzyme inhibitor SnPPIX indicated the important role of HO-1 induction in providing the beneficial effect of CAPE. The partial protection by CO, the end product of HO-1 action does not explain the direct effect in CAPE cytoprotection. Further investigations are required to clarify the role of HO-1 in cytoprotection.

Chapter III: Synthesis and Cytoprotective effects of Caffeic Acid Phenethyl Ester Fluorinated Derivatives in Oxidative Stressed Endothelial Cells

3.1 INTRODUCTION

The cytoprotective effect of caffeic acid phenethyl ester (CAPE) has been demonstrated in a model of oxidative stress produced by treatment of human endothelial cells with a cytotoxic dose of menadione (MD), and the induction of heme oxygenase-1 (HO-1) enzyme may play an important role in this cytoprotection (Chapter II). Understanding the chemical basis of CAPE in cytoprotection will further elucidate its mechanism of action and may improve cytoprotection with proper chemical modification of CAPE. This effort may eventually lead to better candidate drugs for ameliorating ischemia/reperfusion (I/R) injury.

In this chapter, the synthesis of six new fluorinated CAPE derivatives and their evaluation as cytoprotectants in the recently established HUVEC-MD model will be described. In addition to providing structure-activity information, these fluorinated CAPE derivatives may display altered metabolic liability, thereby extending their protection potency *in vivo*. Since the number of the hydroxyl groups within CAPE catechol moiety may also play an important role in antioxidant activity [176, 177], we also examined the effect of replacing one of these hydroxyl groups with a fluorine or hydrogen, or methylating one or both catechol hydroxyl groups, on the cytoprotective activity of the resulting analogs.

3.2 MATERIALS AND METHODS

3.2.1 Materials and Apparatus

Chemical reagents 6-fluoroveratraldehyde (**2d**), 3-fluoro-4-hydroxy-5-methoxybenzaldehyde (**2a**), 3-fluoro-4-methoxybenzaldehyde (**1**), boron tribromide, chloroacetyl chloride, phenethyl alcohol, and triphenylphosphine were purchased from Aldrich (Milwaukee, WI). Phenethyloxycarbonylmethyl-triphenyl-phosphonium chloride (**4**) was prepared from triphenylphosphine and chloroacetic acid phenethyl ester as described in the literature [148]. All solvents were of analytical grade and distilled prior to experiments. Thin-layer chromatography (TLC) was performed on precoated silica gel 60 F_{254} aluminum plates made from EM Science (Gibbstown, NJ). Flash chromatography was performed on silica gel column (230-400 mesh, 40-63 μm) from Fisher Scientific (Pittsburgh, PA).

Melting points were calculated following differential scanning calorimetry using TA Instruments Model 2920 (New Castle, DE) with a heating range of 10 °C /min and rounded to whole numbers. ^{1}H and ^{13}C NMR spectra were recorded on a Bruker AMX-500 or Varian Inova 500 nuclear magnetic resonance spectrometer, using CD_3OD or $CDCl_3$ as solvents. Chemical shifts are reported in ppm (δ) relative to tetramethylsilane (TMS) as internal standard for ^{1}H NMR and in ppm relative to the solvent for ^{13}C NMR. Elemental analyses were performed on a 2400 Perkin-Elmer Elemental Analyzer by Quantitative Technologies Inc (Whitehouse, NJ). Low-resolution MS data were obtained using Finnigan MAT TSQ700 (San Jose, CA). High-resolution MS data were acquired on Micromass ZABE (Manchester, England).

3.2.2 Synthesis of CAPE Derivatives

3.2.2.1 General procedure for demethylation

2-Fluoro-4,5-dihydroxy-benzaldehyde (2e). Compound **2d**, 2-fluoro-4,5-dimethoxybenzaldehyde (500 mg, 2.715 mmol), was dissolved in 12 ml of CH_2Cl_2 and cooled to –70 °C in a dry ice/acetone bath under argon. A 1 M solution of BBr_3 in CH_2Cl_2 (8.15 ml, 8.15 mmol) was added slowly with vigorous stirring. The reaction mixture was stirred overnight without further cooling. After 24 hrs, MeOH (10 ml) was added to the reaction mixture to quench excess BBr_3 and the solvent was evaporated. This process was repeated two additional times and the crude product **2e** was used in the next step without further purification.

3.2.2.2 General procedure for Wittig reaction

3-(2-Fluoro-4,5-dihydroxy-phenyl)-acrylic acid phenethyl ester (3e, CAPE-1). The crude 2-fluoro-4,5-dihydroxybenzaldehyde (**2e**) was dissolved in 7.5 ml of 1,4-dioxane. The phosphonium chloride **4** (1.7 g, 3.7 mmol), 7.5 ml $CHCl_3$, and $KHCO_3$ (815 mg, 8.15 mmol) were added. The reaction was heated under reflux in a 110 °C oil bath with vigorous stirring under argon for 18 hrs. The resulting mixture was filtered, washed with CH_2Cl_2, and concentrated on a rotary evaporator. Column chromatography (EtOAc/CH_2Cl_2 (2:3, v/v)) afforded 456 mg (55 % yield) of **3e** as a white solid: mp 157 ºC; TLC (Silica gel, EtOAc/CH_2Cl_2 (2:3, v/v)), R_f 0.45; ^{1}H NMR (CD_3OD) δ 2.97 (t, J = 7.0 Hz, 2H), 4.35 (t, J = 7.0 Hz, 2H), 6.26 (d, J = 16.0 Hz, 1H), 6.54 (d, J = 11.7 Hz, 1H),

6.97 (d, J = 7.2 Hz, 1H), 7.23 (m, 5H), 7.66 (d, J = 16.0 Hz, 1H); ^{13}C NMR (CD_3OD) δ 36.14, 66.22, 103.96 (d, J_{C-F} = 26.4 Hz), 113.82 (d, J_{C-F} = 12.9 Hz), 114.02 (d, J_{C-F} = 3.9 Hz), 116.98 (d, J_{C-F} =5.4 Hz), 127.52, 129.48, 129.95, 138.87 (d, J_{C-F} = 3.5 Hz), 139.35, 143.39, 150.79 (d, J_{C-F} = 11.9 Hz), 157.21 (d, J_{C-F} = 245.1 Hz), 168.90; CI-MS *m/z* 303 (MH^+, 100). HRCI-MS: Calcd for $C_{17}H_{15}FO_4$; 303.1033, Found 303.1023; Anal. Calcd for $C_{17}H_{15}FO_4$: C, 67.54; H, 5.00; F, 6.28. Found: C, 67.53; H, 4.97; F, 6.18.

3-(3-Fluoro-4-hydroxy-5-methoxy-phenyl)-acrylic acid phenethyl ester (3a, CAPE-3). The 3-fluoro-4-hydroxy-5-methoxy-benzaldehyde (**2a**, 200 mg, 1.18 mmol) was used directly in the Wittig reaction to afford 214 mg (57% yield) of compound **3a** as an off-white solid after column chromatography and recrystallization from EtOAc/hexane: mp 94 ºC; ^{1}H NMR ($CDCl_3$) δ 3.02 (t, J = 7.0 Hz, 2H), 3.94 (s, 3H), 4.42 (t, J = 7.0 Hz, 2H), 6.28 (d, J = 16.1 Hz, 1H), 6.83 (d, J = 1.6 Hz, 1H), 6.95 (dd, J = 10.8, 1.8 Hz, 1H), 7.28 (m, 5H), 7.53 (d, J = 16.1 Hz, 1H); ^{13}C NMR ($CDCl_3$) δ 35.23, 56.54, 65.03, 106.03, 109.54 (d, J_{C-F} = 19.2 Hz),117.07, 126.11 (d, J_{C-F} =7.8 Hz), 126.60, 128.55, 128.92, 135.38 (d, J_{C-F} = 13.9 Hz), 137.88, 143.86, 148.30 (d, J_{C-F} = 6.2 Hz), 150.55 (d, J_{C-F} = 242.6 Hz), 166.77; CI-MS *m/z* 317 (MH^+, 100). HRCI-MS: Calcd for $C_{18}H_{17}FO_4$; 317.1189. Found 317.1184; Anal. Calcd for $C_{18}H_{17}FO_4$: C, 68.35; H, 5.42; F, 6.01. Found: C, 68.24; H, 5.36; F, 5.98.

3-(3-Fluoro-4,5-dihydroxy-phenyl)-acrylic acid phenethyl ester (3b, CAPE-2). Demethylation of 3-fluoro-4-hydroxy-5-methoxy-benzaldehyde (**2a**, 200 mg, 1.18 mmol) with BBr_3 (3 ml, 3 mmol) afforded crude 3-fluoro-4,5-dihydroxy-benzaldehyde (**2b**) which was used in the subsequent Wittig reaction with **4** to give 307 mg (86 % yield) of **3b** as an off-white solid after column chromatography and recrystallization

from EtOAc/CH_2Cl_2: mp 135 ºC; ^{1}H NMR (CD_3OD) δ 2.98 (t, J = 7.0 Hz, 2H), 4.36 (t, J = 7.0 Hz, 2H), 6.25 (d, J = 15.9 Hz, 1H), 6.83 (t, J = 1.5 Hz, 1H), 6.85 (d, J = 2.0 Hz, 1H), 6.87 (d, J = 2.0 Hz, 1H), 7.24 (m, 5H), 7.45 (d, J = 15.9 Hz, 1H); ^{13}C NMR (CD_3OD) δ 36.18, 66.22, 108.36 (d, J_{C-F} = 19.8 Hz), 111.84, 116.75, 126.62 (d, J_{C-F} =8.9 Hz), 127.55, 129.51, 129.97, 137.36, 139.41, 145.92, 148.84 (d, J_{C-F} = 5.9 Hz), 153.43 (d, J_{C-F} = 238.1 Hz), 168.76; CI-MS *m/z* 303 (MH^+, 100). HRCI-MS: Calcd for $C_{17}H_{15}FO_4$; 303.1033, Found 303.1030; Anal. Calcd for $C_{17}H_{15}FO_4$+1/4H_2O: C, 66.55; H, 5.09. Found: C, 66.76; H, 4.84.

3-(3-Fluoro-4-hydroxy-phenyl)-acrylic acid phenethyl ester (3c, CPAE-5). Demethylation of 3-fluoro-4-methoxy-benzaldehyde (**1**, 200 mg, 1.30 mmol) with BBr_3 (3.3 ml, 3.3 mmol) afforded crude 3-fluoro-4-hydroxy-benzaldehyde (**2c**) which was used in the subsequent Wittig reaction with **4** to give 290.6 mg (78 % yield) of compound **3c** as an off-white solid after column chromatography and recrystallization from EtOAc/hexane: mp 80 ºC; ^{1}H NMR ($CDCl_3$) δ 3.01 (t, J = 7.1 Hz, 2H), 4.42 (t, J = 7.1 Hz, 2H), 6.27 (d, J = 16.0 Hz, 1H), 6.98 (s, 1H), 7.00 (s, 1H), 7.01 (s, 1H), 7.26 (m, 5H), 7.55 (d, J = 15.9 Hz, 1H); ^{13}C NMR ($CDCl_3$) δ 35.22, (40.48), 65.10, 114.72 (d, J_{C-F} = 18.5 Hz), 116.83, 117.71, 125.57 (d, J_{C-F} =3.1 Hz), 126.60, 127.67 (d, J_{C-F} = 6.3 Hz), 128.54, 128.94, 137.87, 143.66, 145.79 (d, J_{C-F} = 14.7 Hz), 151.16 (d, J_{C-F} = 238.9 Hz), 167.04; CI-MS *m/z* 287 (MH^+, 100). HRCI-MS: Calcd for $C_{17}H_{15}FO_3$; 287.1083, Found 287.1089; Anal. Calcd for $C_{17}H_{15}FO_3$+1/4H_2O: C, 70.21; H, 5.37; F, 6.53. Found: C, 70.02; H, 5.27; F, 6.50.

3-(2-Fluoro-4,5-dimethoxy-phenyl)-acrylic acid phenethyl ester (3d, CAPE-6). This compound was a co-product from the above reaction leading to compound **3f**. It

was isolated as 69 mg (6 % yield) of an off-white solid after repeated column chromatography and recrystallization from CH_2Cl_2/hexane: mp 86 ºC; ^{1}H NMR ($CDCl_3$) δ (ppm): 3.02 (t, J = 7.1 Hz, 2H), 3.88 (s, 3H), 3.89 (s, 3H), 4.43 (t, J = 7.1 Hz, 2H), 6.36 (d, J = 16.1 Hz, 1H), 6.64 (d, J = 11.6 Hz, 1H), 6.94 (d, J = 6.8 Hz, 1H), 7.26 (m, 5H), 7.78 (d, J = 16.1 Hz, 1H); ^{13}C NMR ($CDCl_3$) δ (ppm): 35.24, 56.28, 56.40, 64.99, 100.15 (d, J_{C-F} = 28.0 Hz), 109.42 (d, J_{C-F} = 4.5 Hz), 113.46 (d, J_{C-F} = 12.7 Hz), 117.64 (d, J_{C-F} = 6.0 Hz), 126.57, 128.53, 128.94, 137.17 (d, J_{C-F} = 3.0 Hz), 137.92, 145.65 (d, J_{C-F} = 2.5 Hz), 152.01 (d, J_{C-F} = 10.2 Hz), 156.51 (d, J_{C-F} = 248.8 Hz), 166.95; CI-MS *m/z* 331 (MH^+, 100). HRCI-MS: Calcd for $C_{19}H_{19}FO_4$; 331.1346. Found 331.1354; Anal. Calcd for $C_{19}H_{19}FO_4$+1/4H_2O: C, 68.15; H, 5.87. Found: C, 68.47; H, 5.70.

3-(2-Fluoro-4–methoxy-5-hydroxyphenyl)-acrylic acid phenethyl ester (3f, CAPE-4). Partial demethylation of 2-fluoro-4,5-dimethoxy-benzaldehyde (**2d**, 600 mg, 3.26 mmol) was carried out with one equivalent of boron tribromide (3.26 ml, 3.26 mmol) to give crude monomethyl-2-fluoro-4,5-dihydroxybenzaldehyde (**2f**) as a mixture of 4- and 5-methyl isomers containing some un-reacted **2d**. This mixture was used directly in the subsequent Wittig reaction with **4** to afford 42 mg (4 % yield) of compound **3f** as of off-white solid after repeated column chromatography and recrystallization from CH_2Cl_2/hexanes: ^{1}H NMR ($CDCl_3$) δ 3.01 (t, J = 7.1 Hz, 2H), 3.89 (s, 3H), 4.41 (t, J = 7.1 Hz, 2H), 6.33 (d, J = 16.1 Hz, 1H), 6.61 (d, J = 11.3 Hz, 1H), 7.05 (d, J = 7.1 Hz, 1H), 7.26 (m, 5H), 7.74 (d, J = 16.1 Hz, 1H); ^{13}C NMR ($CDCl_3$) δ 35.23, 56.30, 65.02, 99.45 (d, J_{C-F} = 28.5 Hz), 112.38 (d, J_{C-F} = 4.0 Hz), 114.52 (d, J_{C-F} = 13.2 Hz), 118.02 (d, J_{C-F} =6.2 Hz), 126.56, 128.52, 128.96, 137.04 (d, J_{C-F} = 3.1 Hz), 137.93, 142.00 (d, J_{C-F} = 2.5 Hz), 149.01 (d, J_{C-F} = 10.2 Hz), 155.76 (d, J_{C-F} = 247.8 Hz), 167.01;

CI-MS *m/z* 317 (MH^+, 100). HRCI-MS: Calcd for $C_{18}H_{17}FO_4$; 317.1189. Found 317.1198; Anal. Calcd for $C_{18}H_{17}FO_4$: C, 68.35; H, 5.42. Found: C, 68.04; H, 5.22. The structural assignment for **3f** is based on the appearance of the 2-fluorocatechol 4-position carbon resonance ($J^3_{C\text{-}F}$ = 10 Hz) at 149 ppm, which is further downfield than expected for the 5-methyl isomer (*c.a.* 140 ppm).

3.2.3 Cell Culture

HUVEC were cultured the same way as described in Chapter II.

3.2.4 Cell Viability (Alamar Blue Assay)

Stock solutions of MD (0.5 M in PBS) or CAPE analogues (1000x in DMSO) were diluted in culture medium and added to plate wells at final concentrations of 10–40 μM for MD and 5-15 μg/ml for CAPE derivatives, respectively. Cell viability was assessed at 24 hours after initiation of treatment versus vehicle (PBS or DMSO) controls using Alamar Blue™. Detailed experimental information was described in Chapter II.

3.2.5 *In Vitro* Cytoprotection Assay

Confluent HUVEC were pretreated with CAPE and its derivatives for 6 hrs. Cytotoxic dose of MD was then added to the HUVEC in the presence of testing CAPE

analogues and DMSO as vehicle control. After 24 hrs incubation, cell viability was measured using the Alamar Blue assay.

3.2.6 Statistical Analysis

Data were represented as the mean ± standard deviation. Differences among the groups were analyzed using the one-way analysis of variance combined with Tukey (equal variances assumed) or Games-Howell (equal variances not assumed) test. A difference of $p < 0.05$ was considered significant for all statistical analyses.

3.3 RESULTS AND DISCUSSION

3.3.1 Synthesis

A Wittig coupling approach was taken to elaborate a number of fluorinated analogues of CAPE (Table 3.1). The required fluorinated benzaldehydes (**2a-f**) were either commercially available, or easily prepared through demethylation of commercially available aldehydes with boron tribromide (Figure 3.1). The demethylated aldehydes were applied directly in the subsequent Wittig reaction employing the phenethyloxycarbonylmethyl-triphenyl-phosphonium chloride **4**, which was prepared as described in the literature [148]. As shown in Figure 3.1 and Table 3.1, the preparation of the fluorinated CAPE derivatives is relatively straightforward due to the commercial availability of a number of fluorinated methoxybenzaldehydes, which can be easily

demethylated and immediately subjected to Wittig coupling. The methylated CAPE derivatives derived from direct Wittig coupling of these aldehydes were also prepared.

In case of 2-fluoro-4,5-dimethoxybenzaldehyde (**2d**), demethylation with one equivalent of boron tribromide afforded a mixture of 4- and 5-monomethylated aldehydes along with some remaining 4,5-dimethylated starting material. This mixture was used directly in the Wittig reaction to give a low yield of the monomethylated CAPE derivative CAPE-4, along with a small amount of the 2-fluoro-dimethyl CAPE analogue CAPE-6. The remaining fluorinated CAPE analogues were isolated in good yield after column chromatography and recrystallization. All of the isolated CAPE analogues were characterized by ^{1}H and ^{13}C NMR and low- and high-resolution mass spectrometry. Typical ^{1}H NMR, ^{13}C NMR, and mass spectrometry spectral data in the case of CAPE-1 are presented in Figure 3.2 – 3.5. All CAPE derivatives gave satisfactory elemental analyses. In agreement with the results reported by others [148], the *(E)*/*(Z)* ratio of the CAPE analogues prepared in this way were generally >9:1, as judged by ^{1}H NMR.

Two series of CAPE analogues were prepared, those bearing a fluorine at the 3-position of the caffeic acid catechol ring (CAPE-2, 3, and 5) and those with fluorine at the 2-position (CAPE-1, 4, and 6). In addition to variation in the position of fluorination, analogues were prepared in which one (CAPE-3 and 4) or both (CAPE-6) of the hydroxyl groups of the catechol functionality of CAPE were methylated. We also examined an analogue in which one of the catechol hydroxyl groups was replaced with fluorine (CAPE-5).

Table 3.1: Synthesis of fluorinated CAPE analogues.

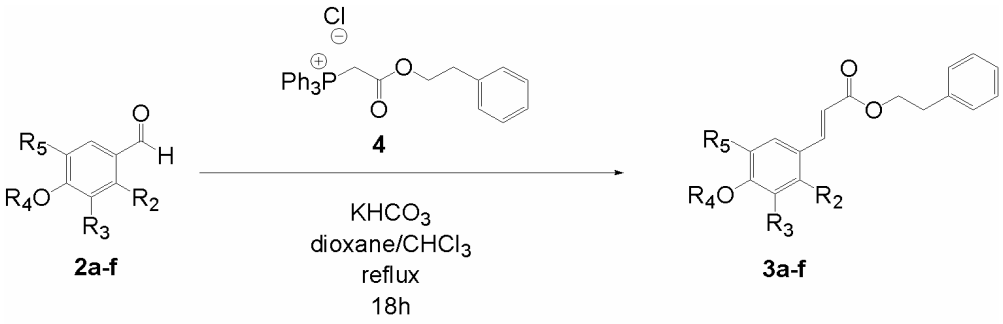

Compound	R_2 =	R_3 =	R_4 =	R_5 =	Yield
a	H	OMe	H	F	57%
b	H	OH	H	F	86%
c	H	H	H	F	78%
d	F	H	Me	OMe	6%[a]
e	F	H	H	OH	55%
f	F	H	Me	OH	4%[a]

[a.] Low yields are due to compound losses during repeated chromatography required to separate **3d** and **3f** from the reaction product of crude **2f**, which contained some of the fully methylated **2d**.

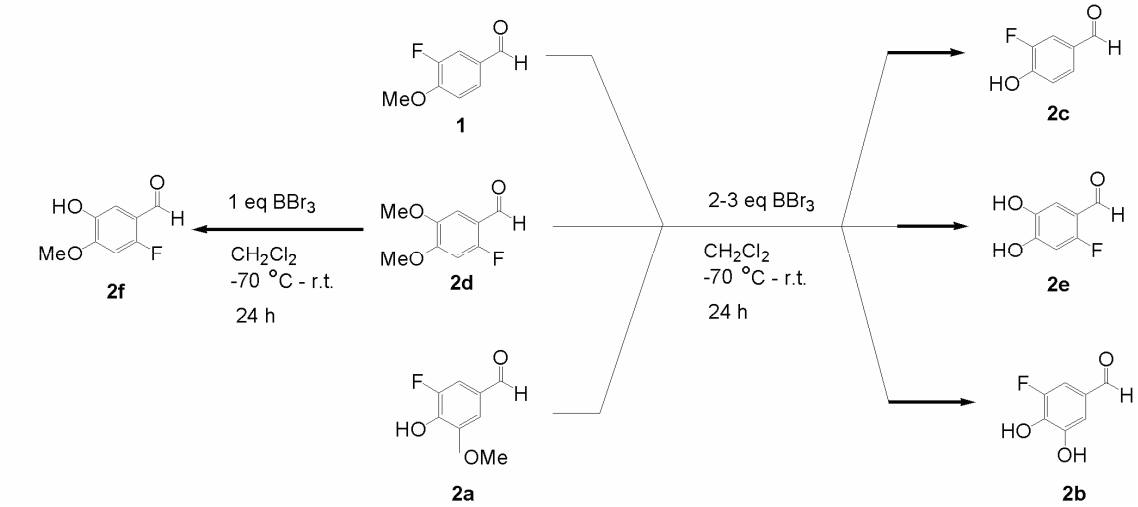

Figure 3.1: Synthesis of fluorinated benzaldehydes.

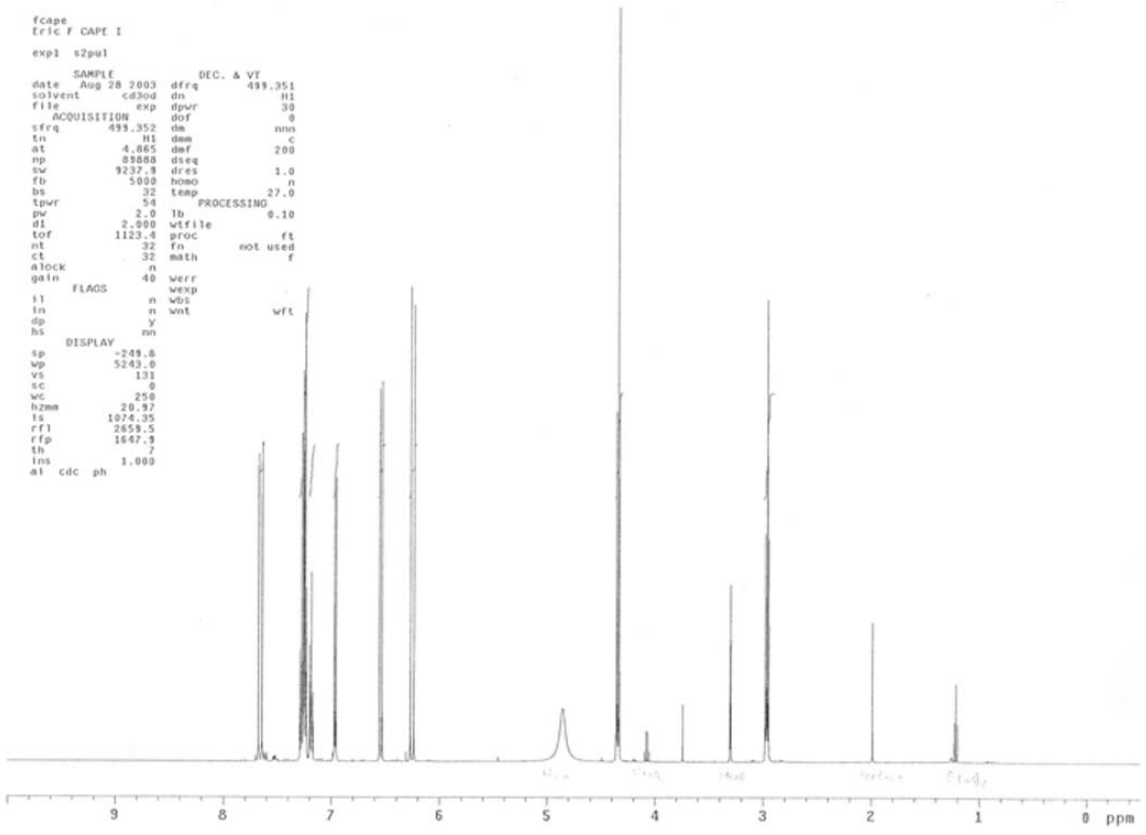

Figure 3.2: Typical ^{1}H NMR spectra of CAPE-1.

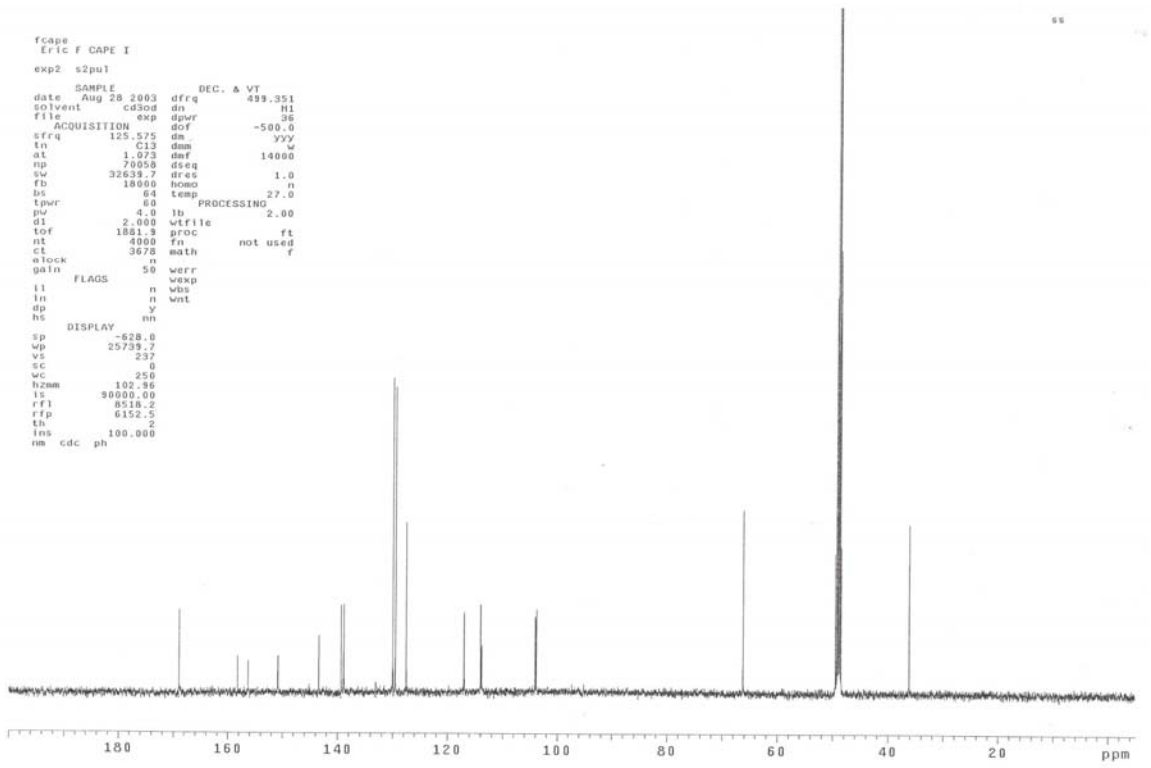

Figure 3.3: Typical ^{13}C NMR spectra of CAPE-1.

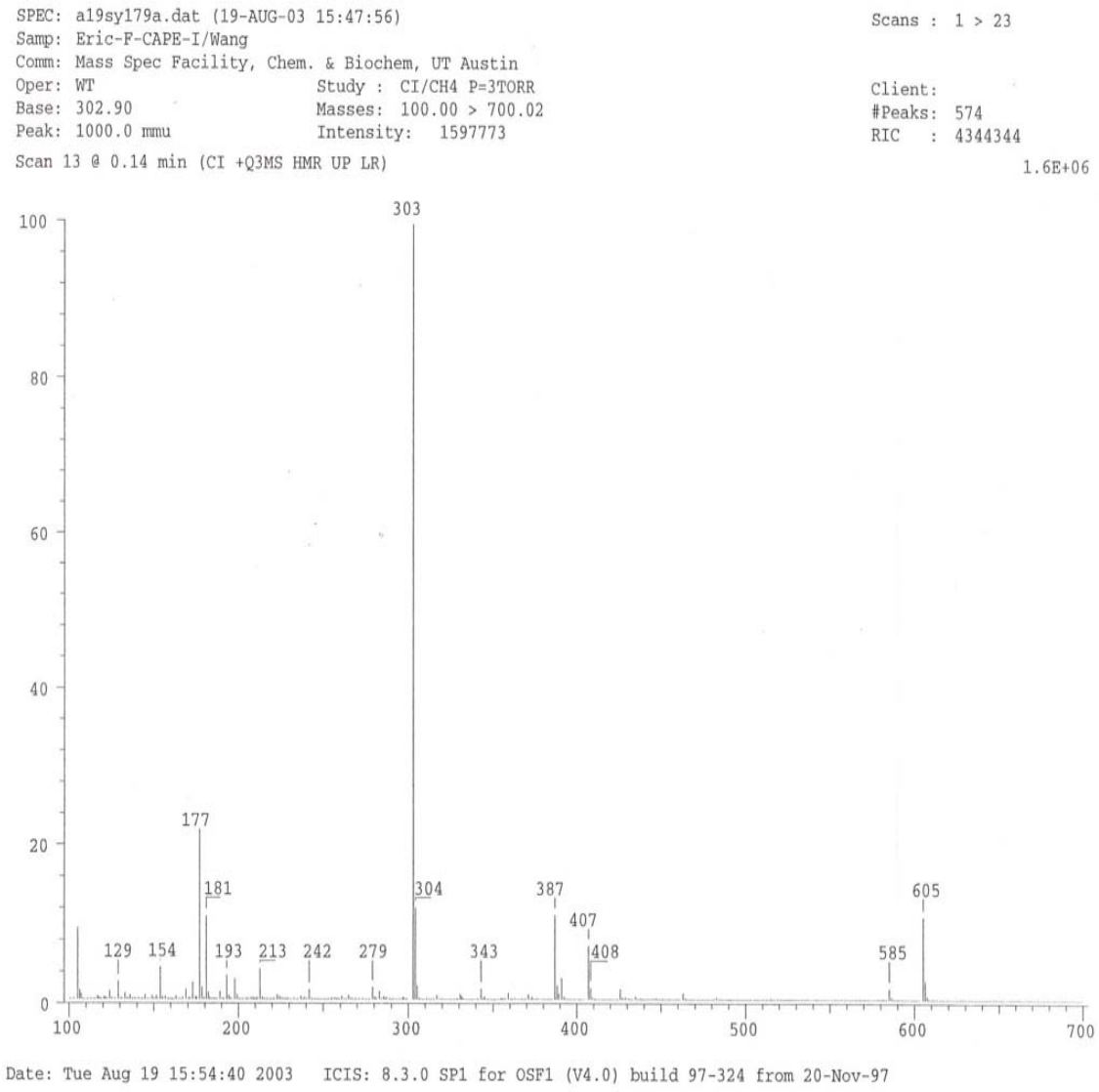

Figure 3.4: Typical low-resolution mass spectrometry spectra of CAPE-1.

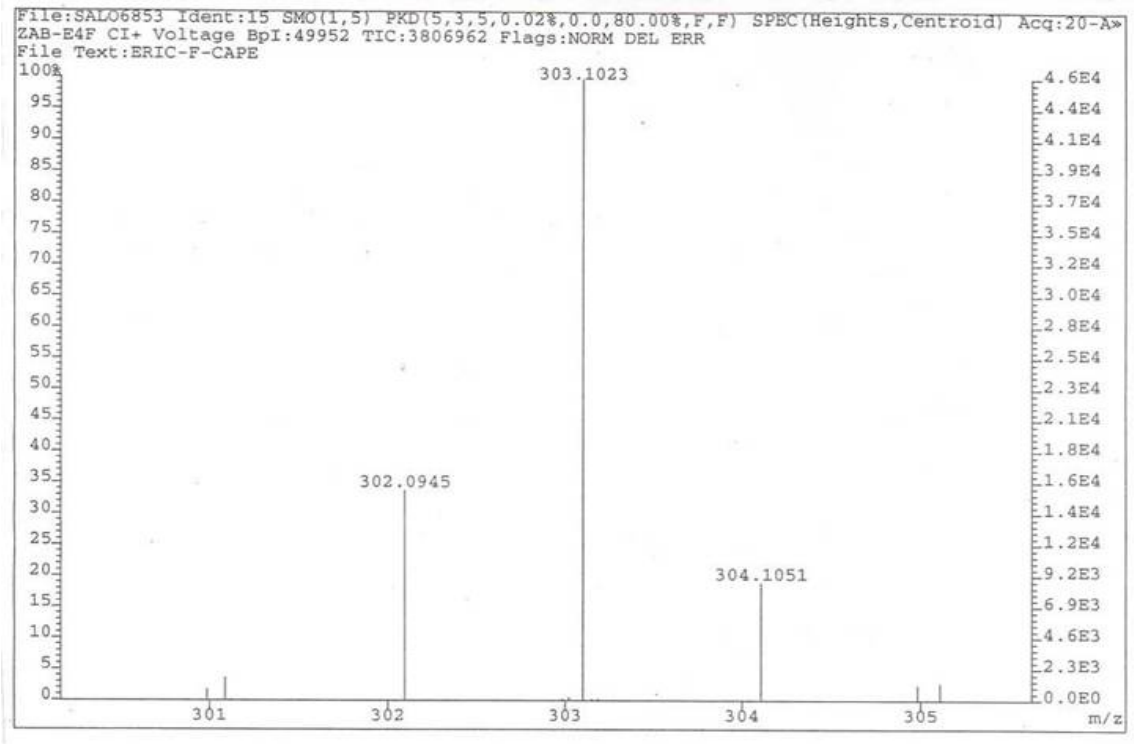

Figure 3.5: Typical high-resolution mass spectrometry spectra of CAPE-1.

3.3.2 Cytotoxicity of Fluorinated CAPE Analogues Compared to CAPE

CAPE and the fluorinated CAPE analogues were initially assayed for cytotoxic effects in HUVEC at the concentrations used in the cytoprotection studies. HUVEC were incubated in the presence of these compounds at 5, 10, and 15 μg/ml for 24 hrs, and the extent of cell viability was determined versus vehicle-treated control cells using the Alamar Blue assay. Cell viability less than 90% of control was considered toxic. The results, shown in Figure 3.6, demonstrate that, compared to CAPE, CAPE-1, 2, 3, and 4 were also toxic at the highest concentration examined (15 μg/ml), while the analogues CAPE-5 and 6 showed no toxicity at any tested concentrations. The data suggest that the cytotoxicity of these CAPE analogs towards HUVEC is not correlated with the position of the fluorine substitution. The 2-fluoroCAPE derivative CAPE-1 and the 3-fluoroCAPE derivative CAPE-2 are cytotoxic at >10 μg/ml, as is CAPE itself. In contrast, derivatives that lack CAPE's catechol functionality, such as the 2-fluoro-4,5-dimethyl analog CAPE-6 and the fluorophenol CAPE-5 are less cytotoxic than CAPE at the highest concentrations examined. It was found that CAPE-2 was less cytotoxic at 10 μg/ml than at 5 and 15 μg/ml. The origin of this phenomenon is not known; however, such non-monotonic dose-responses have been reported for other compounds [178, 179].

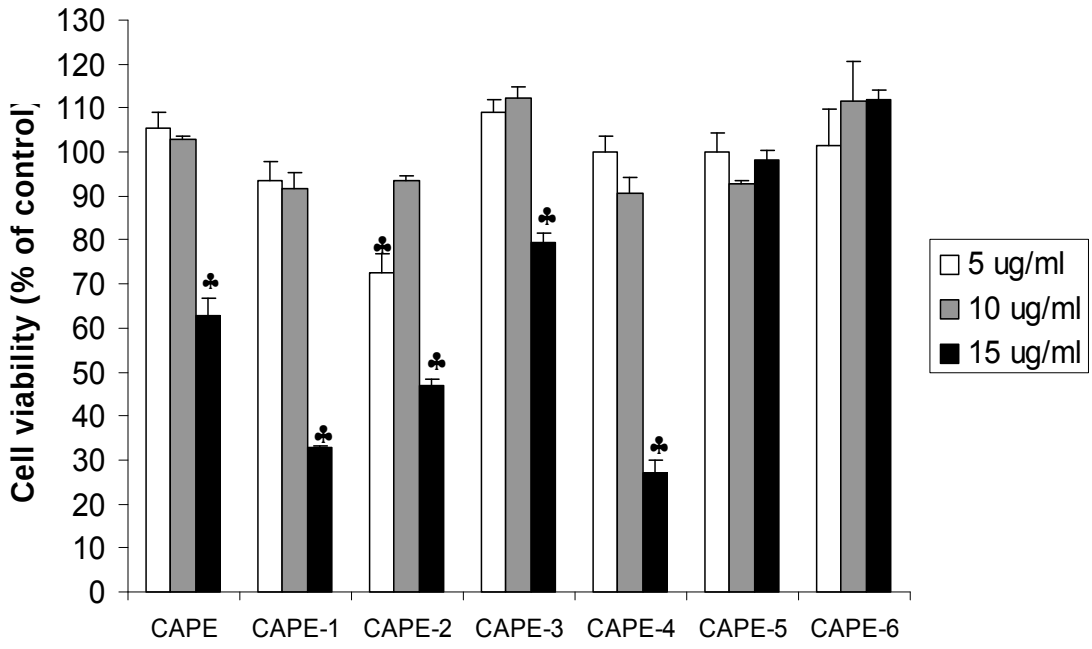

Figure 3.6: The cytotoxicity of CAPE and its derivatives toward HUVEC. HUVEC cells were incubated with CAPE at the indicated concentrations for 24 hrs and the number of viable cells was determined by Alamar Blue assay. Values are reported as mean (n = 3) percent of untreated control with error bars showing the standard deviation. Asterisks indicate significant cytotoxicity relative to no treatment ($P < 0.05$).

3.3.3 Cytoprotection of Fluorinated CAPE Derivatives against Menadione-Induced Oxidative Stress Compared to CAPE

MD treatment of HUVEC for 24 hrs resulted in a concentration-dependent decrease in cell viability as measured by the Alamar Blue assay (Figure 3.7). The lowest dose of menadione that reduced cell viability to about 10 % of untreated cells (e.g., 30 μM) was employed for the cytoprotection assays of CAPE and its analogues. Almost all CAPE derivatives showed dose-dependent cytoprotection against MD-mediated cytotoxicity in HUVEC to some extent except CAPE-2. The dose-dependent cytoprotection profiles for all of the CAPE derivatives are shown in Figure 3.8. Compared to CAPE, CAPE analogues CAPE-3, 4, 5, and 6, demonstrated cytoprotective effects even at the highest concentrations, 10 or 15 μg/ml, while CAPE-1 only showed cytoprotection at 5 μg/ml. Within the same passage of HUVEC, the cytoprotection of CAPE and its derivatives at their maximal cytoprotective dose were compared as shown in Figure 3.9.

The cytoprotection data demonstrated that the position of fluorine substitution on the CAPE catechol ring can have a significant effect on the ability of these derivatives to protect against MD-mediated oxidative stress. The presence of a fluorine at the 2-position of the catechol ring (CAPE-1) results in cytoprotection at a similar level to that of CAPE. In contrast, the presence of a fluorine at 3-position (CAPE-2) completely abolishes cytoprotective activity. The catechol functionality of CAPE and related antioxidants has been reported to be involved in cytoprotection through metal ion chelation [88]. In our studies, fluorinated CAPE derivatives in which the catechol functionality of CAPE is methylated or replaced with a phenol also display cytoprotection. Both 2- and 3-fluoromonomethyl CAPE derivatives CAPE-3 and 4, respectively, retain cytoprotective

activity, although the maximal cytoprotection by these analogs is less than that by CAPE. Interestingly, the 2-fluorodimethyl CAPE derivative CAPE-6 and 3-fluoro-4-hydroxy CAPE analogue CAPE-5 are also both cytoprotective, and these analogues, which are not cytotoxic at higher concentrations, do not show the diminution in cytoprotection at higher concentrations observed for CAPE.

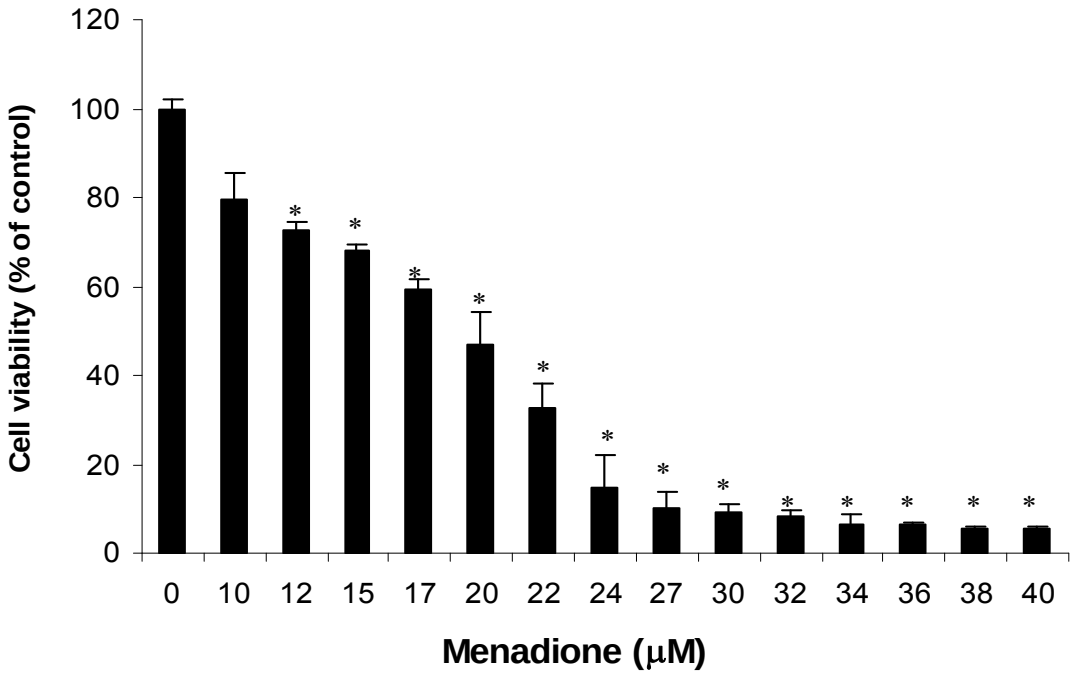

Figure 3.7: MD shows dose-dependent cytotoxicity in HUVEC. HUVEC were incubated with MD for 24 hrs at the indicated concentrations and the number of viable cells was determined by Alamar Blue assay. Values are reported as mean (n = 3) percent of untreated control with error bars showing the standard deviation. The lowest dose of MD causing 90 % loss in cell viability (e.g., 30 μM) was employed in the cytoprotection assays. Asterisks indicate significant cytotoxicity relative to no treatment ($P < 0.05$).

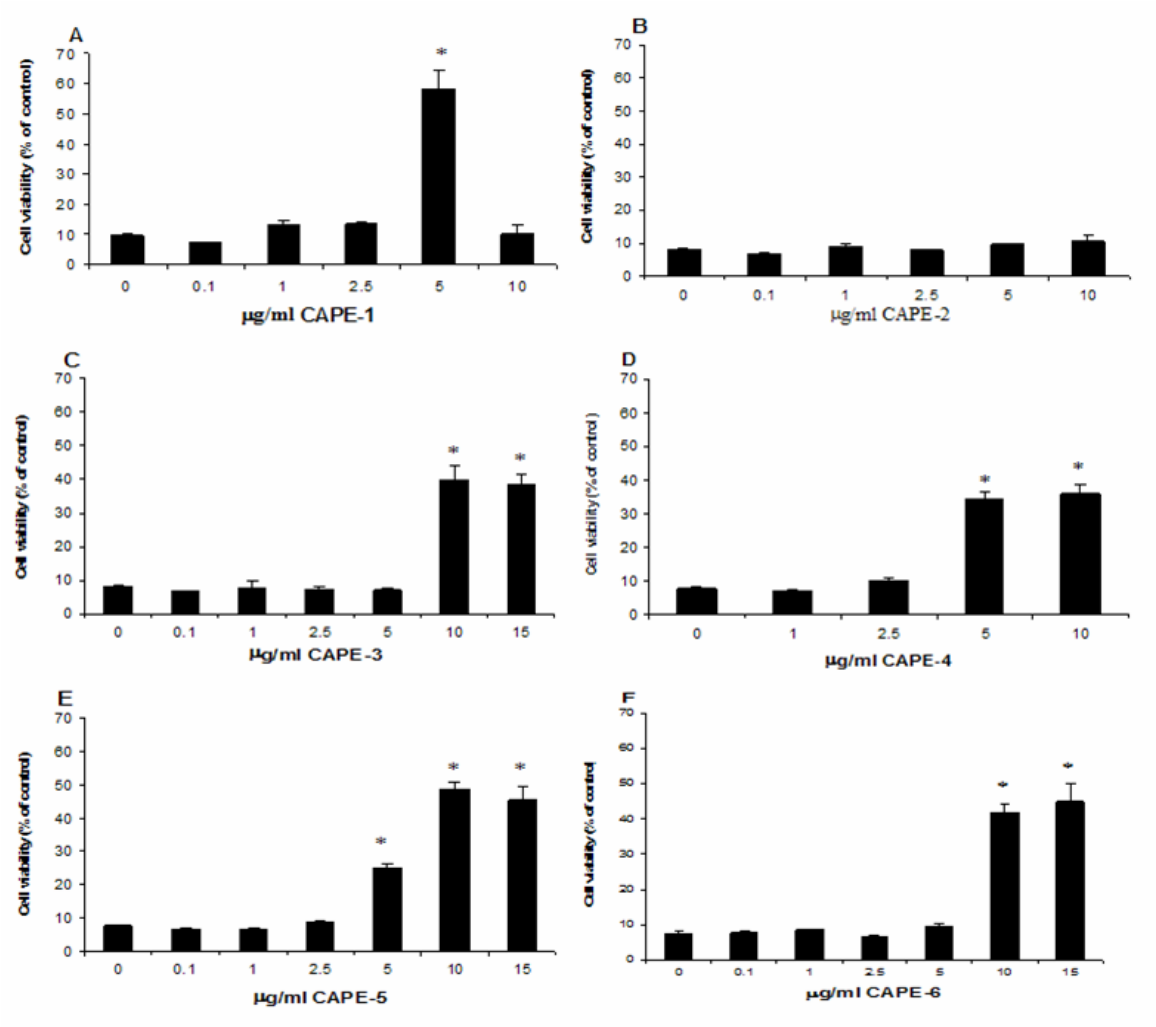

Figure 3.8: Dose-dependent cytoprotection by CAPE derivatives. HUVEC were incubated with CAPE analogs for 6 hrs at the indicated concentrations prior to MD treatment. Values are reported as mean (n = 3) percent of untreated control with error bars showing the standard deviation. Asterisks indicate significant protective effects against MD-caused injury relative to no pretreatment ($P < 0.05$).

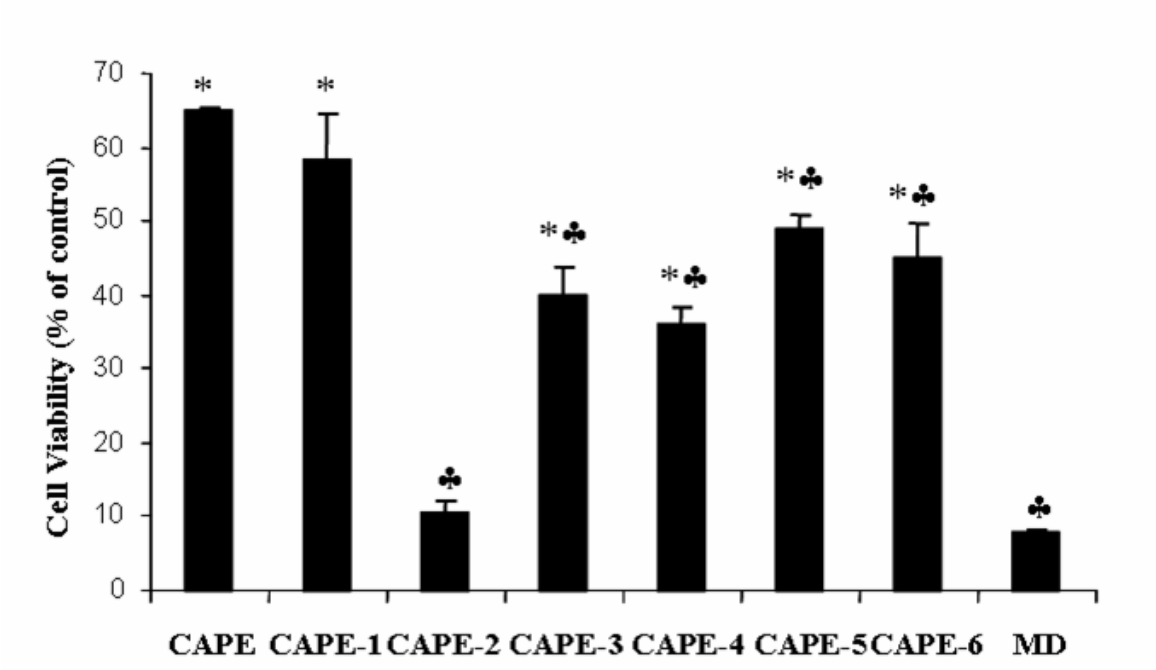

Figure 3.9: Comparison of CAPE and CAPE analogs maximal cytoprotection against MD-induced oxidative stress. CAPE: 5 µg/ml; CAPE-1: 5 µg/ml; CAPE-2: 10 µg/ml; CAPE-3: 10 µg/ml; CAPE-4: 10 µg/ml; CAPE-5: 10 µg/ml; CAPE-6: 15 µg/ml. Values are reported as mean (n = 3) percent of untreated control with error bars showing the standard deviation. Asterisks indicate significant protective effects against MD-caused injury relative to no pretreatment ($P < 0.05$). Clover signs indicate significant difference relative to CAPE pre-treated cells ($P < 0.05$).

3.4 CONCLUSIONS

Six new catechol-ring fluorinated CAPE derivatives were synthesized using the Wittig reaction and characterized to meet criteria of purity. Their cytoprotection profiles were established in the HUVEC-MD model. The results demonstrated that most of the fluorinated CAPE analogues examined were as cytoprotective as CAPE in a dose-dependent manner. CAPE-1 displayed the best cytoprotective effect among the derivatives, and was not significantly different from CAPE. CAPE-3 to 6 all protected HUVEC from MD-induced oxidative injury to some extent. CAPE-5 and 6 extended the beneficial effects to higher dose of 15 μg/ml without exhibiting cytotoxicity. CAPE-2, however, showed no cytoprotection at the doses tested. The cytoprotection data described here provides some insight into the structural basis for CAPE cytoprotection. Further exploration of the mechanism responsible for cytoprotective effects of CAPE and its derivatives is warranted.

Chapter IV: Mechanism Investigation of Cytoprotection of Caffeic Acid Phenethyl Ester and Fluorinated Derivatives: Effects on Heme Oxygenase-1 Induction and Antioxidant Activities

4.1 INTRODUCTION

To study caffeic acid phenethyl ester (CAPE) structure and cytoprotective relationships, six catechol ring-fluorinated CAPE derivatives were synthesized and evaluated for their cytoprotective effects in the human umbilical vein endothelial cells (HUVEC)-menadione (MD) model which simulates ischemia/reperfusion injury *in vitro* (Chapter II and III). Gene expression analysis data showed CAPE induced the cytoprotective gene heme oxygenase-1 (HO-1), which may play an important role in CAPE cytoprotection. That this is the case was suggested by the application of HO-1 inhibitor SnPPIX. To further elucidate the structural effects on the protective mechanism of CAPE, the effect of HO-1 elevation on the cytoprotection of CAPE analogues was examined.

However, antioxidant activity has also been proposed to account for the beneficial effects of polyphenolic compounds such as CAPE, curcumin, and resveratrol in I/R induced oxidative damage [37, 180, 181]. To investigate whether CAPE cytoprotection is due to a transcription-mediated event or pure structure-related antioxidant activity, it was necessary to evaluate the free radical scavenging abilities of CAPE and derivatives in HUVEC cells, which was achieved by measuring the intracellular ROS production using a fluorescent probe 5-(and-6)-chlormethyl-2',7'-dichlorodihydrofluorescein diacetate (CM-H_2DCFDA) [182].

In this chapter, the hypothesis was tested that the cytoprotective effect of CAPE and derivatives on MD-induced oxidative injury in HUVEC is mediated through transcriptional activity, mainly the induction of HO-1, rather than their direct antioxidant function.

4.2 MATERIALS AND METHODS

4.2.1 Chemicals and Reagents

Caffeic acid and 1 M 4-(2-hydroxyethyl)-1-piperazineethanesulfoic acid (HEPES) buffer were obtained from Sigma-Aldrich (Saint Louis, MO). Methyl Caffeate (MC) and phenethyl dimethyl caffeate (PEDMC) were from LKT Laboratories (St. Paul, MN). CM-H_2DCFDA and 10× Hanks' balanced salt solution (no sodium bicarbonate and phenol red) were obtained from Invitrogen (Eugene, OR). Cells-to-cDNA kit was from Ambion (Austin, TX).

4.2.2 Synthesis of Catechol Ring-Fluorinated CAPE Derivatives

The chemical structures of the Fluorinated CAPE analogues examined in this study were reported in Figure 4.1. These compounds were synthesized according to a general procedure described previously (Chapter III).

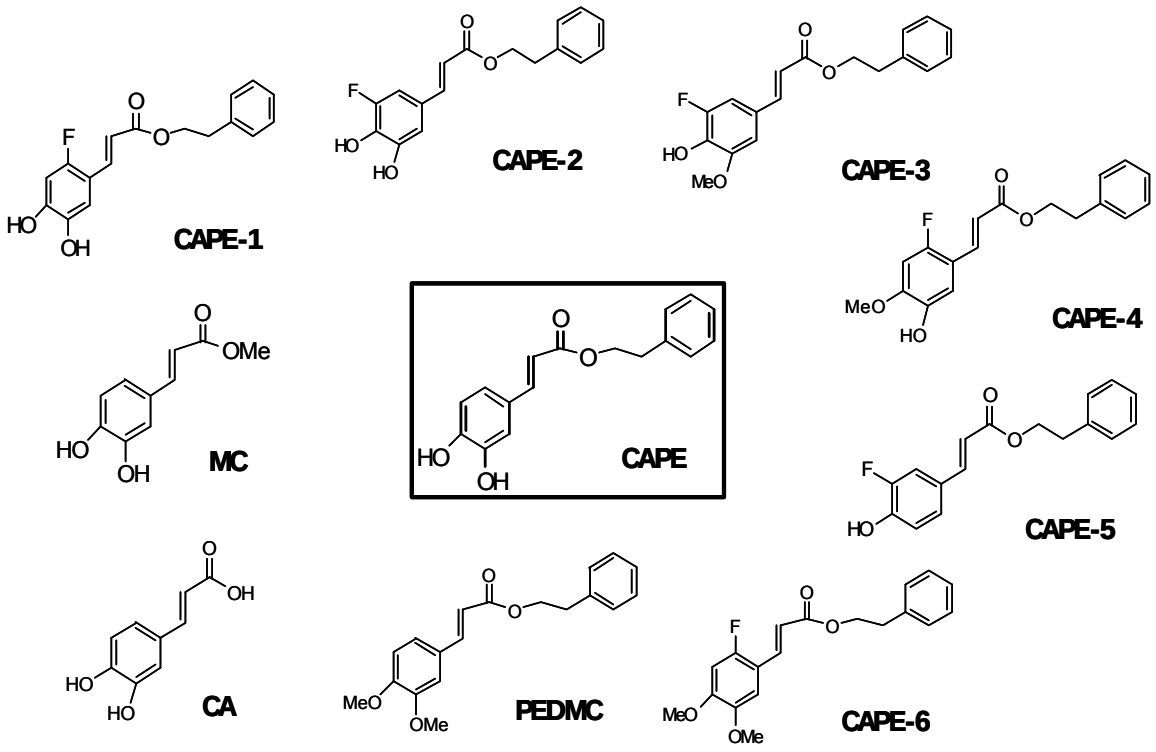

Figure 4.1: Chemical structures of CAPE and derivatives.

4.2.3 Cell Culture

HUVEC were cultured according to experimental section in Chapter II.

4.2.4 Cell Viability and Toxicity Assay

Cell viability was measured in HUVEC using Alamar Blue assay kit (Chapter II). MD was used to induce oxidative injury in HUVEC as previously described (Chapter II).

4.2.5 Cell Protection Assay

CAPE and its derivatives were dissolved in DMSO to 20 mM and diluted 1000-fold with medium before assay. Confluent HUVEC in 48-well plates were initially pretreated with CAPE and its analogues at same concentrations of 20 μM for 6 hrs, and the cytotoxic dose of MD was then administered to the HUVEC in the presence of testing compounds. After 24-hr incubation, cell viability was measured using the Alamar Blue assay.

4.2.6 Determination of Endothelial HO-1 mRNA Levels by Real-time RT-PCR

HUVEC were grown in 48-well plates until confluence and pretreated with 20 μM CAPE and its derivatives for 6 hrs. cDNA was obtained by reverse transcription from cells directly without RNA isolation using the Cells-to cDNA™ II kit according to the manufacturer's instruction (Ambion Inc., Austin, TX). Real-time PCR was performed on

a LightCycler™ thermal cycler (Idaho Technology, Salt Lake City, UT) with Roche LightCycler® TaqMan Master for HO-1 and 18S (Roche Diagnostics, Indianapolis, IN). HO-1 and 18S primer sets were from TaqMan® Gene Expression Assays (Applied Biosystems, Foster City, CA). HO-1 gene was normalized to the expression level of 18S gene for each sample. Relative quantification was acquired by comparative C_T method.

4.2.7 Western Blotting

Detailed experimental procedures were described in Chapter II.

4.2.8 HO-1 Inhibition with SnPPIX

Confluent HUVEC were pretreated with CAPE and its fluorinated derivatives at 20 μM in the presence of different doses of HO-1 inhibitor SnPPIX, respectively, for 6 hrs before exposing to a toxic dose of MD for additional 24 hrs. SnPPIX was dissolved in 0.1 M NaOH and diluted 1000-fold with medium. Cell viability was measured using the Alamar Blue assay.

4.2.9 Cell-Based Antioxidant Assay

Intracellular ROS production while HUVEC were exposed to 20 μM CAPE and derivatives was measured with the fluorescent probe CM-H_2DCFDA [182]. In brief, HUVEC were seeded onto 96-well plates and grown till confluence. The working buffer was prepared by diluting 10× Hanks' balanced salt solution (without sodium bicarbonate

or phenol red; Invitrogen) and 10 mM HEPES buffer in sterile water to make 1× Hanks' HEPES. HUVEC were rinsed twice with prewarmed working buffer, and incubated for 30min at 37 °C in the incubator with DCFDA (8 μM) premixed in the working buffer. HUVEC were then washed twice with prewarmed working buffer and loaded with the testing compounds dissolved in the working buffer. The fluorescence released from the cells was recorded immediately at 480 nm (excitation) and 520 nm (emission) using SpectraMAX® M2 microplate reader at different time intervals over a 2 hr period while the HUVEC were incubated at 37 °C within the plate reader. The fluorescent signals were normalized to the initial readings at time zero. The relative fluorescence was proportional to the ROS production.

4.2.10 Statistical Analysis

Data are presented as mean plus standard deviation. Differences between or among the groups were analyzed using the independent samples T test or one-way analysis of variance combined with Tukey (equal variances assumed) or Games-Howell (equal variances not assumed) test through SPSS statistical software. A difference of p value < 0.05 was considered significant.

4.3 RESULTS AND DISCUSSION

4.3.1 Cytoprotective Comparison of CAPE and Fluorinated Derivatives against Oxidative Stress in HUVEC

To further elucidate the molecular mechanisms of CAPE cytoprotection, we first compared the cytoprotective effects of CAPE and fluorinated derivatives against MD toxicity at the same molar amount. The cytotoxic effect of MD was evaluated in HUVEC and a dose of 22.5 μM was selected and applied in the cytoprotection assay (Figure 4.2). CAPE and fluorinated analogues at 20 μM ameliorated MD-induced oxidative injury in HUVEC to different levels (Figure 4.3). Among all fluorinated derivatives, CAPE-1 showed maximal cytoprotection resulting in about 60% more cell viability compared to MD-treated HUVEC which was not significantly different than that of CAPE itself. CAPE-4 and CAPE-5 exhibited similar protective effects which recovered about 45% more cells from MD toxicity. CAPE-3 protected HUVEC to a relatively low level and about 20% more cells survived from oxidative injury. CAPE-2 and CAPE-6 didn't increase the cell survival significantly compared to MD control at the dose tested. The concentration of CAPE-6 at 20 μM is equal to 6.6 μg/ml, which may not reach its cytoprotective dose yet (10 μg/ml). The cytoprotection results of CAPE analogues are consistent with chapter III.

4.3.2 HO-1 mRNA and Protein Expression in HUVEC by CAPE Fluorinated Derivatives

We examined whether HO-1 up-regulation is also involved in the beneficial effects of CAPE analogues. HUVEC with same batch and passage number as those for the cytoprotection assay were employed to determine HO-1 mRNA levels after 6-hr pretreatment with 20 μM CAPE and analogues. Almost all CAPE fluorinated analogues activated high level of HO-1 mRNA expression compared to the DMSO control except CAPE-6 (Figure 4.4). The cytoprotection correlated well with HO-1 activation for most CAPE derivatives. CAPE, CAPE-1, 3, 4, and 5 showed both cytoprotection and HO-1 mRNA induction (> 15 fold). CAPE-6 neither protected HUVEC nor increased HO-1 expression to the level induced by other analogues. Only CAPE-2 activated HO-1 transcription but did not ameliorate MD-caused oxidative damage in HUVEC. Considering that there may be a nonlinear relationship between HO-1 transcript and protein level, it was necessary to check the HO-1 protein level induced by CAPE-2. Interestingly, the western blot data showed CAPE-2 did not induce HO-1 protein product as CAPE did at 6 hrs (Figure 4.5). A Similar induction of mRNA without a corresponding translation into protein product has been observed in other polyphenols such as resveratrol [183].

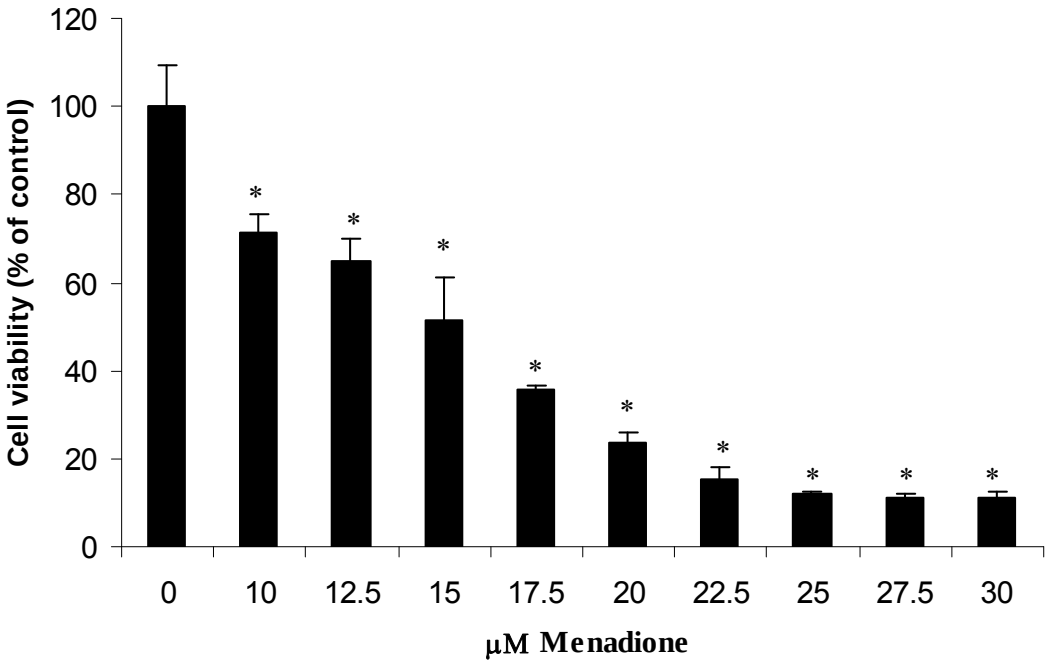

Figure 4.2: Cytotoxicity of MD in HUVEC. Values are represented as means plus standard deviation (n=3). MD caused reduction of HUVEC viability in a dose-dependent manner. The dose of MD at 22.5 μM was used in the cytoprotection assay of CAPE and derivatives. ∗: $P<0.05$ versus control (MD at 0 μM).

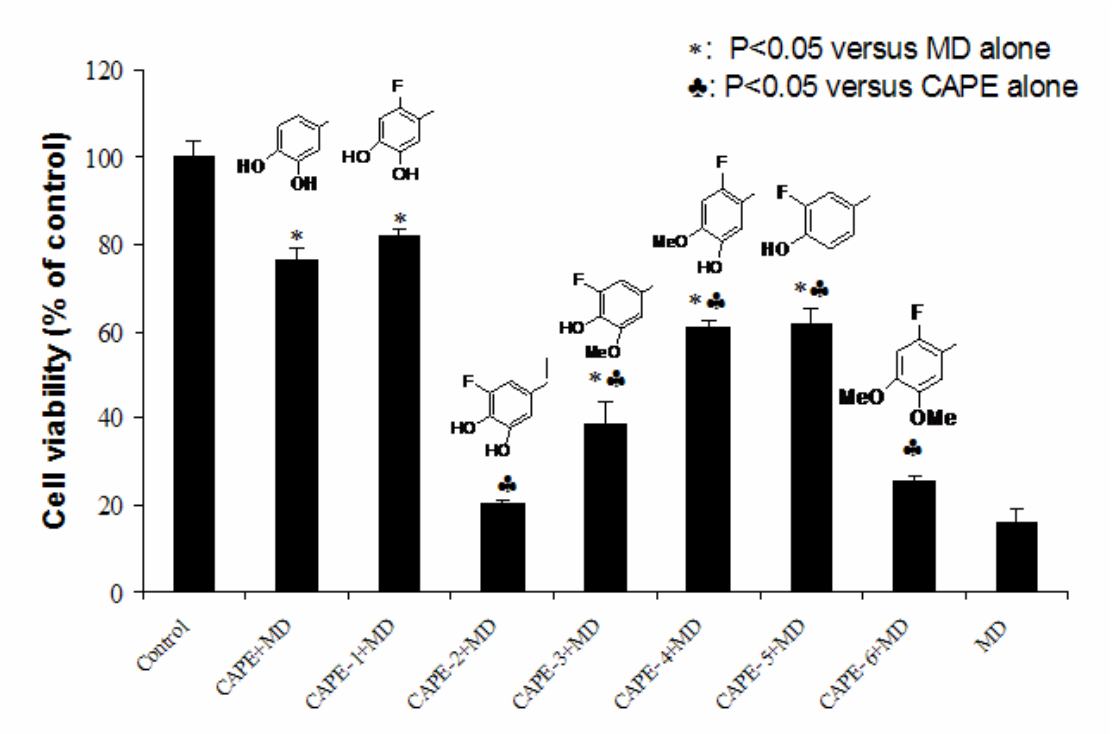

Figure 4.3: CAPE and its fluorinated analogs' cytoprotection against MD-induced injury in HUVEC. Values are represented as means plus standard deviation (n=3). Pretreatment of HUVEC with CAPE and six synthesized derivatives at 20 μM showed different cytoprotective effects against 22.5 μM MD-caused oxidative injury. CAPE-1 exhibited the best cytoprotection among analogues, which was similar to that of CAPE. CAPE-3, 4, and 5 ameliorated MD-resulted oxidative stress in HUVEC to some extent, while CAPE-2 and 6 didn't protect HUVEC at the dose examined.

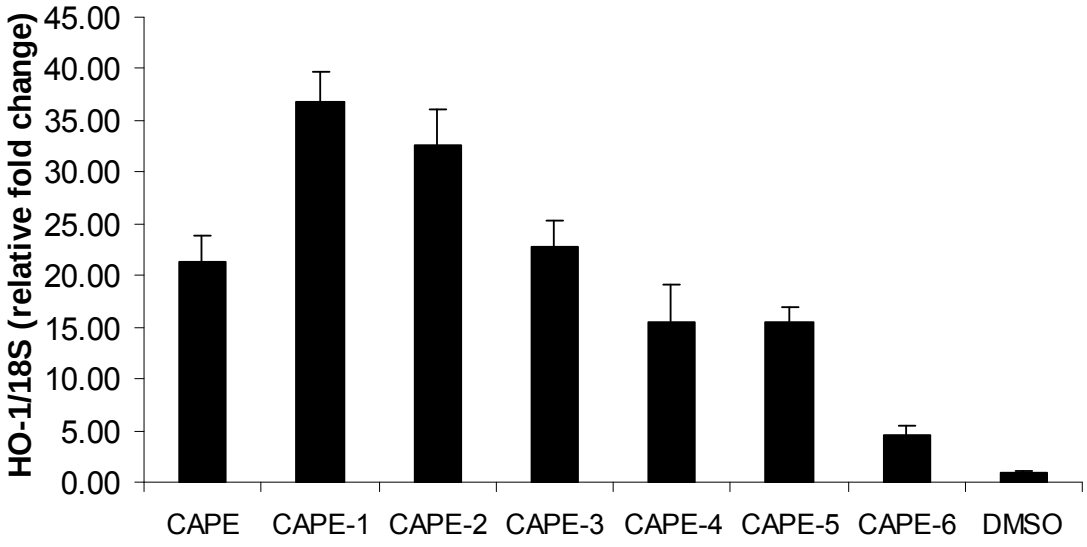

Figure 4.4: HO-1 mRNA induction by CAPE and fluorinated derivatives in HUVEC through RT-PCR. Values were represented as means plus standard deviations (n=4). After 6 hr incubation, CAPE and most analogues highly elevated HO-1 gene expression more than 15 fold compared to DMSO control except CAPE-6.

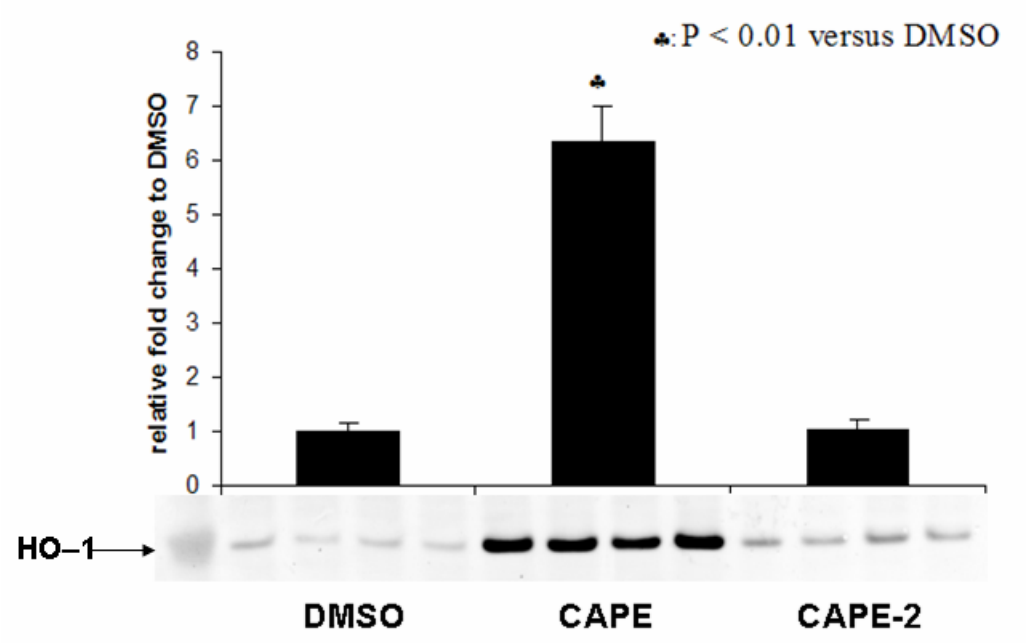

Figure 4.5: HO-1 protein expression in HUVEC by CAPE and CAPE-2. CAPE at 20 μM induced HO-1 protein production about 6 fold compared to DMSO control in 24 hrs, while same amount of CAPE-2 didn't significantly elevate the expression of HO-1 protein.

4.3.3 Effects of HO-1 Inhibitor on Cytoprotection of CAPE Fluorinated Analogues against MD-Induced Oxidative Injury in HUVEC

The application of the HO-1 inhibitor SnPPIX suggested that HO-1 was involved in the beneficial effects of those cytoprotective derivatives of CAPE. Different concentrations of SnPPIX were coincubated in HUVEC with CAPE and its cytoprotective analogues (CAPE-1, 3, 4, and 5) at 20 μM. SnPPIX suppressed the cytoprotection of most CAPE derivatives against MD in a dose-dependent manner except CAPE-1, where CAPE-1 cytoprotection was completely abolished compared to MD-treated cells at any dose applied (Figure 4.6). These data further indicated that HO-1 induction and enzymatic activity played a major role in the cytoprotection mechanisms of CAPE and fluorinated derivatives.

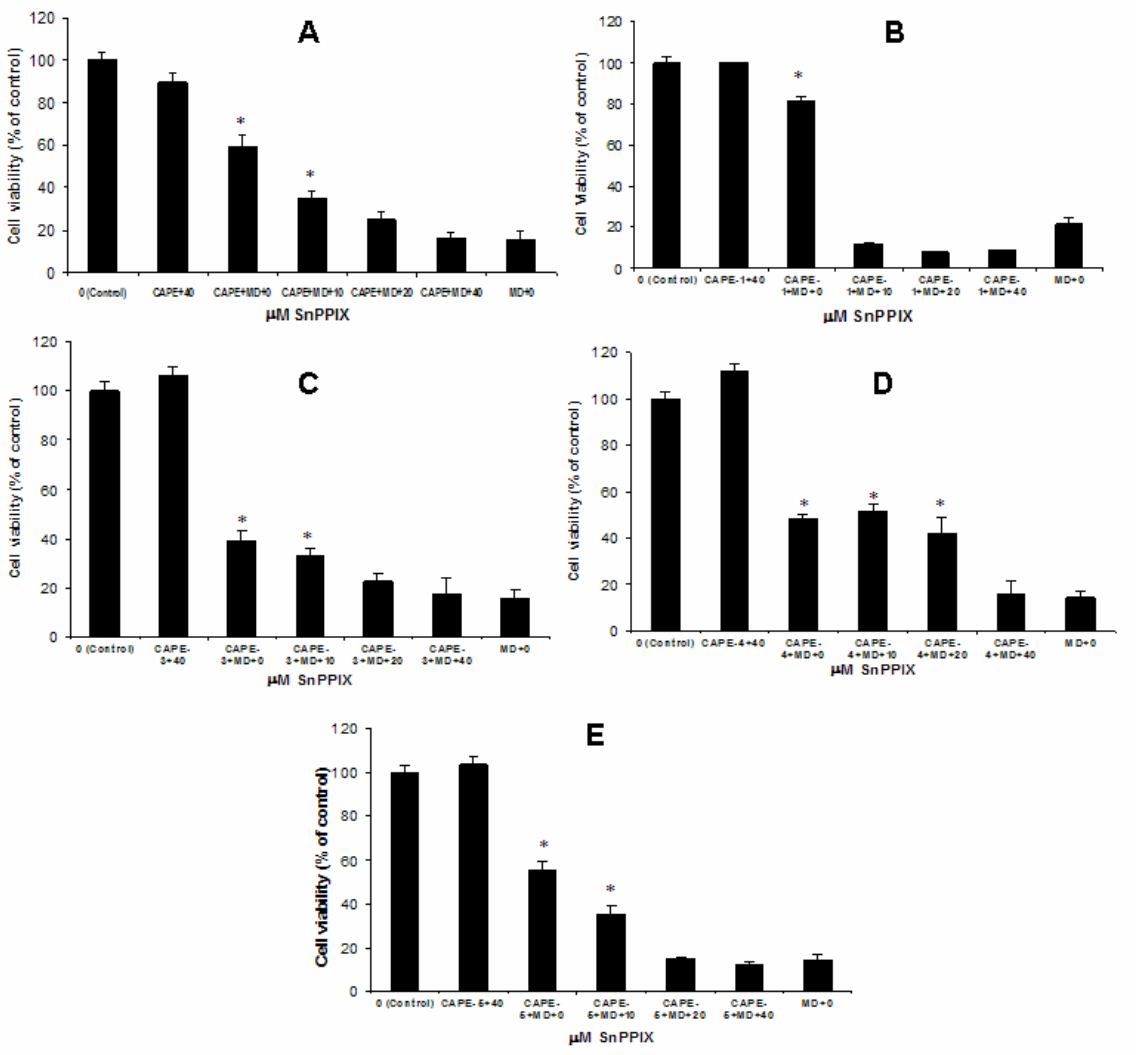

Figure 4.6: The effect of HO-1 inhibitor SnPPIX on CAPE and its cytoprotective derivatives at 20 µM against MD-mediated oxidative injury in HUVEC. Values are represented as means plus standard deviation (n=3). SnPPIX suppressed the cytoprotective effects of CAPE (A) and its analogues 3 (C), 4 (D), and 5 (E) in a dose-dependent manner against 22.5 µM MD-induced oxidative injury, while it completely removed CAPE-1 (B) cytoprotection even at 10 µM. The incubation of CAPE derivatives plus 40 µM SnPPIX alone with HUVEC was not toxic. ∗: $P < 0.01$ versus 22.5µM MD alone.

4.3.4 Antioxidant Activity Comparison of CAPE and Derivatives in HUVEC by Determining the Intracellular ROS Production

Structurally-related antioxidant activity has long been proposed as the major beneficial effect of polyphenols. To elucidate the effects of antioxidant properties of CAPE and analogues on their potential cytoprotection, we evaluated their free radical scavenging abilities in HUVEC through measuring the cellular ROS level with a fluorescent probe CM-H_2DCFDA. The results showed that HUVEC treated with 20 μM CAPE, CAPE-1, and 2 generated ROS less fluorescence than DMSO control, indicating that corresponding ROS production was significantly less at 2 hrs time point compared to DMSO control. This represented a dampening of endogenous ROS generation that normally occurs during metabolism. Interestingly, CAPE-3 and 4 with only one hydroxyl group on the aromatic ring resulting from mono-methylation and CAPE-5 with hydrogen replacement behaved as pro-oxidants in cell culture that produced greater fluorescence than DMSO control. CAPE-6 didn't change the trend of ROS formation in HUVEC (Figure 4.7). By reference to the cytoprotection data of CAPE fluorinated analogues, maintaining cell-based antioxidant activity didn't correlate to cytoprotection of human endothelial cells against the detrimental effects of MD. CAPE-2 maintained antioxidant activity without being cytoprotective, while CAPE-3, 4, and 5 exhibiting pro-oxidant activity were also cytoprotective. CA, a potential CAPE metabolite, MC and PEDMC, commercially available CAPE derivatives, were also tested for antioxidant activities in HUVEC. CA and MC showed similar antioxidant effect compared to CAPE, while PEDMC didn't change much of ROS production compared to DMSO control as CAPE-6 did (Figure 4.7). None of these analogues showed any beneficial effects against MD-caused damage and they didn't elevate much HO-1 mRNA either compare to CAPE at 20

μM (Figure 4.8). The lack of cytoprotection for CA and MC implies the minor role of chemical antioxidant activity in cytoprotection, and the loss of HO-1 induction by those compounds indicates the important role of HO-1 activation indirectly.

The cytoprotection, HO-1 induction, and intracellular ROS scavenging data of CAPE analogues have provided some insights into their structure-activity relationships. In the case of CAPE-6 and PEDMC, the blockage of both hydroxyl groups of CAPE catechol ring by methylation hindered the transcriptional activation of HO-1 gene expression and caused loss of cytoprotection, which was not influenced by the presence of 2-fluorine introduction. The only one hydroxyl methylation of CAPE (CAPE-3 and 4) provided some cytoprotection and elevated HO-1 mRNA as well, where the incorporation of fluorine at different position caused small difference in activities. The presence of only one hydroxyl group accompanied with an ortho-fluorine as CAPE-5 also showed beneficial effect correlated with HO-1 induction. The maintenance of the catechol ring of CAPE was not required for cytoprotection. The phenethyl ester group was a prerequisite feature in CAPE structure necessary to up-regulate HO-1 and provided protection since the replacement by H group for CA or methyl ester for MC abolished both HO-1 induction and cytoprotection of CAPE. The introduction of fluorine at different position of the CAPE catechol ring, however, altered cytoprotection. 2-fluoro-CAPE (CAPE-1) showed maximal cytoprotection among other analogs, while 3-fluoro-CAPE (CAPE-2) didn't protect HUVEC against oxidative damage by MD. Although CAPE-2 also induce HO-1 mRNA expression, the lack of HO-1 protein product supported the correlation between cytoprotection and HO-1 induction for CAPE derivatives. The cell-based antioxidant assay indicates the maintenance of 3, 4-dihydroxyl groups on the aromatic ring ensures the antioxidant function of CAPE and analogues, the total methylation of those groups abolishes their ROS scavenging ability, and the presence of one hydroxyl

group and fluorine on the catechol ring induced more ROS production. However, their free radical scavenging behavior didn't correlate with cytoprotection in the HUVEC-MD model.

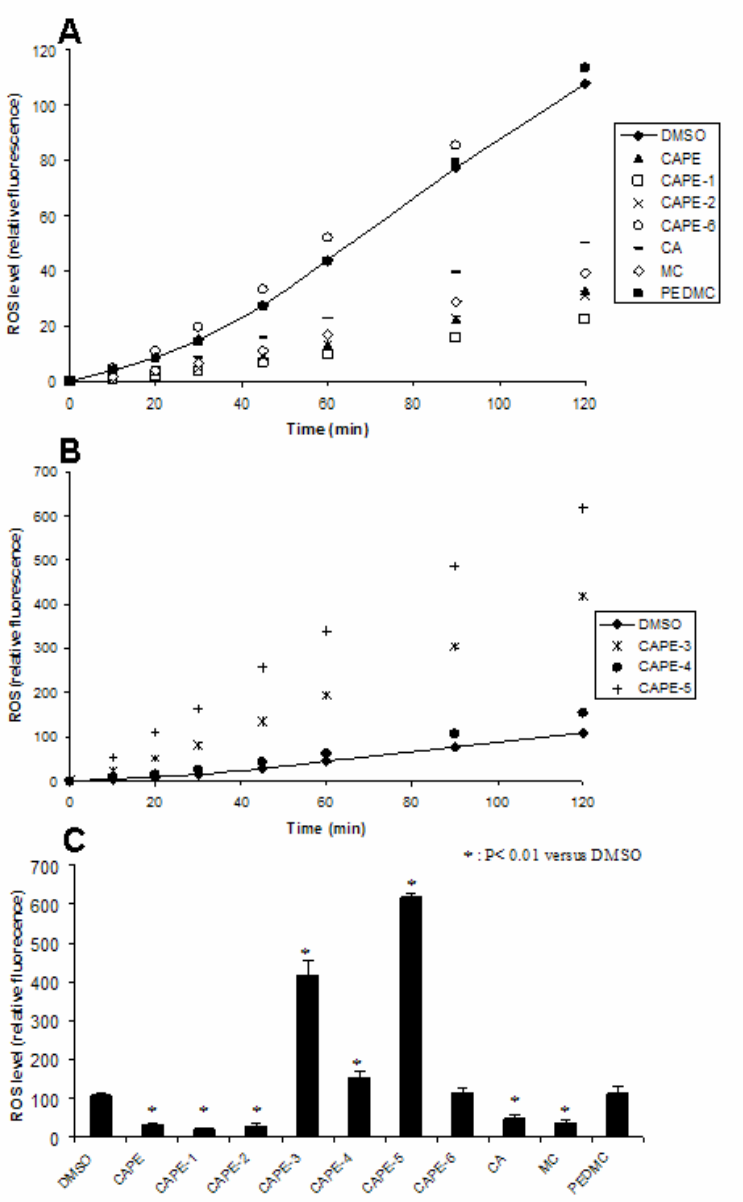

Figure 4.7: Direct antioxidant activities of CAPE and analogs in HUVEC demonstrated by measuring the alteration of intracellular ROS level. The ROS level of DMSO control was represented as a smooth line connecting all the data points (A and B). ROS level after the treatment of CA, MC, CAPE, CAPE-1, and CAPE-2 was decreased compared to that of control in a time-dependent manner, while the incubation of CAPE-6 and PEDMC generated similar ROS level as DMSO (A). The treatment of CAPE-3, 4, and 5 increased ROS level to different extent instead (B). The different ROS level at 2 hrs was shown in panel C, which reflected the antioxidant abilities of CAPE and analogs.

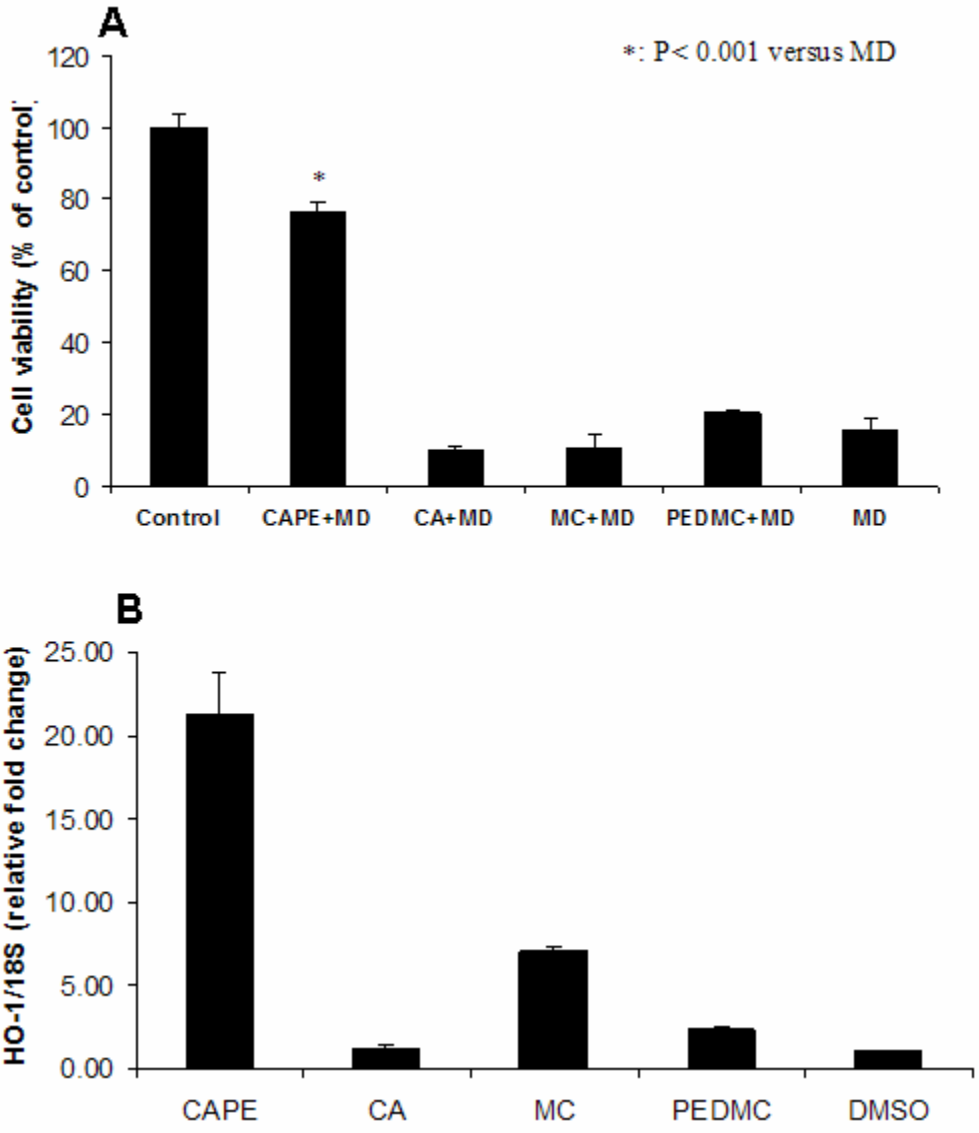

Figure 4.8: The cytoprotection and HO-1 induction profiles of 20 μM CA, MC, and PEDMC in HUVEC compared to CAPE. Values are represented as means plus standard deviation (n=3). Neither of CA, MC, or PEDMC protected HUVEC from MD-induced cytotoxicity (A), nor did they induce much HO-1 mRNA (B) compared to CAPE.

4.4 CONCLUSIONS

The cytoprotection, HO-1 induction, and cell-based antioxidant profiles of CAPE and derivatives at the same molar concentration of 20 μM were determined. The alteration of HO-1 at the transcriptional level correlated with the cytoprotective effects of most CAPE analogues except CAPE-2, which up-regulated HO-1 transcript but showed no protection. This was explained by the failure to produce HO-1 protein levels compared to that of DMSO control and CAPE. The application of the HO-1 inhibitor SnPPIX resulted in loss of protection of CAPE derivatives, which further indicated the importance of HO-1 induction in cytoprotection. CAPE analogues that showed antioxidant activity in HUVEC but didn't yield cytoprotective effects such as CAPE-2, CA, and MC did not induce HO-1. On the other hand, CAPE derivatives with pro-oxidant properties (CAPE-3, 4, and 5) could also protect HUVEC from oxidative stress. In conclusion, transcriptional activation of antioxidant enzyme HO-1 contributed an important portion to CAPE cytoprotection rather than its direct antioxidant activity in HUVEC against MD-induced oxidative stress.

Chapter V: Stability of Caffeic Acid Phenethyl Ester and Fluorinated Derivative FCAPE in Male Sprague Dawley Rat Plasma

5.1 INTRODUCTION

Plasma stability is a very important issue in drug development. It has a direct impact on drug performance *in vivo* and serves as a criterion for drug candidates screening at early stage of preclinical study. In addition, further degradation of drugs in post-collecting samples could compromise the results of subsequent studies such as pharmacokinetics. Samtani et al have demonstrated this issue in the analysis of corticosteroid prodrugs betamethasone sodium phosphate and dexamethasone sodium phosphate from plasma samples [184, 185].

Although CAPE exhibits many beneficial effects in animal models, its stability in biological media has not been well studied. In addition, our previous studies showed one of the CAPE derivatives, 3-(2-fluoro-4,5-dihydroxyphenyl)-acrylic acid phenethyl ester (CAPE-1 or FCAPE), showed good cytoprotective activity in the *in vitro* HUVEC-MD model and ability to induce HO-1 expression as CAPE (Chapter III and IV). Since this structural modification may result in different stability and rate of metabolism, it may have some advantage over CAPE in protective potency and display different pharmacokinetic profile *in vivo*.

The purpose of this study was to investigate the stability of CAPE and FCAPE in rat plasma in the presence and absence of sodium fluoride at pH 6.

5.2 MATERIALS AND METHODS

5.2.1 Materials

FCAPE was synthesized and characterized previously (Chapter III). Taxifolin, sodium fluoride, and formic acid were obtained from Aldrich and Sigma Chemical Co. (St. Louis, MO). Heparinized male Sprague Dawley rat plasma was purchased from Bioreclamation Inc. (Hicksville, NY). All reagents used were of the highest grade commercially available.

5.2.2 Instrumentation

HPLC was performed on a Varian HPLC system equipped with a 9010 pump, a 9050 UV detector, a 9065 diode array detector, and a 9100 autosampler fitted with a 20µl sample injection loop. Instruments were controlled by a Varian Star 4.5 work station (Varian Inc., Palo Alto, CA). Column equilibration was performed prior to analysis.

5.2.3 Chromatographic Conditions

The HPLC analysis was performed on a RP Luna C18(2) column (250 × 3.00mm i.d.; 5 µm, 100 Å) coupled with a security guard C18 cartridge system (4.0 × 2.0mm i.d.; 5 µm, 100 Å) (Phenomenex, Torrance, CA).The mobile phase consisted of A: 0.5% formic acid in acetonitrile and B: 0.5% formic acid in water. Before analysis, the mobile phase was filtered and degassed. The flow rate was maintained at 0.4 ml/min and the

detection wavelengths were set at 325 and 330 nm for CAPE and FCAPE, respectively. The sample volume injected was 20 µl. The temperatures of column and autosampler were controlled at room temperature of 25 °C and 4 °C, respectively. The gradient system was illustrated in Table 5.1. At 15 minutes, the gradient system was changed back to the beginning level (15% A and 85% B) before next run.

Table 5.1: The gradient system for CAPE and FCAPE

Time (min)	Gradient (CAPE)		Gradient (FCAPE)	
	(%)A	(%)B	(%)A	(%)B
0	15	85	15	85
2	15	85	15	85
3	75	25	55	45
10	100	0	100	0
15	100	0	100	0

A: acetonitrile with 0.5% formic acid.
B: water with 0.5% formic acid.

5.2.4 Sample Preparation

The method was based on the extraction of CAPE and FCAPE from plasma with ethyl acetate. Blank rat plasma was spiked with freshly made working solutions of CAPE, FCAPE, and taxifolin in acetonitrile for the preparation of CAPE or FCAPE calibration standard samples. Two hundred microliters of spiked rat plasma samples were transferred to a 1.5-ml centrifuge microtube. Six hundred microliters of ethyl acetate was added to the plasma samples, vortexed for 15 minutes, and centrifuged at 5,000 × g for 15 minutes at 4ºC. The supernatant (organic phase) was transferred to a 2-ml centrifuge microtube. The residue was extracted with 600 µl of ethyl acetate one more time, and the supernatant was collected, pooled, evaporated under a nitrogen stream at room

temperature, and stored at -20 ºC. Samples were reconstituted with 200 µl of mobile phase A: B (50:50, v/v) immediately prior to analysis. After vortexing for 15 minutes and a 15-min centrifugation at 5,000 × g at 4 ºC, the supernatant was transferred to autosampler microvials to be analysed. All plasma samples were handled on ice during the extraction process.

5.2.5 Method Validation

Blank rat plasma was spiked with freshly prepared working solutions (100 µg/ml) of CAPE, FCAPE, and taxifolin (internal standard, IS) to obtain calibration standards of 0.25, 0.5, 1, 5, and 10 µg/ml CAPE or FCAPE in the presence of 10 µg/ml IS. The HPLC method was validated by analyzing six replicates of each calibration standard for three consecutive days. Quantitative determination of CAPE and FCAPE was obtained from the standard curve where the peak height ratios (CAPE/taxifolin or FCAPE/taxifolin) were plotted against corresponding nominal concentrations of CAPE or FCAPE. A linear relationship was observed over the standard curve range from 0.25 to 10 µg/ml. The linear regression equations for the standard curve were found to be $Y=0.711X – 0.048$ for CAPE and $Y=0.551X + 0.031$ for FCAPE (Y, peak height ratio; X, nominal concentration). The coefficient of correlation (r^2) was 0.9994 for CAPE and 0.9999 for FCAPE. Method precision and accuracy were represented as percentage relative standard deviation (%R.S.D.) and percentage deviation (%Deviation), respectively, which ≤ 15% was acceptable for most calibration standards except the lower limit of quantification (LLOQ). LLOQ refers to the smallest quantifiable concentration also known as the lowest concentration point on the calibration curve for which precision and accuracy ≤ 20% were acceptable. The LLOQ was 0.25 µg/ml for both CAPE and FCAPE. The limit

of detection (LOD) regarding as the lowest concentration discriminate from baseline was also determined at signal/noise ratio of 3. CAPE and FCAPE were stable during the three-day analyses in the 4°C autosampler.

The recovery was evaluated as absolute recovery of CAPE or FCAPE at concentrations of 0.25, 1 and 10 μg/ml in the presence of 10 μg/ml IS. The absolute recovery of the extraction procedure was measured by comparing the peak heights of extracted plasma samples with those of neat standards. The absolute recovery of IS was also determined.

5.2.6 Stability Studies

The described reverse-phase HPLC assay was applied to determining CAPE or FCAPE in rat plasma from an *in vitro* stability study. This study was designed to determine the activation energy of CAPE or FCAPE hydrolysis in rat plasma. The stability study was evaluated at five time points (0.5, 1, 2, 6, and 24 hrs), three temperatures (4, 25, and 37 °C), and two concentrations (0.5 and 5 μg/ml) in the presence and absence of 0.4% sodium fluoride and 0.1 M acetate buffer at pH 6. The blank rat plasma was first spiked with the freshly made working solutions of CAPE or FCAPE (1 mg/ml) and taxifolin (2 mg/ml) to yield a final concentration of 0.5 or 5 μg/ml CAPE or FCAPE in the presence of 10 μg/ml taxifolin without the addition of sodium fluoride and pH adjustment. Aliquots of 200 μl of this bulk solution were placed in 1.5-ml centrifuge microtubes, and these microtubes were then tightly capped and incubated in the 37 °C incubator, at room temperature of 25 °C, and 4 °C in a refrigerator. The plasma samples were extracted with ethyl acetate at different time points following the extraction procedure described above. In addition, blank rat plasma was first mixed with 4% sodium

fluoride and acetate buffer (5 M, pH 5) to generate the final concentrations of 0.4% and 0.1 M, respectively. The pretreated rat plasma was then spiked with CAPE or FCAPE and IS to achieve the same concentrations examined above. Aliquots of 200 μl of this bulk solution were stored in a 4 °C refrigerator and extracted at the same time points.

The ability of NaF and pH adjustment to maintain the integrity of CAPE or FCAPE during three freeze-thaw cycles (FTCs), short-term (bench top, 24 hrs) storage, and long-term (-20 °C, four weeks) storage was examined. Two batches of blank rat plasma were mixed with NaF and acetate buffer. One batch was spiked with a low concentration of CAPE or FCAPE plus IS at 10 μg/ml and the other was spiked with a high concentration of CAPE or FCAPE plus IS. Three 200-μl aliquots of plasma samples at each concentration of CAPE or FCAPE were extracted and analyzed immediately serving as the control samples (t = 0). For the three FTCs stability study, three 200-μl aliquots of each concentration (0.5 or 5 μg/ml) were stored at -20 °C for 24 hrs and thawed at room temperature. When thawed completely, the aliquots were refrozen for 12 to 24 hrs. After repeating two more times of this cycle, the aliquots were extracted and analyzed. For the short-term storage study, three aliquots of each concentration (0.25 or 10 μg/ml) were kept at the bench top for 24 hrs before being processed for HPLC assay. For the long-term storage, three aliquots of each concentration (0.5 or 5 μg/ml) were stored at -20°C for four weeks, and processed for analysis. Stability was represented as percent recovery of CAPE or FCAPE by comparing the observed concentrations of plasma samples with corresponding controls.

5.2.7 Data Analysis

The data obtained from the stability study in the absence of 0.4% sodium fluoride and 0.1 M acetate buffer were plotted as natural logarithm (Ln) of the percentage remaining of CAPE or FCAPE versus time. The first-order rate constant for the hydrolysis of CAPE or FCAPE were calculated from the slope of the linear fit of the experimental data.

The energy of activation (E_A) known as the minimum energy required for the occurrence of a reaction was obtained using the Arrhenius equation at 4, 25, and 37°C. The Arrhenius equation is giving by equation 5.1:

$$\ln k = \ln A - E_A/RT \qquad \textbf{(5.1)}$$

Where k is the first order decomposition rate constant, A is the Arrhenius frequency factor, R represents the ideal gas constant, T is the absolute temperature, and E_A is the Energy of Activation.

The effect of 0.4% Sodium fluoride and 0.1 M acetate buffer on the kinetics of hydrolysis of CAPE or FCAPE from rat plasma was evaluated by analysis of variance (ANOVA) of the stability data for CAPE or FCAPE. A difference of $p < 0.05$ was considered significant.

5.3 RESULTS AND DISCUSSION

5.3.1 Assay Validation

To facilitate the stability study of CAPE and its fluorinated derivative FCAPE, we developed a simple HPLC assay with UV detection. The chromatographic separation was specific for CAPE and FCAPE, and no endogenous substances interfered with their determinations. Representative chromatograms for CAPE and FCAPE were shown in Figure 5.1. The retention time was 9.1 minutes for CAPE and 7.3 minutes for IS, and 11.0 minutes for FCAPE and 7.9 minutes for IS over a 15-min run, respectively. The assays were linear over the range of 0.25 – 10 μg/ml for CAPE and FCAPE ($r^2 > 0.999$, n=3). The linear regression parameters, method precision, and accuracy for CAPE and FCAPE were reported in Table 5.2, 5.3, and 5.4, respectively. In brief, the precision ranged from 0.7 to 13.7% for CAPE, and 0.4 to 10.4% for FCAPE. Accuracy ranged from -2.8 to 12.4% for CAPE and -0.6 to 6.8% for FCAPE. The LOD was set at 0.1 μg/ml for both CAPE and FCAPE. The absolute recovery was 84% - 96% (%R.S.D. ≤ 9.7) for CAPE, and 86.8% (%R.S.D. = 13.6) for IS (n=18). The absolute recovery was 89% - 100% (%R.S.D. ≤ 7.9) for FCAPE, and 95.6% (%R.S.D. = 9.4) for IS (n=18). The recovery study was investigated over the entire range of calibration curve (Table 5.5).

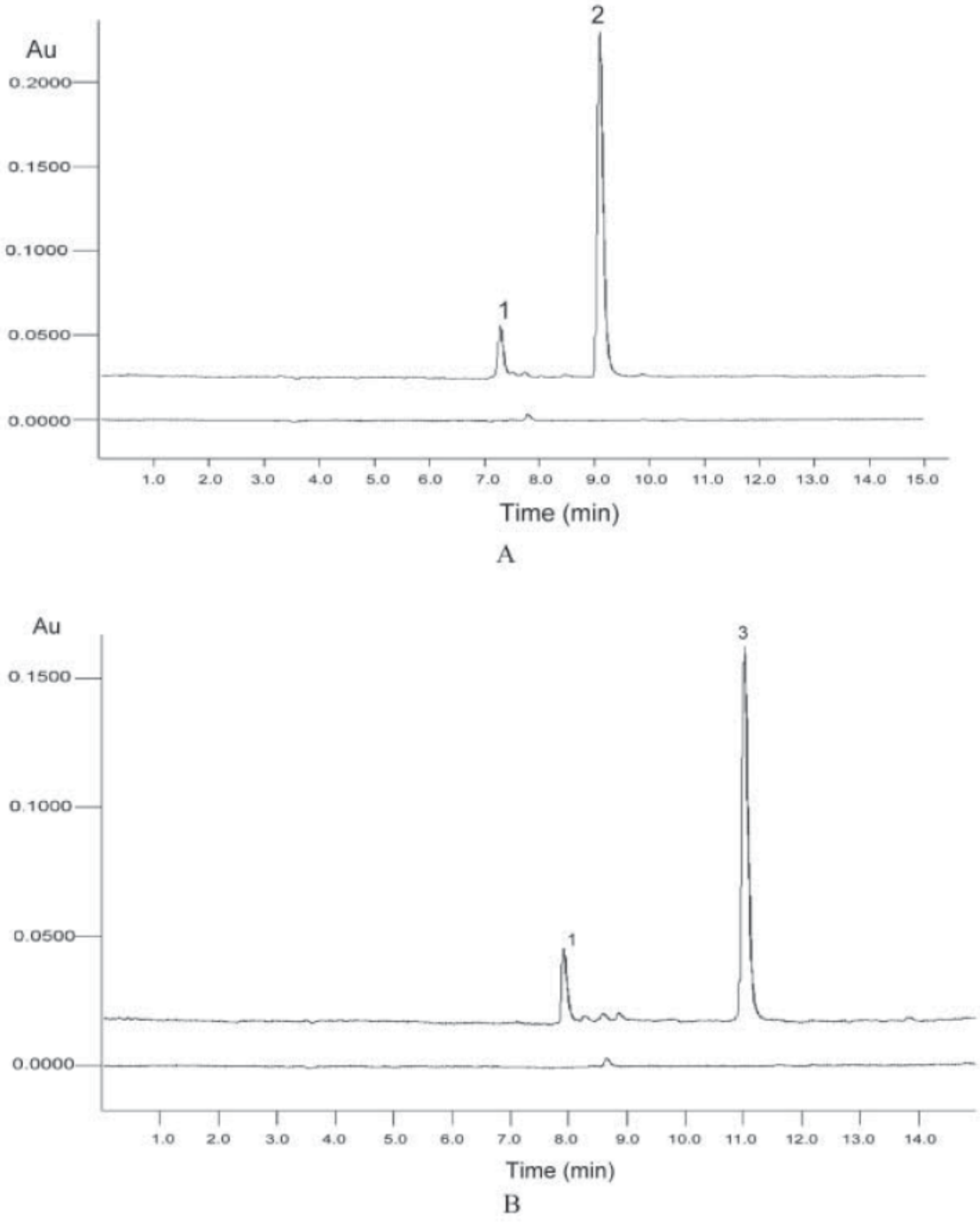

Figure 5.1: Typical chromatograms of (A) CAPE (10 μg/ml) and (B) FCAPE (10 μg/ml) from rat plasma in the presence of 10 μg/ml Taxifolin as internal standard. Peak 1, Taxifolin; peak 2, CAPE; peak 3, FCAPE. Lower line, blank plasma.

Table 5.2: Linear regression parameters.

	CAPE standard curve parameters		
Statistics	Linear slope	Intercept	r^2
	0.7192	-0.0618	0.9994
	0.7264	-0.0659	0.9987
	0.6867	-0.0160	1.0000
Mean	0.711	-0.048	0.9971
SD	0.021	0.028	0.0014
%R.S.D.	3.0	-57.8	0.1
	FCAPE standard curve parameters		
	0.5671	0.0214	1.0000
	0.5530	0.0435	1.0000
	0.5319	0.0278	0.9996
Mean	0.551	0.031	0.9999
SD	0.018	0.011	0.0002
%R.S.D.	7.5	40.3	0.0

Table 5.3: CAPE analytical method validation.

	Nominal concentration (μg/ml)				
	0.25	0.5	1	5	10
	Observed concentration (μg/ml)				
Day1	0.281	0.505	0.986	4.574	10.65
	0.285	0.506	1.045	4.857	10.39
	0.302	0.551	0.979	4.664	9.966
	0.290	0.576	1.035	4.835	9.927
	0.305	0.521	1.027	4.768	9.751
	0.298	0.522	1.031	5.260	9.804
Day2	0.309	0.525	1.112	4.650	9.673
	0.312	0.533	1.075	4.620	10.66
	0.326	0.553	0.993	4.483	10.19
	0.314	0.549	0.958	4.985	9.891
	0.299	0.541	1.039	4.893	9.911
	0.310	0.536	1.050	4.785	10.42
Day3	0.245	0.461	1.021	4.946	10.21
	0.246	0.463	1.015	4.934	9.726
	0.244	0.502	1.042	4.963	9.783
	0.236	0.477	1.026	5.048	10.36
	0.229	0.487	1.056	5.181	9.747
	0.227	0.479	1.038	4.963	10.15
Mean	0.281	0.516	1.029	4.856	10.07
SD	0.033	0.033	0.036	0.207	0.32
%R.S.D.	11.7	6.4	3.5	4.3	3.2
%Deviation [a]	12.4	3.2	2.9	-2.9	0.7

[a] $\%\text{Deviation} = \frac{\text{Mean-Nominal}}{\text{Nominal}} \times 100$

Table 5.4: FCAPE analytical method validation.

	Nominal concentration (μg/ml)				
	0.25	0.5	1	5	10
	Observed concentration (μg/ml)				
Day1	0.274	0.446	0.987	4.852	9.920
	0.244	0.543	1.000	5.182	9.869
	0.228	0.558	1.007	4.953	10.90
	0.245	0.539	0.945	5.067	9.725
	0.235	0.506	1.007	5.007	9.792
	0.230	0.519	0.963	4.979	9.783
Day2	0.248	0.379	1.002	4.886	10.19
	0.255	0.457	1.004	5.199	10.25
	0.318	0.480	0.983	5.118	9.813
	0.293	0.525	1.017	5.197	10.07
	0.209	0.502	0.963	4.723	9.922
	0.242	0.513	0.991	5.100	9.654
Day3	0.214	0.414	1.025	4.755	9.643
	0.304	0.512	1.054	4.926	10.33
	0.360	0.530	0.951	5.058	9.999
	0.334	0.457	0.936	4.934	10.64
	0.325	0.569	0.971	4.729	9.447
	0.244	0.525	1.199	4.791	10.32
Mean	0.267	0.499	1.000	4.970	10.01
SD	0.045	0.051	0.058	0.159	0.37
%R.S.D.	16.9	10.2	5.8	3.2	3.7
%Deviation [a]	6.8	-0.2	0.0	-0.6	0.1

[a] $\%\text{Deviation} = \frac{\text{Mean-Nominal}}{\text{Nominal}} \times 100$

Table 5.5: Absolute recovery of CAPE and FCAPE.

Nominal concentration	CAPE	FCAPE
	Absolute recovery (% recovery)	
0.25 μg/ml	81.1	83.6
	85.6	88.7
	81.9	101.8
	83.7	94.1
	79.9	88.1
	99.8	83.2
Mean	85.3	89.9
SD	7.3	7.1
%R.S.D.	8.6	7.9
1 μg/ml	80.5	92.3
	81.2	102.9
	94.3	92.5
	77.5	106.9
	81.1	106.4
	92.1	94.0
Mean	84.5	99.2
SD	7.0	7.0
%R.S.D.	8.3	7.1
10 μg/ml	82.7	88.3
	105.5	100.5
	85.8	88.5
	102.2	95.7
	95.1	96.1
	101.2	81.4
Mean	95.4	91.8
SD	9.3	7.0
%R.S.D.	9.7	7.6

5.3.2 Stability Study

5.3.2.1 Temperature effect

The effect of temperature on the degradation of CAPE and FCAPE in rat plasma was investigated at 4, 25, and 37 °C. Decomposition of CAPE occurred spontaneously in plasma samples at room temperature, was enhanced at 37 °C and slowed down at 4 °C (Table 5.6 and 5.7 for CAPE, and Table 5.8 and 5.9 for FCAPE). Since CAPE and FCAPE at a low dose of 0.5 μg/ml disappeared dramatically and couldn't be quantified at 37 °C, Their degradation at 5 μg/ml was plotted as the natural logarithm of percent remaining versus time (Figure 5.2 and 5.3). Linear relationships were observed for CAPE and FCAPE at three temperatures tested with the correlation coefficients greater than 0.95. This indicated that CAPE and FCAPE in rat plasma underwent first-order degradation kinetics within the conditions studied. The slope of the plot represented the first-order degradation rate constant (k), which were summarized in Table 5.10. The effect of temperature on the observed rate constant for a uni- or bimolecular reaction could indicate an empirical relation described by Arrhenius equation. In this study, linear Arrhenius plots were observed for the degradation of CAPE and FCAPE (Figure 5.4), which indicated that the hydrolysis mechanism were the same within the temperature range tested. The energy of activation (Ea value) for the hydrolysis reaction of CAPE and FCAPE in rat plasma was calculated from the slope of the Arrhenius plot. The half-lives ($t_{1/2}$) of CAPE and FCAPE at the temperatures studied were determined by equation 5.2:

$$t_{1/2} = 0.693 / k \qquad \textbf{(5.2)}$$

Where k is the first order decomposition rate constant and $t_{1/2}$ is the half-life. The calculated Ea, k, and $t_{1/2}$ were shown in Table 5.10.

Table 5.6: Stability of 0.5 μg/ml CAPE in spiked rat plasma at 37 °C, 25 °C, and 4 °C in the absence of NaF*.

	0 (control)	0.5 hr	1 hr	2 hr	6 hr	24 hr
			Stability (% recovery)			
37 °C		BLOQ	BLOQ	BLOQ	ND	ND
		BLOQ	BLOQ	BLOQ	ND	ND
		BLOQ	BLOQ	BLOQ	BLOQ	ND
		BLOQ	BLOQ	BLOQ	ND	ND
25 °C	96.9	56.9	BLOQ	BLOQ	ND	ND
	100.8	60.2	BLOQ	BLOQ	ND	ND
	102.1	61.7	BLOQ	BLOQ	ND	ND
Mean	99.9	59.6	BLOQ	BLOQ	ND	ND
SD	2.7	2.4				
%R.S.D.	2.7	4.0				
4 °C		87.0	71.0	88.6	49.7	BLOQ
		80.7	73.9	71.4	55.4	BLOQ
		88.2	90.4	64.8	54.4	BLOQ
Mean		85.3	78.5	74.9	53.2	BLOQ
SD		4.0	10.5	12.3	3.0	
%R.S.D.		4.7	13.4	16.4	5.6	

$$\% \text{ recovery} = \frac{\text{Calculated concentration}}{\text{Nominal concentration}} \times 100$$

BLOQ: below lower limit of quantification.
ND: not detectable.
* In the presence of NaF, the hydrolysis was completely inhibited at 4 °C.

Table 5.7: Stability of 5 μg/ml CAPE in spiked rat plasma at 37 °C, 25 °C, and 4 °C in the absence of NaF*.

	0 (control)	0.5 hr	1 hr	2 hr	6 hr	24 hr
			Stability (% recovery)			
37 °C		27.3	14.4	ND	ND	ND
		25.6	14.0	BLOQ	ND	ND
		24.6	13.6	BLOQ	ND	ND
Mean		25.9	14.0	BLOQ	ND	ND
SD		1.4	0.4			
%R.S.D.		5.4	2.9			
25 °C	101.2	58.3	29.2	14.8	BLOQ	ND
	97.1	52.4	29.8	12.3	BLOQ	ND
	101.7	52.4	30.6	16.7	BLOQ	ND
Mean	100.0	54.4	29.9	14.6	BLOQ	ND
SD	2.6	3.4	0.7	2.2		
%R.S.D.	2.6	6.3	2.3	15.1		
4 °C		77.6	72.6	73.7	49.7	18.1
		74.7	69.0	72.2	45.9	16.8
		75.1	70.4	64.4	54.6	14.5
Mean		75.8	70.7	70.1	50.1	16.5
SD		1.5	1.8	5.0	4.4	1.8
%R.S.D.		2.0	2.5	7.1	8.8	10.9

$$\%\ \text{recovery} = \frac{\text{Calculated concentration}}{\text{Nominal concentration}} \times 100$$

BLOQ: below lower limit of quantification.
ND: not detectable.
* In the presence of NaF, the hydrolysis was completely inhibited at 4 °C.

Table 5.8: Stability of 0.5 μg/ml FCAPE in spiked rat plasma at 37 °C, 25 °C, and 4 °C in the absence of NaF*.

	0 (control)	0.5 hr	1 hr	2 hr	6 hr	24 hr
			Stability (% recovery)			
37 °C		BLOQ	BLOQ	BLOQ	ND	ND
		BLOQ	BLOQ	BLOQ	ND	ND
		BLOQ	BLOQ	BLOQ	ND	ND
		BLOQ	BLOQ	BLOQ	ND	ND
25 °C	104.2	82.7	71.8	BLOQ	BLOQ	ND
	96.0	78.5	81.7	BLOQ	BLOQ	ND
	99.8	87.5	69.3	BLOQ	BLOQ	ND
Mean	100.0	82.9	74.3	BLOQ	BLOQ	ND
SD	4.1	4.5	6.6			
%R.S.D.	4.1	5.4	8.9			
4 °C		95.5	86.5	92.2	78.7	BLOQ
		93.4	95.1	87.2	71.1	BLOQ
		106.1	96.1	92.4	79.3	BLOQ
Mean		98.3	92.6	90.6	76.4	BLOQ
SD		6.8	5.3	2.9	4.6	
%R.S.D.		6.9	5.7	3.2	6.0	

$$\%\ \text{recovery} = \frac{\text{Calculated concentration}}{\text{Nominal concentration}} \times 100$$

BLOQ: below lower limit of quantification.
ND: not detectable.
* In the presence of NaF, the hydrolysis was completely inhibited at 4 °C.

Table 5.9: Stability of 5 μg/ml FCAPE in spiked rat plasma at 37 °C, 25 °C, and 4 °C in the absence of NaF*.

	0 (control)	0.5 hr	1 hr	2 hr	6 hr	24 hr
			Stability (% recovery)			
37 °C		53.5	22.5	BLOQ	ND	ND
		53.0	23.0	BLOQ	ND	ND
		51.2	21.3	BLOQ	ND	ND
Mean		52.6	22.3	BLOQ	ND	ND
SD		1.2	0.9			
%R.S.D.		2.3	4.0			
25 °C	99.6	80.4	63.6	43.1	10.6	ND
	99.2	84.5	58.1	42.3	10.6	ND
	101.2	83.6	65.1	42.8	10.9	ND
Mean	100.0	82.8	62.3	42.7	10.7	ND
SD	1.1	2.2	3.7	0.4	0.2	
%R.S.D.	1.1	2.7	5.9	0.9	1.9	
4 °C		96.3	91.6	90.1	74.8	45.5
		95.8	95.6	92.3	74.3	45.3
		95.3	96.2	94.6	77.0	50.8
Mean		95.8	94.5	92.4	75.3	47.2
SD		0.5	2.5	2.2	1.4	3.1
%R.S.D.		0.5	2.6	2.4	1.9	6.6

$$\%\ \text{recovery} = \frac{\text{Calculated concentration}}{\text{Nominal concentration}} \times 100$$

BLOQ: below lower limit of quantification.
ND: not detectable.
* In the presence of NaF, the hydrolysis was completely inhibited at 4 °C.

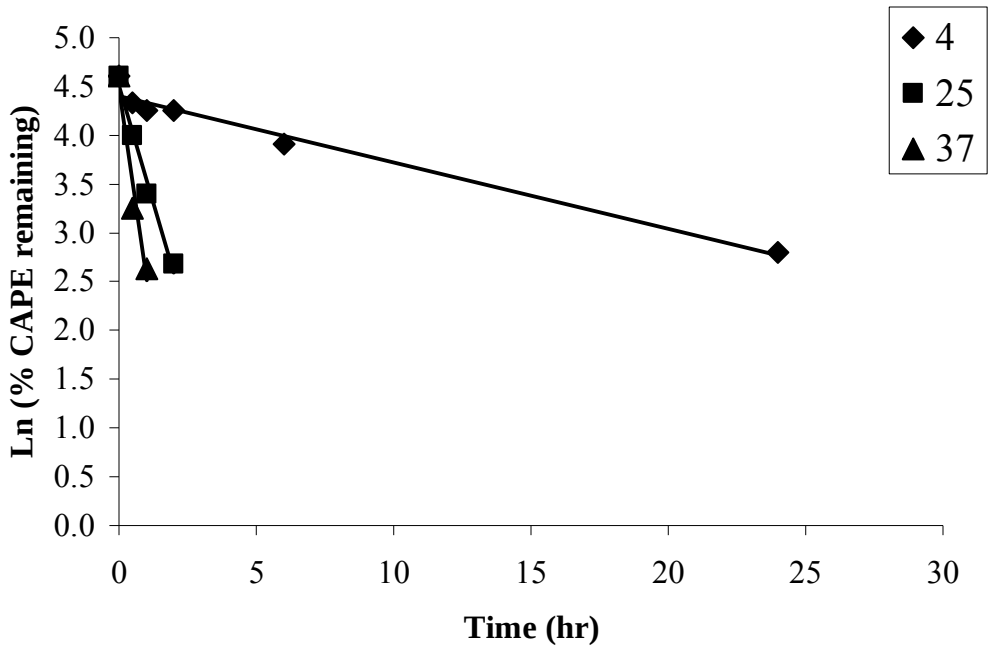

Figure 5.2: First-order hydrolysis kinetics of CAPE at 5 μg/ml in rat plasma at 4, 25, and 37 °C. The linear regression equation at each temperature is shown as follows. 4 °C: $y = -0.0679x + 4.406$, $r^2 = 0.9725$; 25 °C: $y = -0.954x + 4.505$, $r^2 = 0.9793$; 37 °C: $y = -1.97x + 4.482$, $r^2 = 0.9553$.

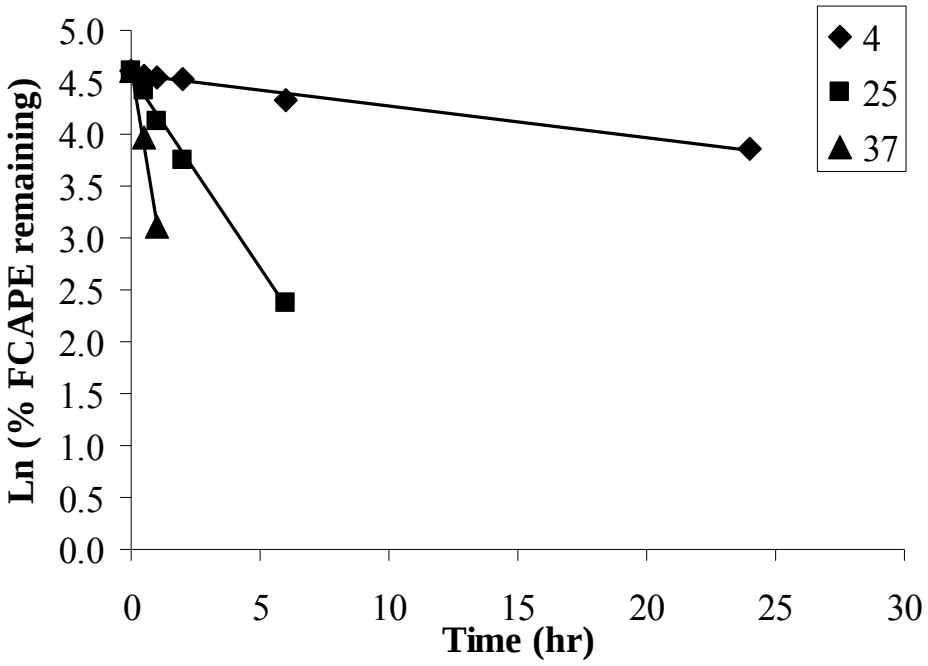

Figure 5.3: First-order hydrolysis kinetics of FCAPE at 5 μg/ml in rat plasma at 4, 25, and 37 °C. The linear regression equation at each temperature is shown as follows. 4 °C: $y = -0.0307x + 4.574$, $r^2 = 0.9853$; 25 °C: $y = -0.369x + 4.557$, $r^2 = 0.9962$; 37 °C: $y = -1.502x + 4.641$, $r^2 = 0.9932$.

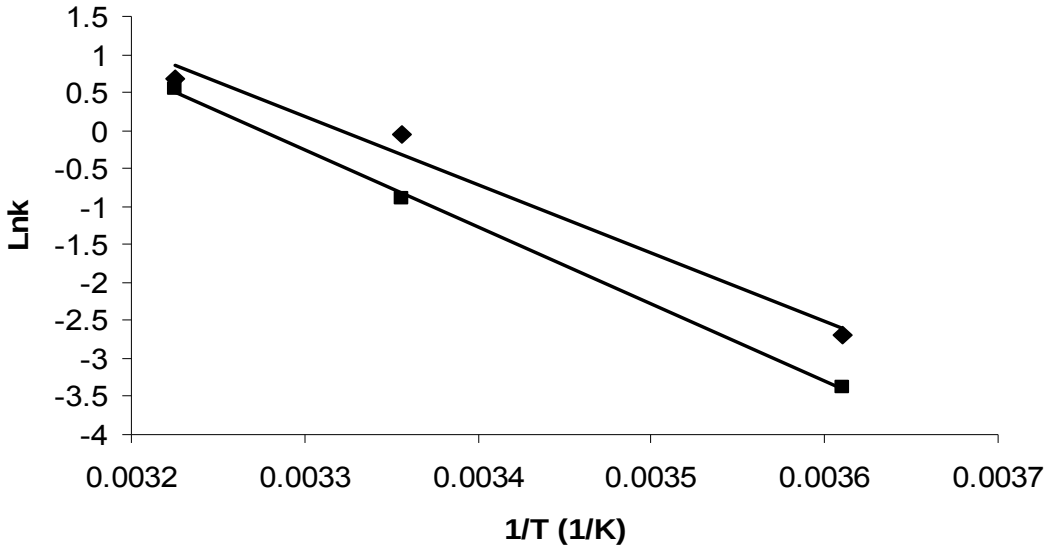

Figure 5.4: Arrhenius plots for the activation energy determination of CAPE (♦) and FCAPE (■). The Arrhenius equations are shown as follows. CAPE: $y = -8985\ x + 29.84$, $r^2 = 0.9824$; FCAPE: $y = -10127\ x + 33.16$, $r^2 = 0.9989$.

Table 5.10: The kinetic parameters of hydrolysis of CAPE and FCAPE at 5 μg/ml in rat plasma at 4, 25, and 37 °C in the absence of NaF*.

		CAPE	
Temperature (°C)	37	25	4
k (h^{-1})	1.97	0.954	0.0679
$t_{1/2}$ (h)	0.35	0.73	10.21
Ea (Kcal/mol)		17.9	
		FCAPE	
Temperature (°C)	37	25	4
k (h^{-1})	1.50	0.369	0.0307
$t_{1/2}$ (h)	0.46	1.88	22.57
Ea (Kcal/mol)		20.1	

* In the presence of NaF, the hydrolysis was completely inhibited at 4 °C.

5.3.2.2 Effects of sodium fluoride and pH

The application of an enzyme inhibitor and maintenance of a weak acid environment are common ways to keep target compounds stable in plasma samples [158]. In the presence of 0.4% sodium fluoride, a reversible esterase inhibitor, and pH adjustment to 6 with acetate buffer (5 M, pH 5), the hydrolysis of CAPE and FCAPE was completely inhibited at 4 °C. The stability of CAPE and FCAPE as percent of control at each time point was not significantly different from each other at a significance level of $p<0.05$ (Figure 5.5). This was also confirmed by the fact that no degradation product peak appeared on the chromatograms. The ability of NaF and pH reduction to preserve the integrity of CAPE or FCAPE in rat plasma was evaluated in the study of freeze-thaw, short-term, and long-term stability. These stability experiments reflect the conditions that may occur during routine sample handling, storage, and analysis. The data showed that the stability of all samples tested was above 85% of the corresponding controls (Table 5.11), which indicated that 0.4% NaF addition and pH adjustment together effectively inhibited the hydrolysis of CAPE or FCAPE.

These results indicated that FCAPE appeared to be more stable than CAPE as reflected by the higher energy of activation. The Ea value estimated for FCAPE was 13% higher than that of CAPE. The potential to limit the metabolism of FCAPE and other fluorinated derivatives may allow them to exert their protective effect longer than CAPE *in vivo*. The addition of 0.4% sodium fluoride and 0.1 M acetate buffer provides a feasible way to prevent the degradation of CAPE and FCAPE for the purpose of establishing their pharmacokinetic profiles and ensures their stability in rat plasma after three freeze and thaw cycles, 24 hrs at room temperature, and four weeks at -20 °C.

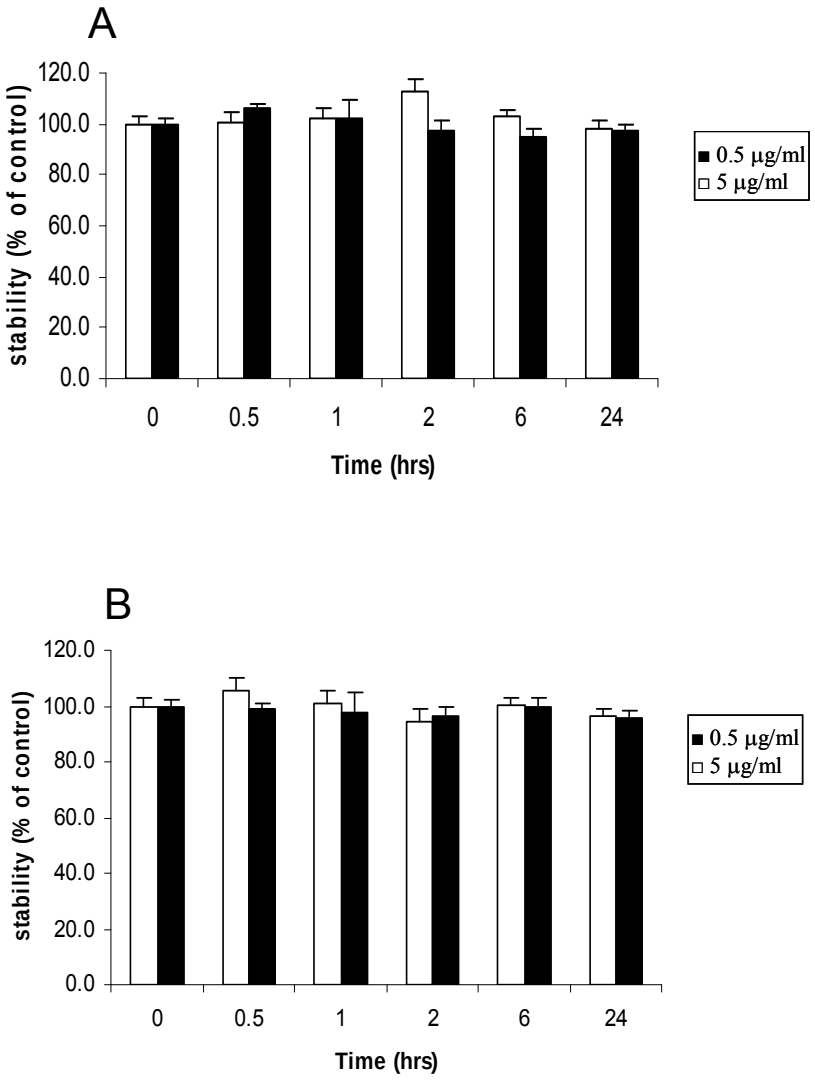

Figure 5.5: Stability of CAPE (A) and FCAPE (B) at 0.5 and 5 µg/ml in rat plasma in the presence of 0.4% Sodium fluoride and 0.1 M acetate buffer at 4 °C. Value were reported as mean (n=3) percent of control (t = 0 hr) with error bars showing the standard deviation. No statistically significant differences were observed at each time point compared to control for the same dose of CAPE and FCAPE ($P < 0.05$).

Table 5.11: Stability of CAPE and FCAPE in rat plasma containing sodium fluoride and acetate buffer, expressed as mean % recovery.

	CAPE		FCAPE	
	0.5 μg/ml	5 μg/ml	0.5 μg/ml	5 μg/ml
Freeze-thaw (three cycles)	102.8	84.3	99.5	95.8
	109.0	87.2	99.9	99.4
	101.9	83.7	96.1	98.1
Mean	104.5	85.1	98.5	97.8
SD	3.9	1.9	2.1	1.9
% R.S.D.	3.7	2.2	2.1	1.9
Long-term storage [a]	99.2	101.9	99.6	104.1
	104.3	96.1	104.6	101.1
	97.8	101.4	106.8	97.8
Mean	100.5	99.8	103.7	101.0
SD	3.4	3.2	3.7	3.2
% R.S.D.	3.4	3.2	3.6	3.2
	0.25μg/ml	10 μg/ml	0.25μg/ml	10 μg/ml
Room temperature (24 hrs)	87.5	95.3	95.1	99.0
	89.1	101.0	82.9	94.7
	95.7	91.7	88.9	97.0
Mean	90.7	96.0	89.0	96.9
SD	4.4	4.7	6.1	2.1
% R.S.D.	4.8	4.9	6.9	2.2

[a] For four weeks at -20 °C

5.4 CONCLUSIONS

A simple HPLC-UV analytical method was developed and validated for the determination of CAPE and FCAPE in rat plasma. The stability profiles of CAPE and FCAPE in rat plasma at 4, 25, and 37 °C were established. The data suggested that both CAPE and FCAPE underwent first-order hydrolysis in rat plasma, enhancing at 37 °C and slowing down at 4 °C compared to 25 °C. The calculated energy of activation from arrhenius plot was 17.9 Kcal/mol for CAPE and 20.1 Kcal/mol for FCAPE, respectively. This result indicates that FCAPE is more difficult to undergo hydrolysis in rat plasma than CAPE. The relatively longer half-lives of FCAPE at each temperature suggested that FCAPE is more stable than CAPE in the conditions tested.

The effects of the esterase inhibitor NaF and pH adjustment were examined. The data suggested that the addition of NaF at 0.4% and acetate buffer at 0.1 M in rat plasma could maintain the integrity of CAPE and FCAPE after three freeze and thaw cycles, at room temperature for 24 hrs, and for at least four weeks at -20 °C.

In conclusion, the chemical modification of CAPE seems to provide a better drug candidate with better stability and longer half-life. The application of sodium fluoride and pH adjustment together could prevent hydrolytic degradation of CAPE and FCAPE in rat plasma.

Chapter VI: Quantitative Determination of Caffeic Acid Phenethyl Ester and Fluorinated Derivative FCAPE from Sprague Dawley Rat Plasma by Liquid Chromatography-Electrospray Ionization Tandem Mass Spectrometry

6.1 INTRODUCTION

The quantitative determination of CAPE and FCAPE in a biological medium is essential for establishing their pharmacokinetic profiles. A literature search showed that only a limited number of quantitative analyses of CAPE have been performed. Ceschel *et al.* reported an HPLC-UV method for the quantification of CAPE in propolis extracts. The separation was performed on a Nova-Pak C18 column at room temperature with mobile phase consisting methanol/acetonitrile (50:50, v/v). The UV detection wavelength was set at 325 nm. Detailed quantitative information, however, was not available from the paper [159]. Del Boccio and Rotilio employed an HPLC system coupled a quadrupole mass spectrometer detector to measure CAPE from crude propolis [160]. Ethyl acetate was used to extract CAPE from propolis and the chromatographic separation was achieved on a Luna RP-C18 column at room temperature with a linear gradient consisting of acetonitrile and water with 0.5% formic acid in both solvents. The analyses were performed by Selected Ion Monitoring mode, monitoring deprotonated molecule peak of CAPE at *m/z* 283. The external standard method was applied to define a linear quantification range of 0.125 – 80 ng/ml. On the basis of Del Boccio and Rotilio's method, Celli *et al.* were able to determine CAPE in rat plasma and urine by liquid chromatography/tandem mass spectrometric analysis with similar separation conditions

[161]. Taxifolin was used as the internal standard. The linear range was validated from 5 to 1000 ng/ml for CAPE. The lower limit of detection was set at 1ng/ml.

In this chapter, a method using ultra-performance liquid chromatography with electrospray ionization tandem mass spectrometry (UPLC-ESI-MS/MS) for the quantification of CAPE and FCAPE in male Sprague Dawley rat plasma was developed. Methyl caffeate (MC, Figure 4.1) was used as the internal standard (IS). This method was validated according to the acceptance criteria for bioanalytical method validation described in the FDA guidelines [186].

6.2 MATERIALS AND METHODS

6.2.1 Materials

CAPE, FCAPE, MC, NaF, formic acid, and heparinized male Sprague Dawley rat plasma were obtained as described in previous chapters. All reagents used were of the highest grade commercially available.

6.2.2 Instrumentation

The quantitative analysis was performed on a Waters® ACQUITY™ TQD tandem quadrupole UPLC-MS/MS system, which consists of an ACQUITY Ultra Performance™ liquid chromatography system and an ACQUITY TQ detector (Waters, Milford, MA). This UPLC-MS/MS system was controlled by MassLynx™ 4.1 software.

6.2.3 UPLC-MS/MS Conditions

The UPLC separation was performed on a Waters ACQUITY ethylene-bridged (BEH™) C18 column (1.7 μm, 2.1 × 50 mm) at 60 °C. The mobile phase consisted of (A) water with 0.2% formic acid and (B) acetonitrile with 0.1% formic acid at a flow rate of 0.4 ml/min. A gradient elution was applied (Table 6.1). The sample injection volume was 10 μl. The sample temperature was controlled at 4 °C prior to analysis. The total UPLC run time was 2.7 min.

Table 6.1: Gradient elution program.

Step	Time (min)	Flow (ml/min)	(%) A	(%) B
1	0.00	0.4	75.0	25.0
2	0.12	0.4	75.0	25.0
3	0.50	0.4	2.0	98.0
4	2.00	0.4	2.0	98.0
5	2.10	0.4	75.0	25.0
6	2.70	0.4	75.0	25.0

A: water with 0.2% formic acid.
B: acetonitrile with 0.1% formic acid.

All MS optimization experiments were performed in MS scan mode and product scan mode. The mass spectrometer was operated in multiple reaction monitoring (MRM) mode using electrospray ionization in negative ion mode. For MRM data collection, the capillary voltage was 2800 V, the cone voltage was 40 V, the source temperature was 125

°C, the desolvation temperature was 350 °C, the cone gas flow was 70 L/Hr, the desolvation gas flow was 650 L/hr, the MS inter-scan delay was 0.01 sec, the polarity/mode switch inter-scan delay was 0.03 sec, the inter-channel delay was 0.01 sec, and the dwell time was 0.1 sec. The MRM transitions for the analytes were: *m/z* 283.00 > *m/z* 134.90 for CAPE, *m/z* 301.00 > *m/z* 152.90 for FCAPE, and *m/z* 192.90 > *m/z* 133.80 for MC.

6.2.4 Preparation of Stock Solutions, Calibration Standards, and Quality Control Samples

Stock solutions of CAPE and FCAPE in acetonitrile were prepared at 1 mg/ml for making spiking solutions with the calibration standards. Separate stock solutions of CAPE and FCAPE were used to prepare spiking solutions for the quality control (QC) samples. A stock solution of MC at 1 mg/ml was prepared to generate an IS working solution at a nominal concentration of 20 μg/ml in acetonitrile. Spiking solutions of CAPE and FCAPE were added to SD rat blank plasma (containing 0.4% sodium fluoride and 0.1 M acetate buffer) to obtain the required concentrations for calibration standards ranging from 10 to 10000 ng/ml and QC samples at low (25 ng/ml), medium (4500 ng/ml), and high (9000 ng/ml) concentrations for either CAPE or FCAPE.

6.2.5 Sample Extraction Procedure

Two hundred microliters of plasma sample in the presence of 0.4% NaF and 0.1 M acetate buffer were transferred to a 1.5-ml centrifuge microtube with the addition of 50 μl of the IS working solution. Six hundred microliters of ethyl acetate were applied to the

extracted plasma sample as previously described (Chapter V). In brief, after a 15-minute vortexing and a 15-minute centrifuging at 4 °C, the supernatant from both extractions was pooled and collected in a 2 ml centrifuge microtube. After evaporation to dryness under a nitrogen flow at room temperature, the resulting residues were stored at – 80 °C until analyzed. Prior to analysis, the extracted residues were reconstituted and diluted in 2 ml water/methanol (50:50, v/v), mixed, and centrifuged. Ten microliters of each sample was injected into the UPLC-MS/MS system.

6.2.6 Assay Validation

Assay validation included determinations of specificity, sensitivity, accuracy, precision, concentration-response function (calibration), recovery, and stability. The calibration curve was obtained by plotting the peak ratios (CAPE/IS or FCAPE/IS) against the nominal concentrations of the analyte (CAPE or FCAPE) and best fitted using a quadratic regression model with 1/X weighting. In order to obtain the appropriate MS detection, the calibration curve was developed within the range from 1 to 1000 ng/ml by reconstitution of the calibration standards in 10-fold dilution after extraction. The limit of detection (LOD) was determined at a signal-to-noise (S/N) ratio of 3. The lower limit of quantification was measured at a minimum S/N ratio of 10. Accuracy was determined by comparing the mean observed concentration to the theoretical concentration and expressed as the ratio in percentage (% theoretical). Precision was presented as the percent coefficient of variation (%CV). The inter-day and intra-day accuracy and precision of QC samples were evaluated in three-day core validation runs. Each validation run consisted of calibration standards in triplicate and six replicates of QC samples at three different concentrations plus a minimum of two blank plasma samples

without IS and two with IS (not used in the regression). The recovery of CAPE or FCAPE and IS was determined by comparing the peak area of extracted plasma samples to that of the pure standard samples in solvent at three QC concentrations (n=3 for CAPE or FCAPE and n=9 for IS). The stability of CAPE or FCAPE in the presence of NaF and acetate buffer was represented as percent recovery and accessed after three freeze and thaw cycles, 24 hrs at room temperature, and at least one month in -30 °C at three concentrations of QC samples in triplicate. The carry-over effect was evaluated by comparing the level of CAPE or FCAPE at upper limit of quantification (ULOQ) to a blank sample which followed and represented as a percentage of the ratio of the peak area of the target analyte in the blank run versus that of the previous ULOQ sample. A carry-over of less than 1% was considered to be acceptable.

6.3 RESULTS AND DISCUSSION

6.3.1 Method Development

A validated method for quantification analysis of CAPE and FCAPE in biological fluid is a prerequisite for investigation of accurate pharmacokinetics. We previously reported an HPLC-UV method used for determination of the stability of CAPE and FCAPE (chapter V). Due to the limit of UV detection, a more sensitive method was required for *in vivo* quantification. We tried an HPLC tandem mass spectrometric method first that was capable of quantitative measurement of CAPE and FCAPE down to a lower limit of 1 ng/ml. However, the carryover effect of more than 6% which compromised the

accuracy of the measurement. The application of an UPLC system solved this problem by minimizing the carryover to less than 1% for both CAPE and FCAPE. The tandem MS detector provided the required sensitivity. The full-scan and product ion mass spectra were performed using the electrospray negative ionization mode since CAPE, FCAPE, and internal standard MC are all polyphenols and readily lost one proton forming deprotonated $[M-H]^-$ ion peaks. The full-scan mass spectra of CAPE, FCAPE, and MC showed abundant deprotonated molecular ion peak at *m/z* = 283.00, 301.00, and 192.90, respectively (Figure 6.1A). The consequent product ion mass spectra for CAPE, FCAPE, and IS exhibited major fragment ions at *m/z* = 134.90, 152.90, and 133.80, respectively (Figure 6.1B). The chromatographic separation was optimized and achieved in 2.7 min using an ACQUITY BEH™ C18 column with 1.7 μm particle size and gradient elution. Representative chromatograms for CAPE, FCAPE, and IS in rat plasma are shown in Figure 6.2. No endogenous interference was found in the area of interest from different sources of blank rat plasma. Sample clean-up procedures were adopted from our previous described method (chapter V). The addition of 0.4% NaF and pH adjustment of the rat blank plasma was necessary to maintain the integrity of CAPE and FCAPE during the preparation of calibration standards and QC samples. This step was necessary to assure the quality of the data to establish the pharmacokinetic profiles of CAPE and FCAPE.

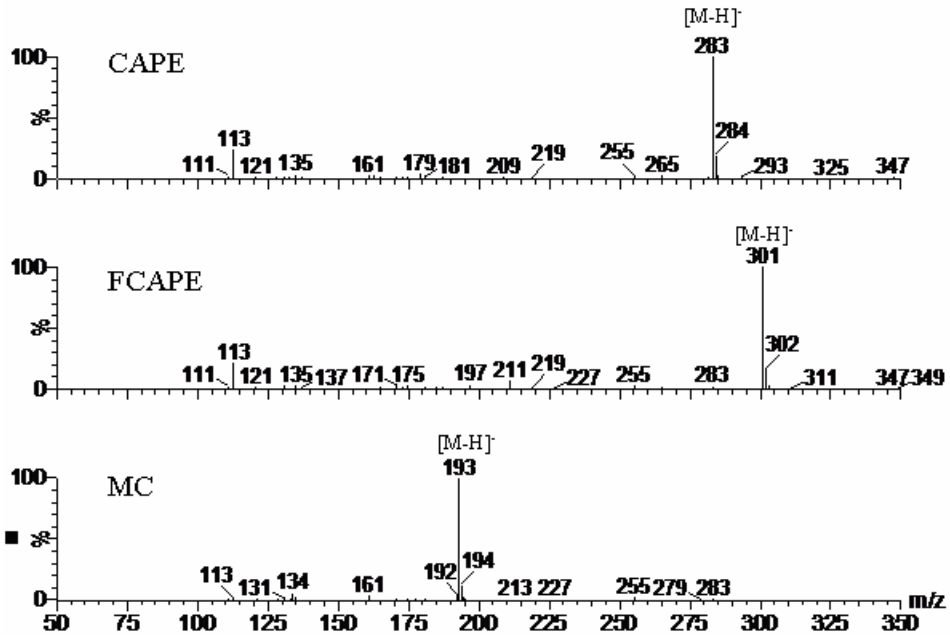

A

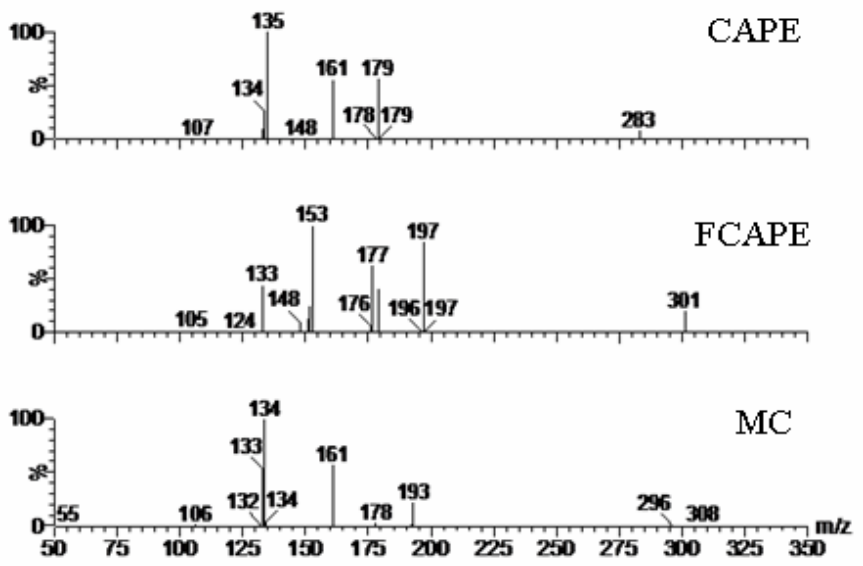

B

Figure 6.1: Full scan mass spectra for CAPE, FCAPE, and MC (A) and product ion mass spectra where product ions m/z 135, m/z 153, and m/z 134 were monitored for CAPE, FCAPE, and MC, respectively (B).

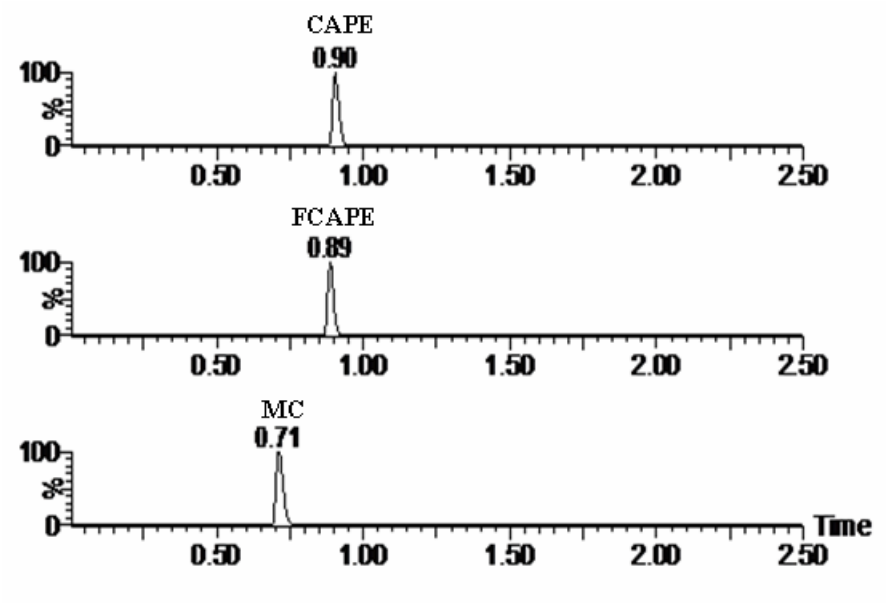

A

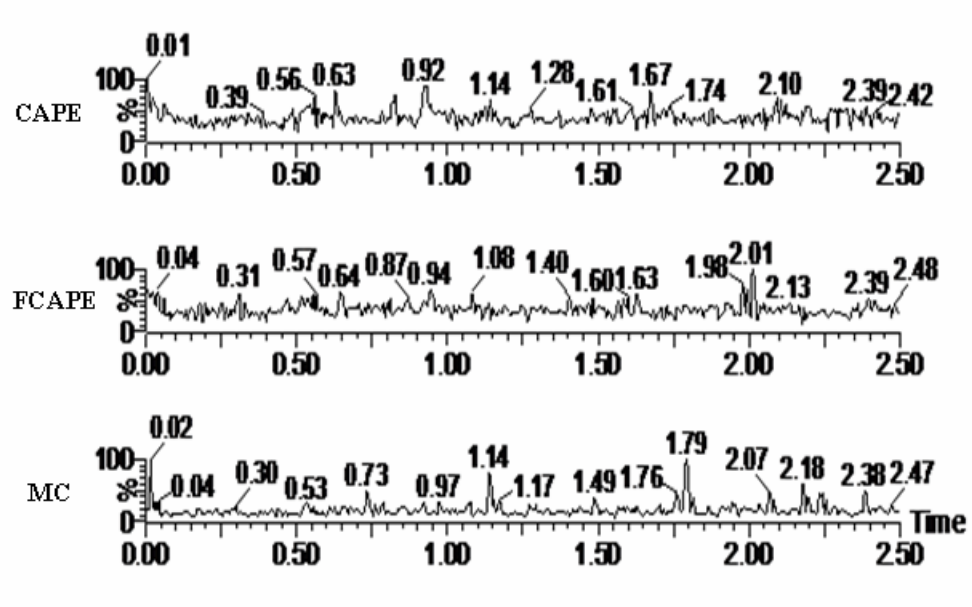

B

Figure 6.2: Typical MRM chromatograms of CAPE, FCAPE, and MC at 100 ng/ml (A) and corresponding blank plasma (B).

6.3.2 Method Validation

For calibration purposes, the standard curves were obtained over the concentration range of 1 -1,000 ng/ml after 10-fold dilutions of CAPE or FCAPE by plotting CAPE or FCAPE to IS peak area ratios against their nominal concentrations with weighted regression analysis. A quadratic regression with 1/X weighting gave the best fit for the concentration/detector response relationship for CAPE and FCAPE in rat plasma. The mean quadratic calibration equations for the validation runs were: $Y= -0.0007830X^2 + 2.112X + 0.696$ for CAPE and $Y= -0.0006568X^2 + 1.769X + 0.509$ for FCAPE. The mean coefficients of determination (r^2) for the validation runs were 0.9971 for CAPE and 0.9969 for FCAPE. The parameters were present in Table 6.2. Linear regression of the data was also performed but with much lower r^2 (<0.9900) than that obtained using a quadratic regression. For the LC-MS(/MS) analysis, especially with ESI, calibration curves with a dynamic range over 2 orders of magnitude is not always linear possibly due to the concentration-sensitive behavior of ESI. The analyte ion signal can become saturated with an increase of sample concentration [187]. The lower limit of quantification (LLOQ) refers to the lowest calibration standard, which is 1 ng/ml for both CAPE and FCAPE. The typical chromatograms for CAPE and FCAPE at LLOQ were shown in Figure 6.3. The limit of detection was set at 0.1ng/ml for both CAPE and FCAPE. The calibration curves for CAPE and FCAPE were acceptable according to the validation criteria as the back-calculated values were within ± 15% of the nominal concentrations (± 20% at the LLOQ) in the three-day validation (Table 6.3 and Table 6.4).

For the QC samples, the inter-day and intra-day accuracy (% theoretical) of CAPE ranged from 91.6 to 113.2, and the inter-day and intra-day precision (%CV) was

less than 14.2 (Table 6.5); the inter-day and intra-day accuracy (% theoretical) of FCAPE ranged from 92.3 to 110.0, and the inter-day and intra-day precision (%CV) was less than 9.5 (Table 6.6).

The recovery of CAPE and FCAPE was estimated using QC samples by comparing the peak area of spiked plasma samples that were extracted versus neat samples. The mean absolute recovery ranged from 80.2% to 100.7% (%R.S.D. < 12.7) for CAPE and 49.9% to 86.3% (%R.S.D. < 9.5) for FCAPE, respectively (Table 6.7). The mean absolute recovery for I.S. was 98.7% (%R.S.D. = 3.1, n = 9). The stability issue of CAPE and FCAPE has been addressed in our previous study (Chapter V). The addition of NaF and pH adjustment prevented degradation of CAPE and FCAPE after three freeze-thaw cycles (-30 °C to 20 °C), 24 hr at room temperature (20 °C), and at least one month in -30 °C (Table 6.8 and 6.9).

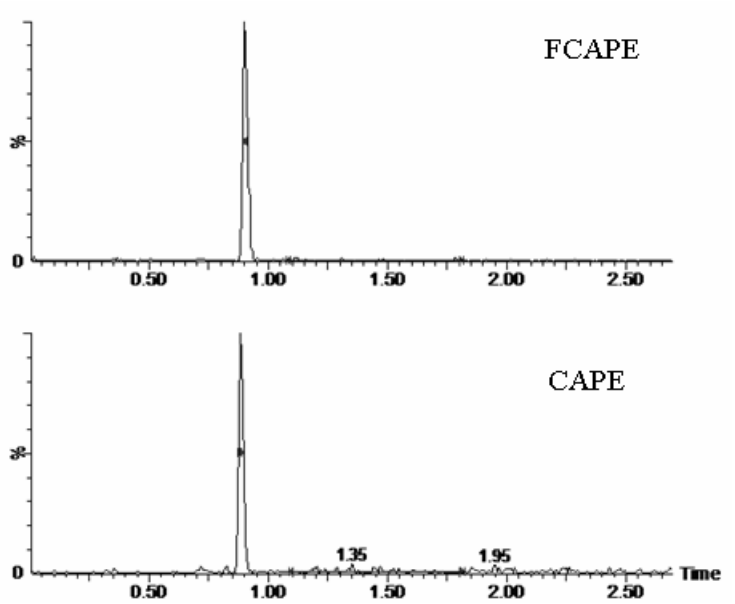

Figure 6.3: Representative chromatograms of CAPE and FCAPE at the LLOQ levels.

Table 6.2: Quadratic regression parameters.

	CAPE calibration curve parameters			
Statistics	Quadratic slope (a) [a]	Linear slope (b) [a]	Intercept (c) [a]	r^2
	-7.460E-04	1.916	0.9232	0.9975
	-7.382E-04	2.148	0.5417	0.9982
	-8.648E-04	2.272	0.6226	0.9955
Mean	-7.830E-04	2.112	0.6958	0.9971
SD	7.095E-05	0.181	0.2010	0.0014
%R.S.D.	9.1	8.6	28.9	0.14
	FCAPE calibration curve parameters			
	-6.468E-04	1.635	0.7309	0.9971
	-5.884E-04	1.772	0.4665	0.9966
	-7.352E-04	1.899	0.3280	0.9969
Mean	-6.568E-04	1.769	0.5085	0.9969
SD	7.391E-05	0.132	0.2047	0.0003
%R.S.D.	11.3	7.5	40.3	0.03

[a] Quadratic regression model: $Y = a \cdot X^2 + b \cdot X + c$

Table 6.3: CAPE calibration curve validation.

	Nominal concentration (ng/ml)					
	1	5	10	100	500	1000
	Observed concentration (ng/ml)					
Day1	0.914	5.893	12.42	107.1	478.4	1023
	0.807	6.165	11.26	109.3	456.5	1127
	0.670	5.311	10.68	108.5	479.9	989.0
Day2	0.857	6.108	11.05	102.6	485.8	1039
	0.962	5.253	11.22	111.3	497.5	1051
	0.909	5.098	10.84	106.0	454.5	975.4
Day3	0.891	5.978	12.11	111.3	436.4	1097
	0.860	5.088	11.76	117.9	487.7	1171
	0.701	5.265	10.82	105.0	470.4	929.2
Mean	0.841	5.573	11.35	108.8	471.9	1045
SD	0.099	0.451	0.61	4.5	19.4	77
%R.S.D.	11.8	8.1	5.4	4.1	4.1	7.4
%Deviation	-15.9	11.5	13.5	8.8	-5.6	4.5

[a] $\%\text{Deviation} = \frac{\text{Mean-Nominal}}{\text{Nominal}} \times 100$

Table 6.4: FCAPE calibration curve validation.

	Nominal concentration (ng/ml)					
	1	5	10	100	500	1000
	Observed concentration (ng/ml)					
Day1	0.810	6.041	12.39	109.7	471.0	1038
	0.830	6.030	11.21	110.2	461.5	1178
	0.653	5.252	11.08	107.5	474.1	974.1
Day2	0.707	6.189	10.84	103.0	481.3	1001
	0.951	4.710	12.24	119.1	500.0	1070
	0.960	5.106	10.78	106.1	437.0	1010
Day3	0.797	5.498	11.39	102.5	479.6	972.4
	0.891	5.023	10.70	111.2	497.6	[b]
	0.962	5.313	10.46	107.1	458.5	892.0
Mean	0.840	5.462	11.23	108.5	473.4	1017
SD	0.112	0.517	0.67	5.0	19.6	84
%R.S.D.	13.3	9.5	6.0	4.6	4.1	8.3
%Deviation	-16.0	9.2	12.3	8.5	-5.3	1.7

[a] $\%\text{Deviation} = \frac{\text{Mean-Nominal}}{\text{Nominal}} \times 100$

[b] Not applicable.

Table 6.5: Intra/inter-day precision and accuracy for CAPE QC samples.

Nominal concentration	Intra-day			Inter-day (n=18)
	Day1	Day2	Day3	
2.5ng/ml	Observed concentration (ng/ml)			
1	2.486	2.554	2.378	
2	2.698	2.795	2.877	
3	2.796	2.744	2.822	
4	2.518	2.639	3.043	
5	2.320	2.596	2.757	
6	2.338	2.447	3.075	
Mean	2.526	2.629	2.825	2.660
SD	0.191	0.127	0.252	0.224
%CV	7.56	4.83	8.92	8.42
% theoretical [a]	101.04	105.16	113.00	106.40
450ng/ml				
1	445.8	463.3	450.8	
2	440.4	420.0	436.0	
3	414.7	434.7	444.6	
4	387.7	414.1	424.6	
5	387.3	412.4	426.2	
6	397.9	419.8	292.7 [b]	
Mean	412.30	427.38	436.44	426.84
SD	25.90	19.27	11.38	21.67
%CV	6.28	4.51	2.61	5.08
% theoretical	91.62	94.98	96.98	94.85
900 ng/ml				
1	790.0	805.5	897.7	
2	1091.4	850.5	965.8	
3	982.1	849.9	877.8	
4	779.5	812.6	772.0	
5	809.0	863.4	889.7	
6	865.1	834.7	907.3	
Mean	886.18	836.10	885.05	869.11
SD	125.18	22.95	63.29	80.74
%CV	14.13	2.74	7.15	9.29
% theoretical	98.46	92.90	98.34	96.57

[a] $\%\ \text{theoretical} = \frac{\text{Mean}}{\text{Nominal}} \times 100$

[b] Rejected as an outlier.

Table 6.6: Intra/inter-day precision and accuracy for FCAPE QC samples.

Nominal concentration	intraday			interday (n=18)
	Day1	Day2	Day3	
2.5ng/ml	Observed concentration (ng/ml)			
1	2.960	2.974	2.631	
2	2.501	2.781	2.738	
3	2.671	2.688	2.897	
4	2.744	2.946	2.731	
5	2.692	2.523	2.668	
6	2.536	2.642	2.840	
Mean	2.684	2.759	2.751	2.731
SD	0.165	0.177	0.101	0.146
%CV	6.15	6.42	3.67	5.35
% theoretical [a]	107.36	110.36	110.04	109.24
450ng/ml				
1	447.4	452.7	411.4	
2	435.9	442.6	369.0	
3	453.2	439.6	462.2	
4	450.3	424.5	433.9	
5	430.8	428.9	399.3	
6	443.3	438.5	193.7 [b]	
Mean	443.48	437.80	415.16	432.11
SD	8.66	10.05	35.21	24.02
%CV	1.95	2.30	8.48	5.56
% theoretical	98.56	97.29	92.27	96.02
900 ng/ml				
1	919.6	823.3	926.5	
2	972.3	873.7	916	
3	880.4	854.4	871.4	
4	804.5	786.7	821.2	
5	882.8	912.3	879.6	
6	1056.0	847.4	909.2	
Mean	919.27	849.63	887.32	885.41
SD	86.63	42.87	38.78	63.62
%CV	9.42	5.05	4.37	7.19
% theoretical	102.14	94.40	98.59	98.38

[a] $\%\ \text{theoretical} = \frac{\text{Mean}}{\text{Nominal}} \times 100$

[b] Rejected as an outlier.

Table 6.7: Recovery of CAPE and FCAPE.

Nominal concentration	CAPE	FCAPE
	Absolute recovery (% recovery)	
2.5 μg/ml	77.0	48.7
	91.5	54.6
	72.2	46.3
Mean	80.2	49.9
SD	10.1	4.3
%R.S.D.	12.6	8.6
450 μg/ml	89.3	74.9
	92.5	72.8
	92.7	70.7
Mean	91.5	72.8
SD	1.9	2.1
%R.S.D.	2.1	2.9
900 μg/ml	97.2	83.0
	101.7	91.3
	103.1	84.5
Mean	100.7	86.3
SD	3.1	4.4
%R.S.D.	3.1	5.1

Table 6.8: Stability of CAPE in rat plasma expressed as mean % recovery.

Storage conditions	Nominal concentrations (ng/ml)		
	2.5	450	900
Room temperature (24hrs)	104.4	105.3	109.7
	90.9	107.7	109.2
	90.9	109.8	104.3
Mean	95.4	107.6	107.7
SD	7.8	2.3	3.0
% R.S.D.	8.2	2.1	2.8
Freeze-thaw (three cycles)	97.6	104.4	93.9
	104.4	103.3	100.3
	90.9	99.7	94.4
Mean	97.6	102.5	96.2
SD	6.7	2.4	3.5
% R.S.D.	6.9	2.3	3.6
Long-term storage [a]	101.0	104.2	98.5
	87.5	100.6	96.5
	90.9	103.8	94.6
Mean	93.2	102.9	96.5
SD	7.0	2.0	1.9
% R.S.D.	7.5	1.9	2.0

[a] For one month at -30 °C

Table 6.9: Stability of FCAPE in rat plasma expressed as mean % recovery.

Storage conditions	Nominal concentrations (ng/ml)		
	2.5	450	900
Room temperature (24hrs)	110.5	102.3	100.0
	96.3	102.5	106.7
	[b]	106.2	105.1
Mean	103.4	103.7	103.9
SD	10.0	2.2	3.5
% R.S.D.	9.7	2.1	3.4
Freeze-thaw (three cycles)	99.2	97.4	96.4
	90.7	102.3	105.6
	85.0	98.8	92.7
Mean	91.6	99.5	98.2
SD	7.1	2.5	6.6
% R.S.D.	7.8	2.5	6.7
Long-term storage [a]	87.8	99.1	91.7
	82.2	98.7	92.7
	[b]	98.2	95.1
Mean	85.0	98.6	93.2
SD	4.0	0.4	1.8
% R.S.D.	4.7	0.4	1.9

[a] For one month at -30 °C
[b] Not applicable.

6.4 CONCLUSIONS

A rapid and sensitive UPLC-ESI-MS/MS method was developed, validated, and applied to the quantitative determination of CAPE and FCAPE in male Sprague Dawley rat plasma. The chromatographic separation within 3 minutes allowed a fast sample analysis time and high-throughput capability favoring a high sample load. The calibration curve showed best fit over the concentration range of 1-1,000 ng/ml using a quadratic regression with 1/concentration weighting. The intra and inter-day accuracy and precision for QC samples were all within the FDA suggested acceptance criteria. CAPE and FCAPE were stable in rat plasma with the addition of 0.4% NaF and 0.1 M acetate buffer under the storage conditions. These results support an acceptable and reliable method for the pharmacokinetic study of CAPE and FCAPE.

Chapter VII: Pharmacokinetics of caffeic acid phenethyl ester and its fluorinated derivative FCAPE after intravenous bolus administration to male Sprague Dawley rats

7.1 INTRODUCTION

Data from previous stability studies demonstrated that caffeic acid phenethyl ester (CAPE) and 3-(2-fluoro-4,5-dihydroxyphenyl)-acrylic acid phenethyl ester (FCAPE) are subject to rapid hydrolysis in male Sprague Dawley rat plasma and determined that further degradation in post-collected biological samples could be prevented by the addition of 0.4% NaF and 0.1 M acetate buffer (Chapter V). The quantitative determination of CAPE and FCAPE in male Sprague Dawley rat plasma was established by liquid chromatography with electrospray ionization tandem mass spectrometry and validated to provide sufficient sensitivity and selectivity provided (Chapter VI). Both studies supported the determination of the pharmacokinetic (PK) profiles of CAPE and FCAPE in rats.

Three doses of CAPE were administered to determine if CAPE follows linear pharmacokinetics in male Sprague Dawley rats after intravenous administration. The non-compartmental PK analyses and bi-exponential fit of the plasma concentration (Cp) time data were performed to obtain major PK parameters for CAPE and FCAPE.

7.2 MATERIALS AND METHODS

7.2.1 Materials

Helix silastic tubing (0.02 × 0.37) and St. Gobain Tygon tubing (0.02 × 0.06) were from VWR International (West chester, PA). Cannula guides (22 Guage) and stainless steel screws were from Plastics One (Roanoke, VA). Ethicon silk sutures and dental cement were from Henry Schein (Melville, NY).

7.2.2 Animals

Male Sprague Dawley (SD) rats weighing 300 ± 50 grams were purchased from Harlan (Indianapolis, IN). Rats were housed 2-3 per cage in a temperature-controlled animal room under a 12:12 light: dark cycle (lights on 0700h) and allowed to acclimate for 1 week with food and water provided *at libitum* prior to surgery. Rats were housed individually after the surgery. The following experimental protocols were approved by University of Texas at Austin Animal Resource Center and met the Institutional Animal Care and Use Committee (IACUC).

7.2.3 Surgical Procedures

The rats were subjected to jugular vein catheterization surgery. During the whole surgical process, rats were deeply anesthetized with isoflurane gas (Henry Schein) through a gas anesthesia machine (induction at 4% and maintenance at 2%). Aseptic

procedures were performed in an isolated area dedicated for surgery. All surgical tools were sterilized prior to use. The surgical area including the skull and neck on each rat was shaved and cleaned with iodine followed by 70% alcohol and treated with 2% xylocaine (Henry Schein). An incision was made on the skin of the skull with a scalpel. Then, the jugular vein was located on the neck and a small incision was made. The jugular vein was isolated, hemisected and a sterile catheter introduced and secured with sutures. After verifying the blood flow, the catheter was pulled routed subcutaneously from the neck to the skull. The neck incision was sutured and cleaned with betadyne followed by wound powder. The animal was stabilized with a stereotax equipped with an isoflurane breathing adaptor. Four small holes were drilled into the skull to allow sterile screws to be inserted for the purpose of fixing cranioplast dental cement. Both cannula and jugular catheter tubing were secured on the skull with dental cement. The surgical area was cleaned and treated post-operatively. The catheter was flushed daily with 0.1 ml filtered heparinized saline (200 U/ml) till the end of the experiment. The catheterized rats were allowed at least 5-day to recover before the start of pharmacokinetic study.

7.2.4 Pharmacokinetic Study

Male Sprague Dawley rats weighing 300 ± 50 grams were randomly divided into four groups, each containing 5 rats. Different group of rats were intravenously administered CAPE at doses of 5, 10, or 20 mg/kg and FCAPE at a dose of 20mg/kg. CAPE or FCAPE was dissolved in 15% ethanol, 45% propylene glycol, and 40% sterile saline and prepared freshly before each experiment. The Rats were administered 0.5 ml of drug solution via the jugular vein catheter over a 30-second period. The cannula and catheter were immediately flushed with a small volume of isotonic heparinized saline to

ensure complete drug delivery. Blood samples (400 µl) were collected at 0 (pre-dose), and at 5, 10, 20, 40, 60, 90, 120, and 180 minutes post administration. The blood samples were immediately transferred to heparinized vials containing 0.4% sodium fluoride and 0.1 M acetate buffer and placed on ice. Plasma samples were harvested by centrifugation at 10,000 g for one minutes and stored at -80 °C until assayed.

7.2.5 Sample Extraction

Two hundred microliters of plasma sample were transferred to a 1.5 ml centrifuge microtube with the addition of 50 µl of the IS working solution. Six hundred microliters of ethyl acetate were applied twice to extract the plasma sample as previously described in chapter VI.

7.2.6 Quantitative Analysis of CAPE or FCAPE in Rat Plasma

The concentration of CAPE or FCAPE was determined by the validated analytical procedure using UPLC-ESI-MS/MS described in chapter VI.

7.2.7 Data Analysis

Non-Compartmental Analysis (NCA) was performed using WinNonlin professional Edition version 2.1 (Pharsight Cooperation, Mountain View, CA). The data points within the terminal phase were chosen to determine the terminal elimination rate constant λ_z. The area under the plasma concentration time curve (AUC) was estimated

using linear trapezoidal rule. AUC from the time of last measurable concentration (t_{last}) to infinity was calculated as C_{last}/λ_z, where C_{last} is the drug concentration at t_{last}. The AUC from time zero to infinity (AUC_∞) was calculated using equation 7.1. The area under the product of the concentration and time versus time curve is referred to the area under the first moment curve (AUMC). The AUMC from time zero to t_{last} was estimated using the linear trapezoidal rule. The AUMC from t_{last} to infinity was computed as the sum of $C_{last} \times t_{last}/\lambda_z$ and C_{last}/λ_z^2. The computation of the $AUMC_\infty$ was achieved using equation 7.2. Total body clearance (CL), volume of distribution (Vd), elimination phase half-life ($t_{1/2\text{-}\lambda z}$), mean residence time (MRT), and volume of distribution at steady state (V_{ss}) were calculated using equations 7.3 to 7.7, respectively.

$$AUC_\infty = \sum_{i=0}^{n-1} \frac{t_{i+1} - t_i}{2} (C_i + C_{i+1}) + \frac{C_{last}}{\lambda_z} \quad \textbf{(7.1)}$$

$$AUMC_\infty = \sum_{i=0}^{n-1} \frac{t_{i+1} - t_i}{2} (C_i\, t_i + C_{i+1}\, t_{i+1}) + \frac{C_{last} \cdot t_{last}}{\lambda_z} + \frac{C_{last}}{\lambda_z^2} \quad \textbf{(7.2)}$$

$$CL = \frac{Dose}{AUC_\infty} \quad \textbf{(7.3)}$$

$$V_d = \frac{Dose}{AUC_\infty \lambda_z} \quad \textbf{(7.4)}$$

$$t_{1/2\text{-}\lambda z} = \frac{ln2}{\lambda_z} \quad \textbf{(7.5)}$$

$$MRT = \frac{AUMC_\infty}{AUC_\infty} \quad \textbf{(7.6)}$$

$$V_{ss} = CL \cdot MRT = \frac{Dose \cdot AUMC_\infty}{AUC_\infty^2} \quad \textbf{(7.7)}$$

The plasma concentration time data of CAPE or FCAPE, which declined in an apparent bi-exponential trend after intravenous bolus administration, were also fitted by non-linear regression to the equation (7.8).

$$C_p = A \cdot e^{-\alpha \cdot t} + B \cdot e^{-\beta \cdot t} \qquad \textbf{(7.8)}$$

Parameters A, B, α, and β were estimated graphically from the slopes and intercepts by methods of residuals, and used to fit the plasma concentration time data by WinNonlin. The calculation of the AUC, AUMC, Vd, and half life ($t_{½}$) was achieved using equations 7.9 to 7.12, respectively. The computation of parameters such as Cl, MRT, and Vss was achieved from equation 7.3, 7.6, and 7.7, respectively.

$$AUC_{\infty} = \frac{A}{\alpha} + \frac{B}{\beta} \qquad \textbf{(7.9)}$$

$$AUMC_{\infty} = \frac{A}{\alpha^2} + \frac{B}{\beta^2} \qquad \textbf{(7.10)}$$

$$Vd = \frac{\text{Dose}}{\text{AUC} \cdot \beta} \qquad \textbf{(7.11)}$$

$$t_{1/2} = \frac{\ln 2}{\beta} \qquad \textbf{(7.12)}$$

7.2.8 Statistical Analysis

Differences between or among the mean value for each group were analyzed using the independent samples t-test or one-way analysis of variance using SPSS for Windows Standard Version 11.0.0. Statistical significance was set at $p < 0.05$.

7.3 RESULTS AND DISCUSSION

7.3.1 Pharmacokinetics of CAPE

The plasma concentrations (normalized by individual dose in mg) of CAPE after intravenous bolus administration to male Sprague Dawley rats at doses of 5, 10, and 20 mg/kg of CAPE are summarized in Table 7.1 – 7.3. The validated calibration curve ranged from 10 to 10,000 ng/ml of CAPE. Therefore, concentration values less than 80% of LLOQ (10 ng/ml) were considered below lower limit of quantification (BLOQ) and not applied in pharmacokinetic analysis. Plasma samples with concentration over 10,000 ng/ml of CAPE were diluted and reanalyzed in order to ensure that the corresponding concentrations after dilution fall within the calibration curve range. The plasma concentrations of CAPE following intravenous administration of 20 mg/kg CAPE at 5 minutes were determined after 10-fold dilution. The graphic representations of CAPE plasma concentration-time profiles in semi-log scale are illustrated in Figure 7.1 – 7.3. CAPE shows a rapid distribution phase reflected by the rapid decline of the plasma concentrations from 5 to 15 minutes after 5, 10, and 20 mg/kg CAPE administered intravenously. The average CAPE plasma concentration-time profiles after three intravenous dose administrations are presented in Figure 7.4.

Table 7.1: Observed plasma concentrations normalized by individual dose (ng/ml·mg) of CAPE following intravenous bolus administration of 5 mg/kg CAPE to male Sprague Dawley rats.

Time (min)	rat1	rat2	rat3	rat4	rat5	Mean	SD
5	1570.9	679.2	797.7	464.1	1404.1	983.2	479.3
10	200.5	107.6	62.0	44.7	131.6	109.3	61.7
20	53.9	32.6	22.9	19.1	20.5	29.8	14.5
40	23.4	8.0	11.1	10.4	7.9	12.1	6.4
60	13.3	7.3	7.5	5.2	5.6	7.8	3.2
90	NU	BLOQ	BLOQ	NU	BLOQ		
120	NU	BLOQ	BLOQ	BLOQ	BLOQ		
180	BLOQ	BLOQ	BLOQ	BLOQ	BLOQ		
Dose (mg)	1.65	1.61	1.54	1.695	1.52	1.60	0.03
Weight (kg)	0.330	0.322	0.308	0.339	0.304	0.321	0.015

NU: not usable for pharmacokinetic analysis.
BLOQ: below lower limit of quantification.

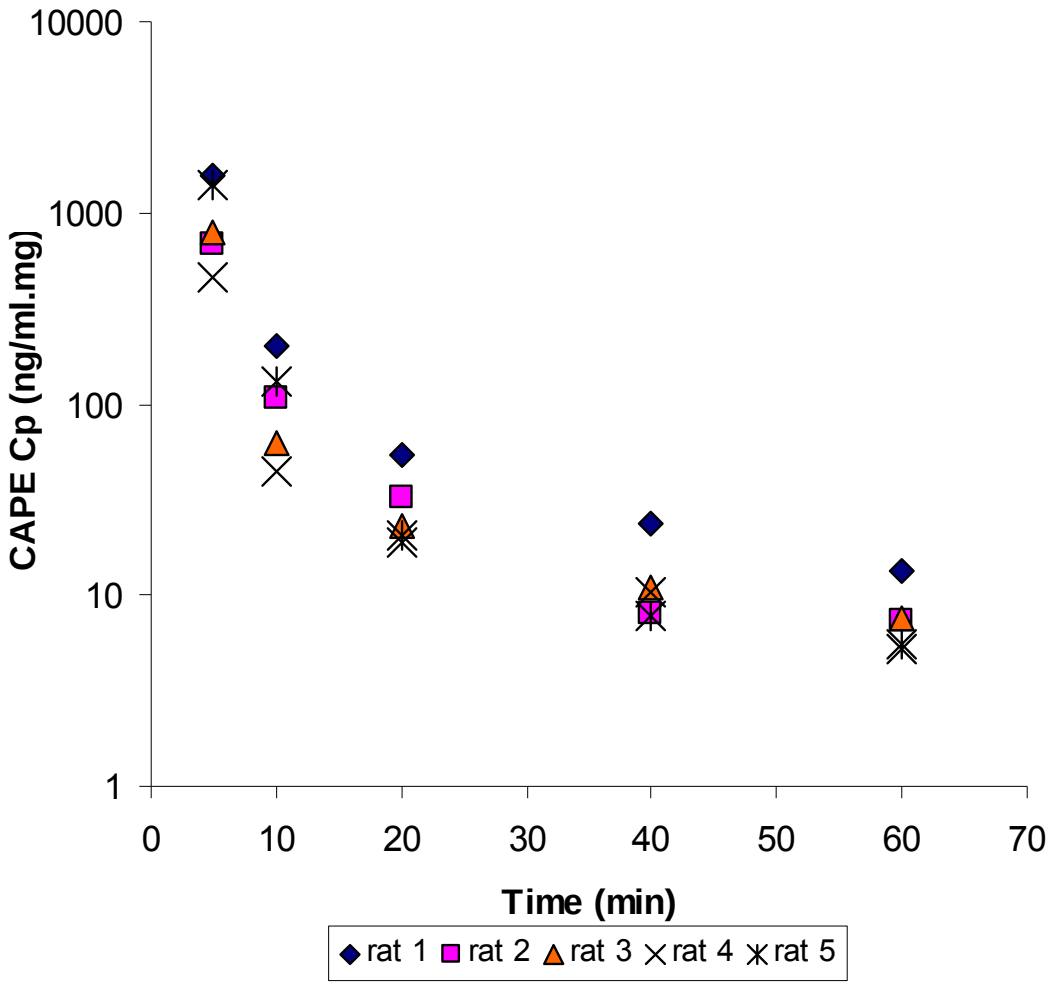

Figure 7.1: Semi logarithmic representation of the individual normalized plasma concentration (Cp) time profile of CAPE after intravenous bolus administration of 5 mg/kg CAPE to male Sprague Dawley rats.

Table 7.2: Observed plasma concentrations normalized by individual dose (ng/ml·mg) of CAPE following intravenous administration of 10 mg/kg CAPE to male Sprague Dawley rats.

Time (min)	Rat 1	Rat 2	Rat 3	Rat 4	Rat 5	Mean	SD
5	1092.1	2778.0	1422.8	1251.2	1887.8	1686.4	679.0
10	143.3	570.7	329.6	86.5	195.1	265.0	193.1
20	41.5	180.9	59.4	22.0	44.0	69.6	63.7
40	11.4	133.7	45.7	NU	14.9	51.0	49.4
60	NU	152.1	NU	5.2	NU	NU	
90	2.7	88.4	10.4	3.8	3.4	21.7	37.4
120	BLOQ	NU	NU	BLOQ	NU		
180	BLOQ	NU	NU	BLOQ	BLOQ		
Dose (mg)	3.57	3.23	2.67	3.51	3.78	3.35	0.43
Weight (kg)	0.357	0.323	0.267	0.351	0.378	0.335	0.043

NU: not usable for pharmacokinetic analysis.
BLOQ: below lower limit of quantification.

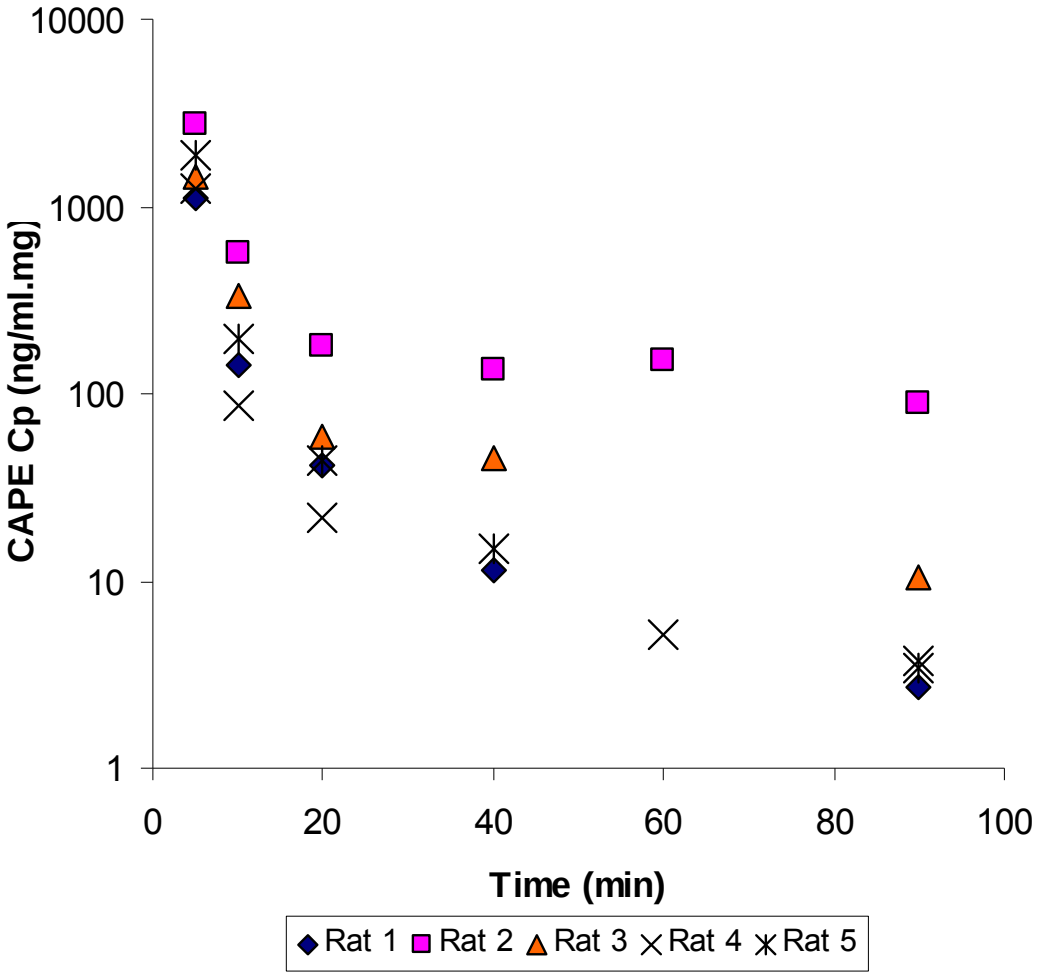

Figure 7.2: Semi logarithmic representation of the individual normalized plasma concentration (Cp) time profile of CAPE after intravenous bolus administration of 10 mg/kg CAPE to male Sprague Dawley rats.

Table 7.3: Observed plasma concentrations normalized by individual dose (ng/ml·mg) of CAPE following intravenous administration of 20 mg/kg CAPE to male Sprague Dawley rats.

Time (min)	Rat 1	Rat 2	Rat 3	Rat 4	Rat 5	Mean	SD
5	3675.5[a]	3988.8[a]	3175.7[a]	3976.2[a]	3251.2[a]	3613.5	387.0
10	280.4	278.2	306.1	558.2	619.8	408.6	166.5
20	71.7	49.3	106.8	432.2	355.7	203.1	177.4
40	45.9	32.9	48.3	173.9	116.2	83.4	60.1
60	23.6	21.2	37.8	76.8	67.7	45.4	25.5
90	7.0	13.5	24.0	30.4	NU	25.0	16.8
120	NU	NU	NU	18.4	NU	NU	
180	NU	NU	NU	NU	NU	NU	
Dose (mg)	5.78	5.88	5.72	6.36	5.2	5.79	0.41
Weight (kg)	0.289	0.294	0.286	0.318	0.260	0.289	0.021

[a] Plasma concentrations were determined after 10-fold dilution.
NU: not usable for pharmacokinetic analysis.

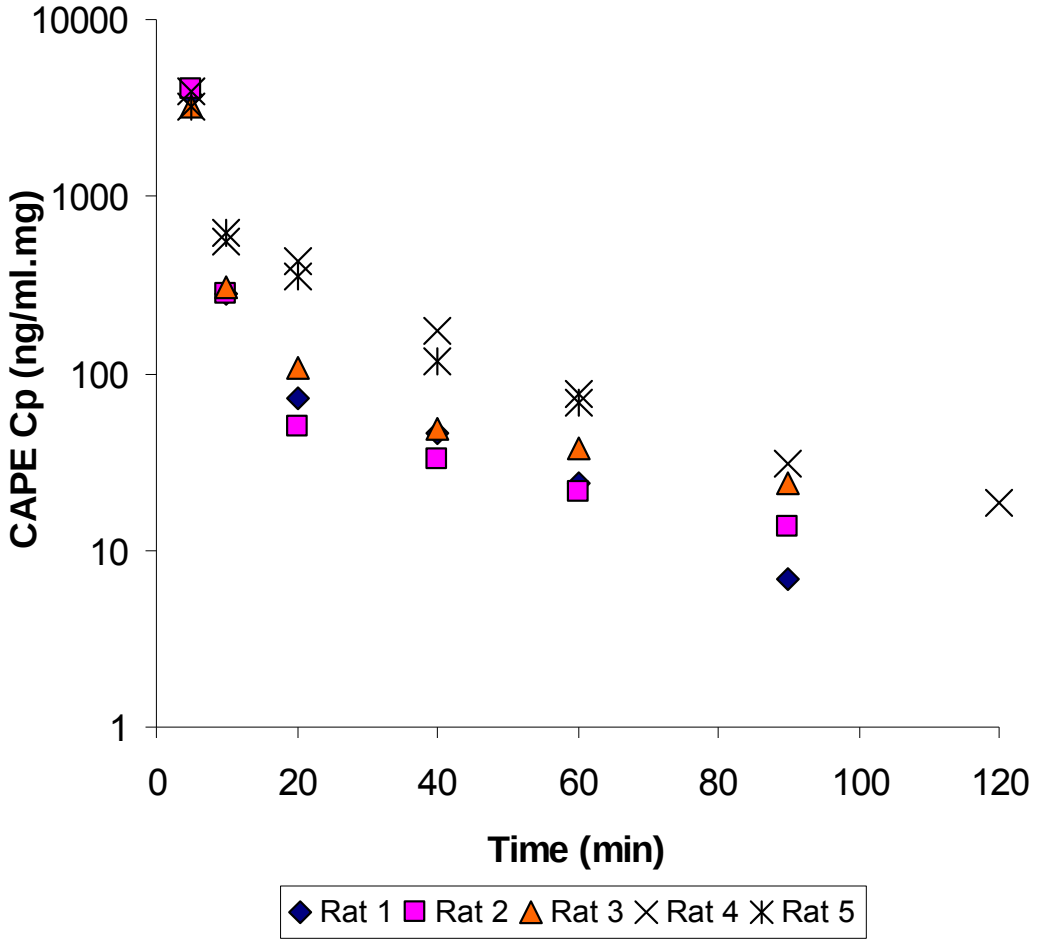

Figure 7.3: Semi logarithmic representation of the individual normalized plasma concentration (Cp) time profile of CAPE after intravenous bolus administration of 20 mg/kg CAPE to male Sprague Dawley rats.

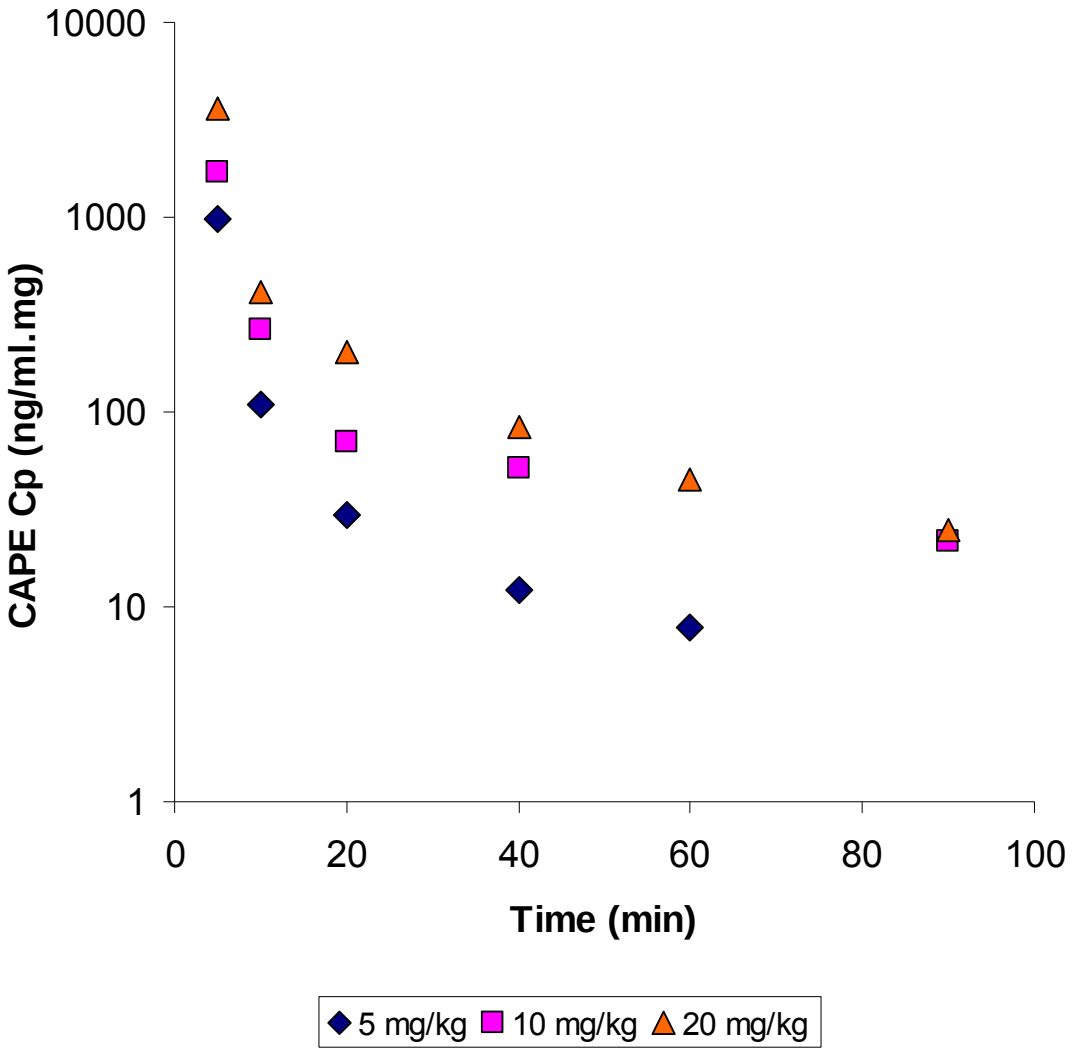

Figure 7.4: Superposition of dose-normalized average plasma concentrations (Cp) of CAPE as a function of time after intravenous bolus administration of 5, 10, and 20 mg/kg of CAPE to male Sprague Dawley rats (n=5).

Non-Compartmental Analysis Following Intravenous Bolus Administration of CAPE

Non-Compartmental Analysis (NCA) of the blood plasma concentration time data for CAPE at three doses was performed. The pharmacokinetic parameters obtained from the individual rat data are summarized in Table 7.4 – 7.6. The average of the pharmacokinetic parameters obtained from the individual plasma time curve were compared to the pharmacokinetic parameters obtained from the mean plasma concentration time curve for 5, 10, and 20 mg/kg of CAPE, respectively, in Table 7.7. Good agreement exists between the average of pharmacokinetic parameters obtained from the individual plasma concentration time data and from the pharmacokinetic parameters obtained from the mean plasma concentration time curve.

One-way analysis of variance (ANOVA) test comparing the mean PK parameters obtained following three doses of CAPE administration intravenously to Sprague Dawley rats were performed and the results were summarized in Table 7.8. There were statistically significant differences found in body weight normalized AUC_{∞}, total body clearance Cl, and volume of distribution Vd ($P < 0.05$). There were no statistically significant differences found in the terminal elimination rate constant (λ_z), elimination phase half-life ($t_{1/2-\lambda z}$), mean residence time (MRT), and volume of distribution at steady state (V_{ss}) ($P > 0.05$).

Figure 7.5 illustrates the relationship between dose and the area under the plasma concentration time curve from time zero to infinity (AUC_{∞}). It can be observed that as the dose increases the AUC_{∞} does not increase proportionally. It can be concluded from the data that dose proportionality does not exist in dose range studied in this investigation. The observed square of the correlation coefficient is 0.7058, which strengthens this conclusion.

Table 7.4: Pharmacokinetic parameters of CAPE obtained following intravenous bolus administration of 5 mg/kg CAPE to male Sprague Dawley rats (non-compartmental analysis).

PK parameter	Rat 1	Rat 2	Rat 3	Rat 4	Rat 5	Mean	SD
AUC_{∞}(μg·min/ml·kg)	209.6	80.4	155.1	77.0	230.8	150.6	71.2
Cl (ml/min·kg)	72.3	193.2	104.7	191.4	71.3	126.6	61.5
Vd (ml/kg)	2066	5163	3751	5886	2197	3813	1717
λ_Z (min^{-1})	0.035	0.037	0.028	0.033	0.032	0.033	0.004
λ_Z half-life (min)	19.8	18.5	24.8	21.3	21.4	21.2	2.4
MRT (min)	3.1	4.2	2.3	3.0	1.7	2.9	0.9
V_{ss} (ml/kg)	225.7	805.4	238.2	579.4	118.1	393.4	288.2
Weight (kg)	0.330	0.322	0.308	0.339	0.304	0.321	0.015

AUC_{∞}, Cl, Vd, and V_{ss} were normalized by body weight.

Table 7.5: Pharmacokinetic parameters of CAPE obtained following intravenous bolus administration of 10 mg/kg CAPE to male Sprague Dawley rats (non-compartmental analysis).

PK parameter	Rat 1	Rat 2	Rat 3	Rat 4	Rat 5	Mean	SD
AUC_{∞}(μg·min/ml·kg)	285.0	721.9	232.2	697.8	579.3	503.3	230.5
Cl (ml/min·kg)	98.3	42.9	161.3	40.8	45.7	77.8	52.5
Vd (ml/kg)	2651	4706	6255	1574	1296	3297	2129
λ_Z (min^{-1})	0.037	0.009	0.026	0.026	0.035	0.027	0.011
λ_Z half-life (min)	18.7	76.1	26.9	26.7	19.7	33.6	24.0
MRT (min)	2.8	35.4	7.7	1.6	2.0	9.9	14.5
V_{ss} (ml/kg)	279.4	1520.0	1247.6	63.9	90.6	640.3	690.5
Weight (kg)	0.357	0.323	0.267	0.351	0.378	0.335	0.043

AUC_{∞}, Cl, Vd, and V_{ss} were normalized by body weight.

Table 7.6: Pharmacokinetic parameters of CAPE obtained following intravenous bolus administration of 20 mg/kg CAPE to male Sprague Dawley rats (non-compartmental analysis).

PK parameter	Rat 1	Rat 2	Rat 3	Rat 4	Rat 5	Mean	SD
AUC_{∞}(μg·min/ml·kg)	2876	3357	2112	2172	1470	2398	732
Cl (ml/min·kg)	24.1	20.3	33.1	29.0	52.3	31.7	12.5
Vd (ml/kg)	715	1087	1645	1034	1262	1148	340
λ_Z (min^{-1})	0.034	0.019	0.020	0.028	0.042	0.028	0.010
λ_Z half-life (min)	20.6	37.2	34.4	24.7	16.7	26.7	8.8
MRT (min)	1.7	1.9	4.1	6.8	6.9	4.3	2.5
V_{ss} (ml/kg)	40.3	38.1	134.4	198.0	359.7	154.1	133.2
Weight (kg)	0.289	0.294	0.286	0.318	0.260	0.289	0.021

AUC_{∞}, Cl, Vd, and V_{ss} were normalized by body weight.

Table 7.7: Average of the pharmacokinetic parameters obtained from the individual plasma time curve and pharmacokinetic parameters obtained from the mean plasma concentration time curve at 5, 10, and 20 mg/kg of CAPE (non-compartmental analysis).

	5 mg/kg		10 mg/kg		20 mg/kg	
Pharmacokinetic parameters	Mean of Individual	Mean Cp	Mean of Individual	Mean Cp	Mean of Individual	Mean Cp
AUC_{∞}(μg·min/ml·kg)	150.6	144.2	503.3	419.2	2398	2162
Cl (ml/min·kg)	126.6	108.3	77.8	71.2	31.7	32.0
Vd (ml/kg)	3813	3233	3297	4253	1148	1087
λ_Z (min^{-1})	0.033	0.034	0.027	0.017	0.028	0.029
λ_Z half-life (min)	21.2	20.7	33.6	41.4	26.7	23.6
MRT (min)	2.9	2.7	9.9	9.5	4.3	4.2
V_{ss} (ml/kg)	393.4	289.1	640.3	674.6	154.1	134.8

AUC_{∞}, Cl, Vd, and V_{ss} were normalized by body weight.

Table 7.8: ANOVA results comparing the mean values of pharmacokinetic parameters of CAPE obtained following intravenous bolus administration of CAPE at 5 mg/kg, 10 mg/kg, and 20 mg/kg to Sprague Dawley rats.

Pharmacokinetic parameters	5 mg/kg Mean ± SD	10 mg/kg Mean ± SD	20 mg/kg Mean ± SD	ANOVA P value
AUC_{∞}(μg·min/ml·kg)	150.6 ± 71.2	503.3 ± 230.5	2398 ± 732	0.000*
Cl (ml/min·kg)	126.6 ± 61.5	77.8 ± 52.5	31.7 ± 12.5	0.026*
Vd (ml/kg)	3813 ± 1717	3297 ± 2129	1148 ± 340	0.048*
λ_Z (min^{-1})	0.033 ± 0.004	0.027 ± 0.011	0.028 ± 0.010	0.513
λ_Z half-life (min)	21.2 ± 2.4	33.6 ± 24.0	26.7 ± 8.8	0.439
MRT (min)	2.9 ± 0.9	9.9 ± 14.5	4.3 ± 2.5	0.410
V_{ss} (ml/kg)	393.4 ± 288.2	640.3 ± 690.5	154.1 ± 133.2	0.103

* P value < 0.05 was considered significantly different.
AUC_{∞}, Cl, Vd, and V_{ss} were normalized by body weight.

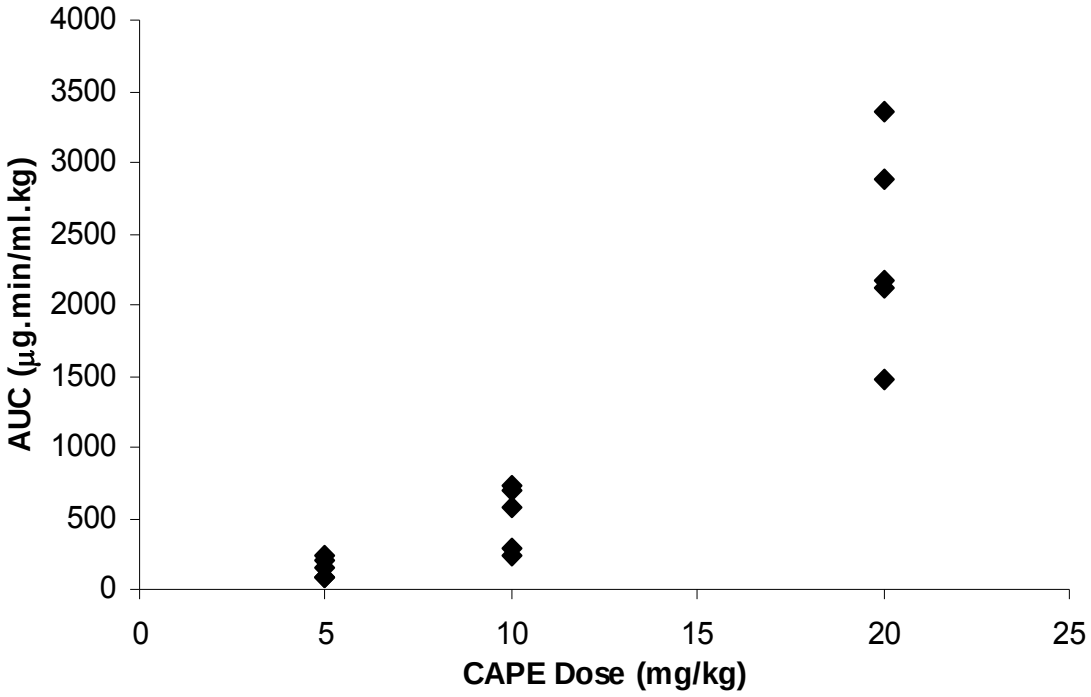

Figure 7.5: Relationship of the area under the plasma concentration time curve versus dose of CAPE (non-compartmental analysis).

Bi-Exponential Fit Following Intravenous Bolus Administration of CAPE

The individual blood plasma concentration time data for CAPE at three doses were fitted by non-linear regression to a bi-exponential equation (7.8). The individual pharmacokinetic parameters obtained from the individual plasma concentration time profile are summarized in Table 7.9 – 7.11. The average of the pharmacokinetic parameters obtained from the individual plasma time curve were compared to the pharmacokinetic parameters obtained from the mean plasma concentration time curve for 5, 10, and 20 mg/kg of CAPE, respectively, and shown in Table 7.12. There is a relatively good agreement between the average of the individual pharmacokinetic parameters and the pharmacokinetic parameters obtained from the mean plasma concentration time curve. The fit of the mean plasma concentration time curves for the 5, 10, and 20 mg/kg CAPE is represented in Figure 7.6 to 7.8, respectively. The average of the individual pharmacokinetic parameters and the pharmacokinetic parameters from the mean plasma concentration time curve both obtained from the bi-exponential fit were compared to those both obtained from the non-compartmental analysis (NCA). The results are shown in Table 7.13. The data suggest that the PK parameters estimated from both NCA and bi-exponential fit are relatively in good agreement. Some of the differences may be attributable to the large variance observed in the individual data.

Figure 7.9 illustrates the relationship between dose and the area under the plasma concentration time curve from time zero to infinity (AUC_∞). It can be observed that as the dose increases the AUC_∞ does not increase proportionally. It can be concluded from the data that dose proportionality does not exist in the dose range studied in this investigation. The observed square of the correlation coefficient is 0.7715, which strengthens this conclusion.

Table 7.9: Pharmacokinetic parameters of CAPE obtained following intravenous bolus administration of 5 mg/kg CAPE to male Sprague Dawley rats (bi-exponential fit).

PK parameter	Rat 1	Rat 2	Rat 3	Rat 4	Rat 5	Mean	SD
AUC (μg·min/ml·kg)	192.8	72.6	150.9	86.3	180.8	136.7	54.7
Cl (ml/min·kg)	78.6	214.0	107.6	171.0	90.9	132.4	57.8
Vd (ml/kg)	2068	5632	3587	5344	2674	3861	1584
$t_{1/2}$ (min)	18.5	18.5	23.1	22.0	20.4	20.5	2.1
MRT (min)	3.9	4.7	3.0	3.6	2.8	3.6	0.8
Vss (ml/kg)	307.8	1012.2	324.1	610.9	256.1	502.2	317.0
A (μg/ml·kg)	88.2	28.8	91.6	50.8	90.2	69.9	28.6
B (μg/ml·kg)	0.558	0.275	0.205	0.180	0.196	0.283	0.158
α (min^{-1})	0.496	0.441	0.636	0.631	0.515	0.544	0.086
β (min^{-1})	0.038	0.038	0.030	0.032	0.034	0.034	0.003
Weight (kg)	0.330	0.322	0.308	0.339	0.304	0.321	0.015

AUC_{∞}, Cl, Vd, V_{ss}, A, and B were normalized by body weight.

Table 7.10: Pharmacokinetic parameters of CAPE obtained following intravenous bolus administration of 10 mg/kg CAPE to male Sprague Dawley rats (bi-exponential fit).

PK parameter	Rat 1	Rat 2	Rat 3	Rat 4	Rat 5	Mean	SD
AUC (μg·min/ml·kg)	254.0	677.7	207.1	567.9	492.8	439.9	202.8
Cl (ml/min·kg)	110.3	45.7	180.9	50.2	53.7	88.1	58.1
Vd (ml/kg)	2981	4570	7236	1859	1492	3628	2346
$t_{1/2}$ (min)	18.7	69.3	27.7	25.7	19.3	32.1	21.1
MRT (min)	3.9	34.0	8.6	2.8	3.2	10.5	13.3
Vss (ml/kg)	434.0	1554.0	1560.2	139.4	171.4	771.8	725.9
A (μg/ml·kg)	112.0	177.3	58.4	333.9	243.3	185.0	108.4
B (μg/ml·kg)	0.692	2.187	0.787	0.491	0.869	1.005	0.675
α (min^{-1})	0.476	0.386	0.333	0.607	0.519	0.464	0.108
β (min^{-1})	0.037	0.010	0.025	0.027	0.036	0.027	0.011
Weight (kg)	0.357	0.323	0.267	0.351	0.378	0.335	0.043

AUC_{∞}, Cl, Vd, V_{ss}, A, and B were normalized by body weight.

Table 7.11: Pharmacokinetic parameters of CAPE obtained following intravenous bolus administration of 20 mg/kg CAPE to SD rats (bi-exponential fit).

PK parameter	Rat 1	Rat 2	Rat 3	Rat 4	Rat 5	Mean	SD
AUC (μg·min/ml·kg)	2480	2507	1907	2733	2264	2378	311
Cl (ml/min·kg)	27.9	27.1	36.7	23.0	34.0	29.7	5.5
Vd (ml/kg)	846	1426	1748	821	791	1126	436
$t_{1/2}$ (min)	21.0	35.7	33.0	24.4	16.1	26.0	8.2
MRT (min)	2.7	3.2	5.1	6.8	5.0	4.6	1.6
Vss (ml/kg)	74.9	86.7	187.9	155.9	170.9	135.3	51.1
A (μg/ml·kg)	1439	1404	984	1389	1191	1281	192
B (μg/ml·kg)	2.92	1.43	2.91	11.85	15.55	6.93	6.35
α (min^{-1})	0.602	0.577	0.556	0.600	0.625	0.592	0.026
β (min^{-1})	0.033	0.019	0.021	0.028	0.043	0.029	0.010
Weight (kg)	0.289	0.294	0.286	0.318	0.260	0.289	0.021

AUC_{∞}, Cl, Vd, V_{ss}, A, and B were normalized by body weight.

Table 7.12: Average of the pharmacokinetic parameters obtained from the individual plasma time curve and pharmacokinetic parameters obtained from the mean plasma concentration time curve at 5, 10, and 20 mg/kg of CAPE (bi-exponential fit).

	5 mg/kg		10 mg/kg		20 mg/kg	
Pharmacokinetic parameters	Mean of Individual	Mean Cp	Mean of Individual	Mean Cp	Mean of Individual	Mean Cp
AUC (μg·min/ml·kg)	136.7	131.7	439.9	379.5	2378	2639
Cl (ml/min·kg)	132.4	118.5	88.1	78.6	29.7	26.2
Vd (ml/kg)	3861	3118	3628	4913	1126	819
$t_{1/2}$ (min)	20.5	18.1	32.1	44.1	26.0	21.7
MRT (min)	3.6	3.4	10.5	11.9	4.6	4.2
V_{ss} (ml/kg)	502.2	402.3	771.8	932.9	135.3	108.7
A (μg/ml·kg)	69.9	65.2	185.0	138.1	1281	1509
B (μg/ml·kg)	0.283	0.314	1.005	0.930	6.93	7.27
α (min^{-1})	0.544	0.528	0.464	0.431	0.592	0.626
β (min^{-1})	0.034	0.038	0.027	0.016	0.029	0.032

AUC_{∞}, Cl, Vd, V_{ss}, A, and B were normalized by body weight.

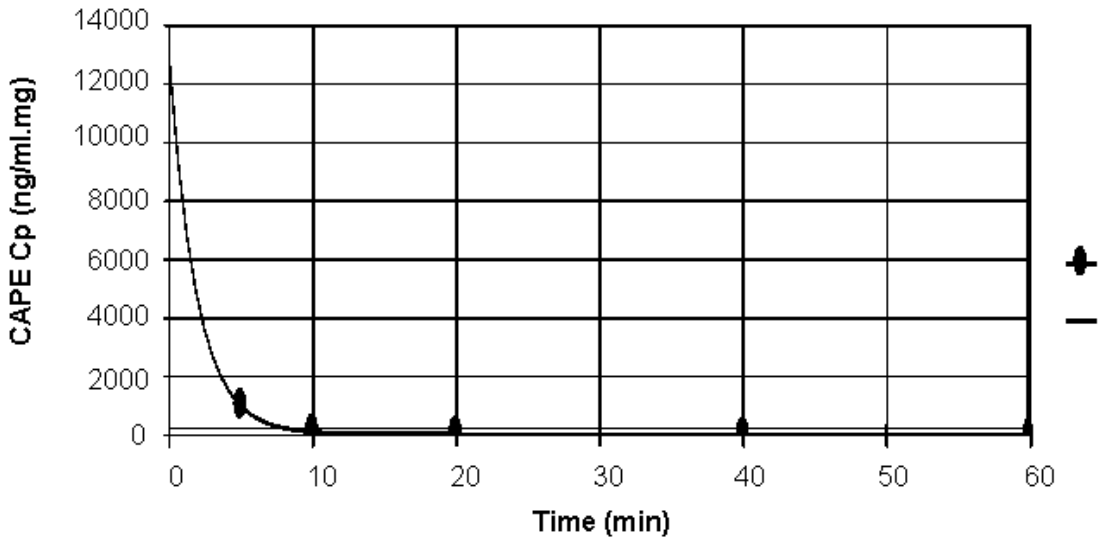

Figure 7.6: The typical bi-exponential fit obtained from the mean plasma concentration time data for 5 mg/kg of CAPE. –: fitted line; ●: observed plasma concentration.

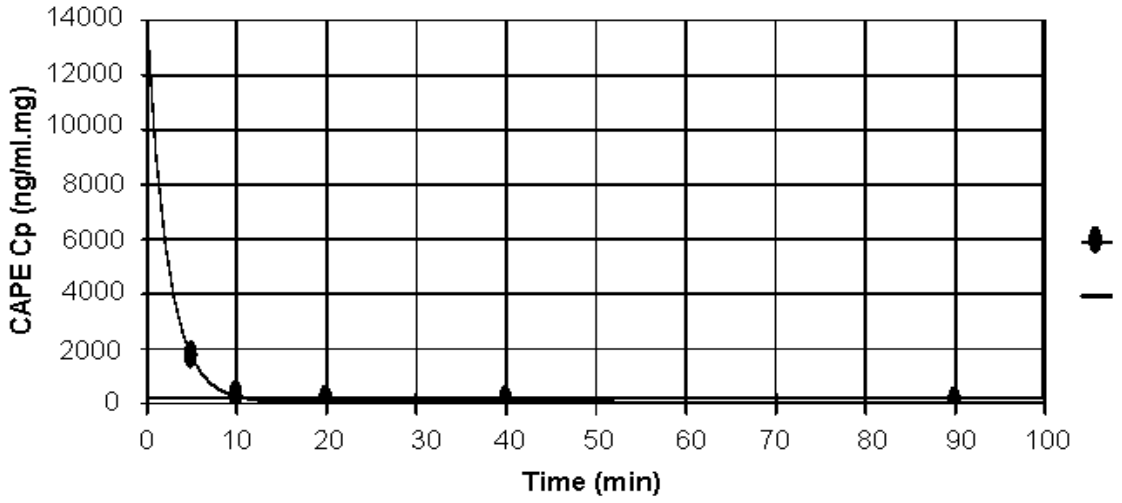

Figure 7.7: The typical bi-exponential fit obtained from the mean plasma concentration time data for 10 mg/kg of CAPE. –: fitted line; ●: observed plasma concentration.

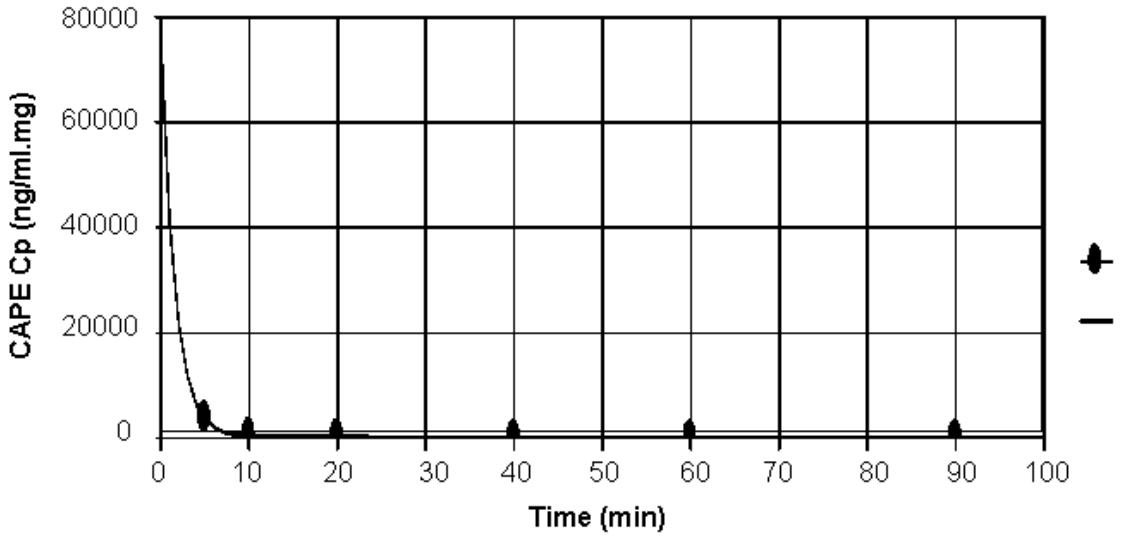

Figure 7.8: The typical bi-exponential fit obtained from the mean plasma concentration time data for 20 mg/kg of CAPE. –: fitted line; ●: observed plasma concentration.

Table 7.13: Comparison of average of the pharmacokinetic parameters obtained from the individual plasma concentration (Cp) time curve and pharmacokinetic parameters obtained from the mean Cp time curve at 5, 10, and 20 mg/kg of CAPE by non-compartmental analysis (NCA) and bi-exponential fit.

Pharmacokinetic parameters	Average of Individual					
	5 mg/kg		10 mg/kg		20 mg/kg	
	NCA	fit	NCA	fit	NCA	fit
AUC_{∞}(μg·min/ml·kg)	150.6	136.7	503.3	439.9	2398	2378
Cl (ml/min·kg)	126.6	132.4	77.8	88.1	31.7	29.7
Vd (ml/kg)	3813	3861	3297	3628	1148	1126
$t_{1/2}$ (min)	21.2	20.5	33.6	32.1	26.7	26.0
MRT (min)	2.9	3.6	9.9	10.5	4.3	4.6
V_{ss} (ml/kg)	393.4	502.2	640.3	771.8	154.1	135.3
	Mean Cp					
	NCA	fit	NCA	fit	NCA	fit
AUC_{∞}(μg·min/ml·kg)	144.2	131.7	419.2	379.5	2162	2639
Cl (ml/min·kg)	108.3	118.5	71.2	78.6	32.0	26.2
Vd (ml/kg)	3233	3118	4253	4913	1087	819
$t_{1/2}$ (min)	20.7	18.1	41.4	44.1	23.6	21.7
MRT (min)	2.7	3.4	9.5	11.9	4.2	4.2
V_{ss} (ml/kg)	289.1	402.3	674.6	932.9	134.8	108.7

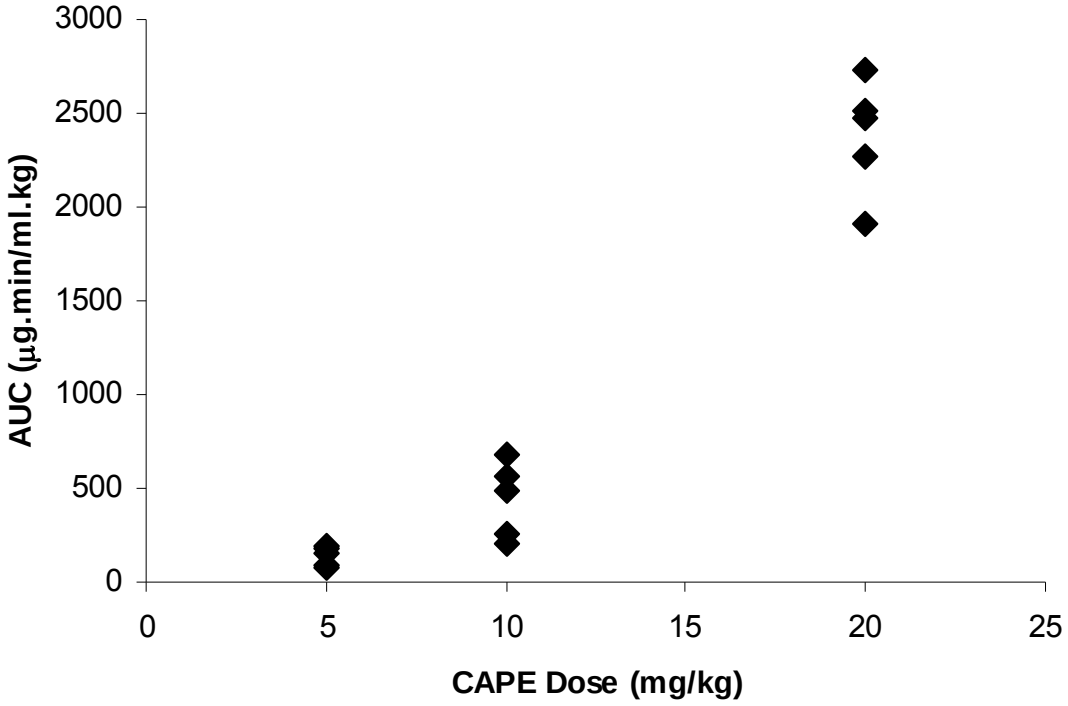

Figure 7.9: Relationship of the area under the plasma concentration time curve versus dose of CAPE (bi-exponential fit).

7.3.2 Pharmacokinetics of FCAPE

The plasma concentrations (normalized by individual dose in mg) of FCAPE after intravenous bolus administration to male Sprague Dawley rats at dose of 20 mg/kg of FCAPE are summarized in Table 7.14. The graphic representation of FCAPE plasma concentration-time profile in semi-log scale is illustrated in Figure 7.10. FCAPE shows a rapid distribution phase reflected by the rapid decline of the plasma concentrations from 5 to 15 minutes after intravenous administration of 20 mg/kg FCAPE.

Table 7.14: Observed plasma concentrations normalized by individual dose (ng/ml·mg) of FCAPE following intravenous administration of 20 mg/kg FCAPE to male Sprague Dawley rats.

Time (min)	Rat 1	Rat 2	Rat 3	Rat 4	Rat 5	Mean	SD
5	1310.6	1053.4	683.8	1351.0	877.2	1055.2	283.9
10	196.6	227.8	113.8	NA	174.2	178.1	48.2
20	54.9	125.1	25.7	281.2	72.3	111.9	101.3
40	30.9	70.4	14.3	212.6	26.5	70.9	82.0
60	26.6	44.8	7.7	117.8	15.0	42.4	44.4
90	15.5	23.1	4.3	75.3	NU	26.4	28.1
120	12.3	15.7	NU	51.0	NU	19.4	18.0
180	NU	NU	NU	NU	NU	NU	
Dose (mg)	5.1	5.84	5.52	6.18	5.76	5.68	0.40
weight (kg)	0.255	0.292	0.276	0.309	0.288	0.284	0.020

NA: not available.
NU: not usable for pharmacokinetic analysis.

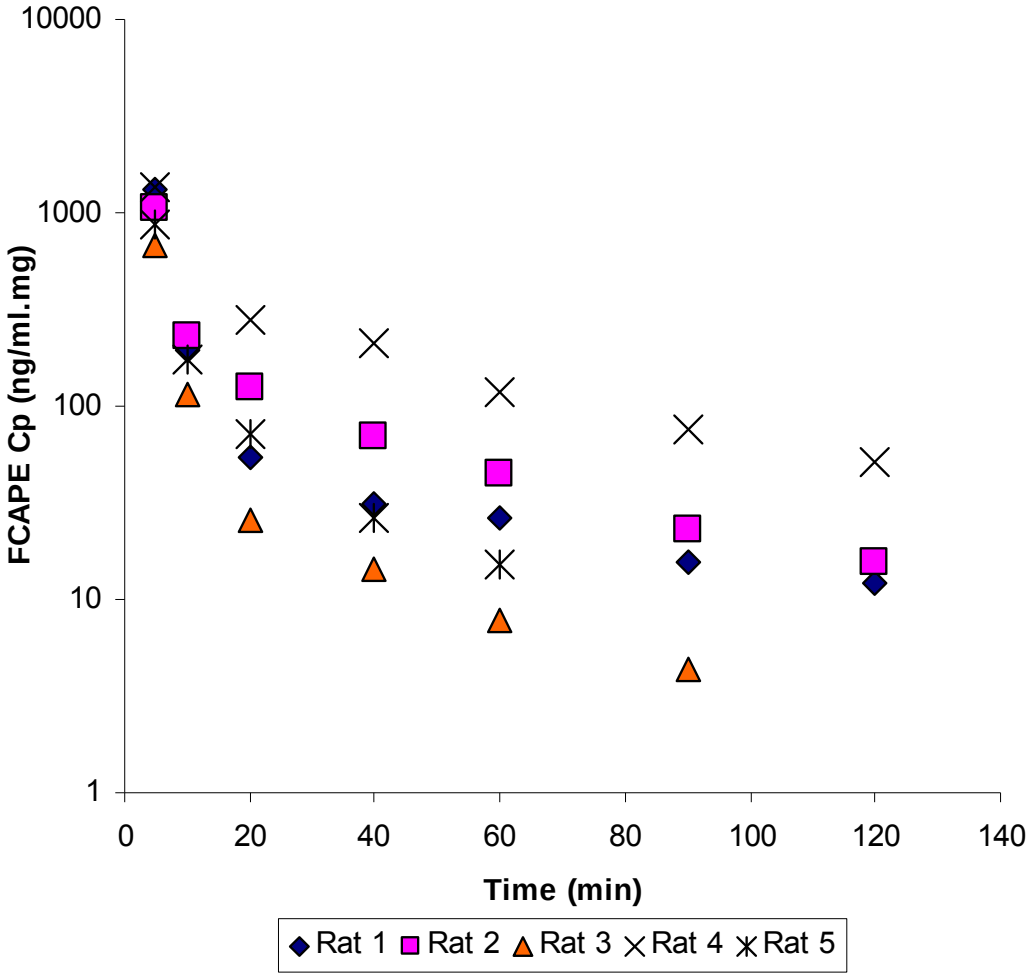

Figure 7.10: Semi logarithmic representation of the individual normalized plasma concentration (Cp) time profile of FCAPE after intravenous bolus administration of 20 mg/kg FCAPE to male Sprague Dawley rats.

Non-Compartmental Analysis Following Intravenous Administration of FCAPE

Non-Compartmental Analysis (NCA) of the blood plasma concentration time data for FCAPE was performed. The pharmacokinetic parameters obtained from the individual rat data are summarized in Table 7.15. The average of the pharmacokinetic parameters obtained from the individual plasma time curve were compared to the pharmacokinetic parameters obtained from the mean plasma concentration time curve for FCAPE in Table 7.16. The comparison showed that the majority of PK parameters obtained from both analyses appear to be in good agreement.

Independent Samples t-test comparing the PK parameters of CAPE versus FCAPE at 20 mg/kg dose was performed and the results are summarized in Table 7.17. Statistically significant differences were found in body weight normalized AUC_{∞}, total body clearance Cl, volume of distribution Vd, and volume of distribution at steady state (V_{ss}) ($P < 0.05$). There were no statistically significant differences found in the terminal elimination rate constant (λ_z), elimination phase half-life ($t_{1/2-\lambda z}$), and mean residence time (MRT) ($P > 0.05$). The results suggest that total body clearance for FCAPE is significantly greater than that of CAPE, probably indicating that the change in clearance was due to a change in volume of distribution.

Table 7.15: Pharmacokinetic parameters of FCAPE obtained following intravenous bolus administration of 20 mg/kg FCAPE to rats (non-compartmental analysis).

PK parameter	Rat 1	Rat 2	Rat 3	Rat 4	Rat 5	Mean	SD
AUC_{∞}(μg·min/ml·kg)	672.5	504.8	312.8	744.9	377.6	522.5	185.2
Cl (ml/min·kg)	116.6	135.7	231.7	86.9	183.9	150.9	57.3
Vd (ml/kg)	9492	6520	9013	4933	4677	6927	2244
λ_Z (min^{-1})	0.012	0.021	0.026	0.018	0.039	0.023	0.010
λ_Z half-life (min)	56.4	33.3	27.0	39.4	17.6	34.7	14.5
MRT (min)	11.7	16.7	5.4	35.4	6.3	15.1	12.2
V_{ss} (ml/kg)	1367.2	2267.9	1239.7	3078.5	1163.6	1823.4	830.2
Weight (kg)	0.255	0.292	0.276	0.309	0.288	0.284	0.020

AUC_{∞}, Cl, Vd, and V_{ss} were normalized by body weight.

Table 7.16: Average of the pharmacokinetic parameters obtained from the individual plasma time curve and pharmacokinetic parameters obtained from the mean plasma concentration time curve at 20 mg/kg of FCAPE (non-compartmental analysis).

Pharmacokinetic parameters	Mean of Individual	Mean Cp
AUC_{∞} (μg·min/ml·kg)	522.5	571.6
Cl (ml/min·kg)	150.9	123.2
Vd (ml/kg)	6927	6977
λ_Z (min^{-1})	0.023	0.018
λ_Z half-life (min)	34.7	39.3
MRT (min)	15.1	17.3
V_{ss} (ml/kg)	1823.4	2129.1

AUC_{∞}, Cl, Vd, and V_{ss} were normalized by body weight.

Table 7.17: Independent Samples t-test results of pharmacokinetic parameters of CAPE and FCAPE obtained following intravenous bolus administration of CAPE and FCAPE at 20 mg/kg to rats, respectively.

Pharmacokinetic parameters	FCAPE Mean ± SD	CAPE Mean ± SD	t-test P value
AUC_{∞} (μg·min/ml·kg)	522.5 ± 185.2	2398 ± 732	0.004*
Cl (ml/min·kg)	150.9 ± 57.3	31.7 ± 12.5	0.008*
Vd (ml/kg)	6927 ± 2244	1148 ± 340	0.004*
λ_Z (min^{-1})	0.023 ± 0.010	0.028 ± 0.010	0.415
λ_Z half-life (min)	34.7 ± 14.5	26.7 ± 8.8	0.323
MRT (min)	15.1 ± 12.2	4.3 ± 2.5	0.089
V_{ss} (ml/kg)	1823.4 ± 830.2	154.1 ± 133.2	0.010*

* P value < 0.05 was considered significantly different.
AUC_{∞}, Cl, Vd, and V_{ss} were normalized by body weight.

Bi-Exponential Fit Following Intravenous Bolus Administration of FCAPE

The individual blood plasma concentration time data for FCAPE were fitted by non-linear regression to a bi-exponential equation (7.8). The individual pharmacokinetic parameters obtained from the individual plasma concentration time profile are summarized in Table 7.18. The average of the pharmacokinetic parameters obtained from the individual plasma time curve were compared to the pharmacokinetic parameters obtained from the mean plasma concentration time curve for 20 mg/kg of FCAPE and shown in Table 7.19. There is a good agreement between the average of the individual pharmacokinetic parameters and the pharmacokinetic parameters obtained from the mean plasma concentration time curve. The fit of the mean plasma concentration time curve for 20 mg/kg of FCAPE is represented in Figure 7.11. The average of the individual pharmacokinetic parameters and the pharmacokinetic parameters from the mean plasma concentration time curve both obtained from bi-exponential fit were compared to those both obtained from non-compartmental analysis (NCA) in Table 7.20. The data suggest that the PK parameters estimated from both NCA and bi-exponential fit are relatively in good agreement. Some of the differences may be attributable to the large variance observed in the individual data.

Table 7.18: Pharmacokinetic parameters of FCAPE obtained following intravenous bolus administration of 20 mg/kg FCAPE to male Sprague Dawley rats (bi-exponential fit).

PK parameter	Rat 1	Rat 2	Rat 3	Rat 4	Rat 5	Mean	SD
AUC (μg·min/ml·kg)	597.0	592.1	278.4	751.9	430.3	530.0	180.8
Cl (ml/min·kg)	131.4	115.7	260.3	86.1	161.4	151.0	66.9
Vd (ml/kg)	7729	4628	9641	4783	3587	6074	2520
$t_{1/2}$ (min)	41.1	28.0	25.7	38.2	15.5	29.7	10.3
MRT (min)	10.3	12.5	6.3	33.6	5.7	13.7	11.5
Vss (ml/kg)	1351.6	1450.9	1632.2	2889.1	919.8	1648.7	741.2
A (μg/ml·kg)	226.5	215.8	102.3	102.6	173.9	164.2	59.7
B (μg/ml·kg)	1.41	4.01	0.84	8.00	3.50	3.552	2.826
α (min^{-1})	0.442	0.502	0.413	0.330	0.493	0.436	0.070
β (min^{-1})	0.017	0.025	0.027	0.018	0.045	0.026	0.011
Weight (kg)	0.255	0.292	0.276	0.309	0.288	0.284	0.020

AUC_{∞}, Cl, Vd, V_{ss}, A, and B were normalized by body weight.

Table 7.19: Average of the pharmacokinetic parameters obtained from the individual plasma time curve and pharmacokinetic parameters obtained from the mean plasma concentration time curve at 20 mg/kg of FCAPE (bi-exponential fit).

Pharmacokinetic parameters	Mean of Individual	Mean Cp
AUC (μg·min/ml·kg)	530.0	761.3
Cl (ml/min·kg)	151.0	92.5
Vd (ml/kg)	6074	4205
$t_{1/2}$ (min)	29.7	32.2
MRT (min)	13.7	10.8
V_{ss} (ml/kg)	1648.7	999.0
A (μg/ml·kg)	164.2	363.5
B (μg/ml·kg)	3.552	3.347
α (min^{-1})	0.436	0.600
β (min^{-1})	0.026	0.022

AUC_{∞}, Cl, Vd, V_{ss}, A, and B were normalized by body weight.

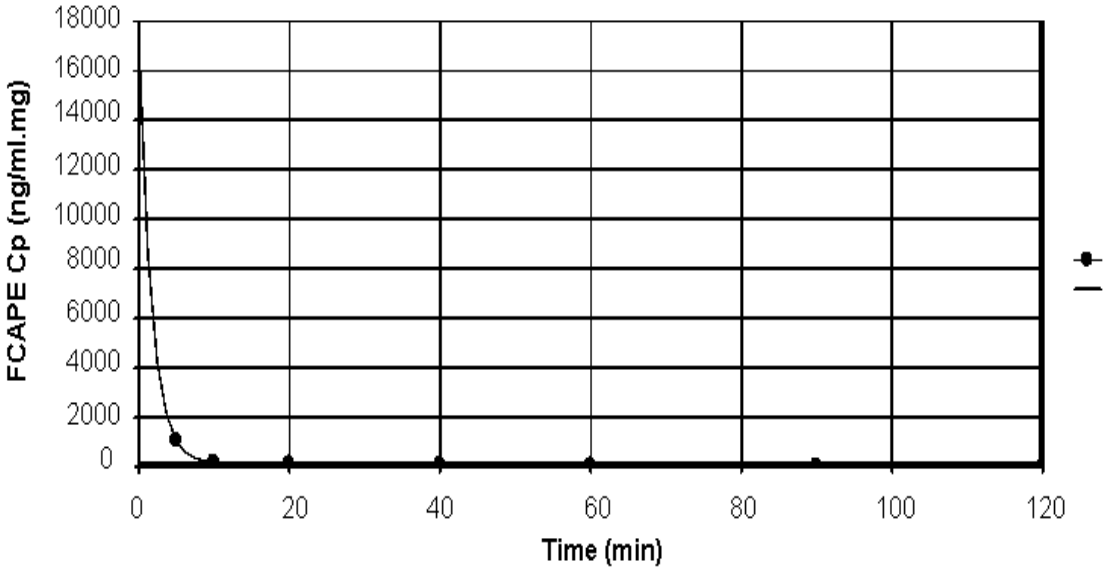

Figure 7.11: The typical bi-exponential fit obtained from the mean plasma concentration time data for 20 mg/kg of FCAPE. –: fitted line; ●: observed plasma concentration.

Table 7.20: Comparison of average of the pharmacokinetic parameters obtained from the individual plasma time curve and pharmacokinetic parameters obtained from the mean plasma concentration (Cp) time curve at 20 mg/kg of FCAPE by non-compartmental analysis (NCA) and bi-exponential fit.

Pharmacokinetic	Mean of Individual		Mean Cp	
parameters	NCA	fit	NCA	fit
AUC_{∞}(μg·min/ml·kg)	522.5	530.0	571.6	761.3
Cl (ml/min·kg)	150.9	151.0	123.2	92.5
Vd (ml/kg)	6927	6074	6977	4205
$t_{1/2}$ (min)	34.7	29.7	39.3	32.2
MRT (min)	15.1	13.7	17.3	10.8
V_{ss} (ml/kg)	1823.4	1648.7	2129.1	999.0

7.4 CONCLUSIONS

The pharmacokinetic profiles of CAPE and FCAPE were characterized following single intravenous bolus administration of 5, 10, and 20 mg/kg of CAPE and 20 mg/kg of FCAPE to male Sprague Dawley rats, respectively. The plasma concentrations of both CAPE and FCAPE at the doses tested declined very fast with approximate distribution half life of 1.31 min and 1.16 min for CAPE and FCAPE, respectively. The pharmacokinetic parameters estimated from the bi-exponential fit are relatively in good agreement with those obtained from non-compartmental analysis.

The total body clearance of CAPE decreased significantly as the doses of CAPE increased followed by a significant increase in area under the plasma concentration time curve, which suggests a possible saturation process. The data showed that dose proportionality dose not exist within the dose range studied in this investigation for CAPE, which is in agreement with the change of clearance among the doses examined. The dose-normalized average plasma concentrations of CAPE were not superimposable suggesting non-linearity. The change in the clearance appears to be due to the change in volume of distribution. It should be noted that the elimination half life is not significantly different within three dose group of CAPE.

The elimination half life was found not to be significantly different between CAPE and FCAPE ($P > 0.05$). However, there are significant differences ($P < 0.05$) between the clearance of FCAPE and CAPE suggesting that the volume of distribution of these compounds is different. Thus, further investigation is needed to elucidate the cause(s) of the differences observed in the total body clearance of these compounds. It can be postulated that differences in plasma protein binding and/or tissue binding and/or

renal excretion and/or hepatic metabolism might exist, which may help explain this observation.

Chapter VIII: Conclusions

Ischemia/reperfusion (I/R) injury is a serious pathological condition associated with cardiovascular diseases, surgical procedures, and traumatic injury, which may lead to death. Recently, caffeic acid phenethyl ester (CAPE), a plant-derived polyphenolic compound, has been shown to ameliorate I/R injury in organs and tissues in a variety of different animal models. In this dissertation, to better understand the mechanism of cytoprotection by CAPE, an *in vitro* model simulating I/R injury was developed and investigated. The structure cytoprotective relationships of CAPE and its fluorinated derivatives (FCAPEs) were also investigated, and the pharmacokinetic profiles of CAPE and its most cytoprotective analogue FCAPE were determined in rats.

CAPE cytoprotection mechanism investigation:

An *in vitro* model was developed using menadione (MD)-induced oxidative stress to human umbilical vein endothelial cells (HUVEC). This model produced an oxidant stress that simulated I/R injury. Good dose-dependent cytoprotection of CAPE was observed against MD cytotoxicity in HUVEC after 6 hr pretreatment. CAPE at 5 μg/ml exhibited the best cytoprotection. Gene expression analysis was performed to examine the alteration of endothelial cell gene transcription induced by 5 μg/ml CAPE for 6 hrs. Heme oxygenase-1 (HO-1) was found to be significantly upregulated in its expression by microarray analysis. This result was confirmed by real time RT-PCR and western blot. The importance of HO-1 induction for CAPE cytoprotection was suggested by the HO-1 inhibitor SnPPIX, which dose-dependently abrogated the cytoprotective effect of CAPE.

CAPE structure cytoprotection relationship:

Six new CAPE derivatives fluorinated on the catechol ring were prepared with the Wittig reaction. The cytotoxicity profiles of these derivatives in HUVEC and their cytoprotection profiles in the HUVEC-MD model were established. CAPE-1, 2, 3, and 4 showed cytotoxicity at the highest dose (15 μg/ml) tested, similar to CAPE. CAPE-5 and 6 did not show any cytotoxicity at any tested dose. Most fluorinated derivatives of CAPE showed dose-dependent cytoprotection except CAPE-2. At equimolar concentrations (20 μM), CAPE-1 (FCAPE) showed the greatest cytoprotection with no significant difference from CAPE.

Further mechanism investigation: HO-1 induction versus antioxidant activity:

Cell-based antioxidant activities of CAPE and derivatives at 20 μM were examined by measuring the alteration of ROS level in HUVEC. HO-1 mRNA induction by 20 μM CAPE and derivatives was performed by real time RT-PCR. The correlation between cytoprotection by CAPE derivatives and antioxidant activity could not be confirmed. The best correlation of structure and cytoprotection was with HO-1 mRNA induction for most CAPE derivatives except CAPE-2. It was able to induce HO-1 mRNA, but was not cytoprotective. The lack of HO-1 protein production by CAPE-2 may account for its failure to be cytoprotective. The results suggested that CAPE and most of its derivatives are cytoprotective against oxidative stress in human endothelial cell culture, and this *in vitro* beneficial effects correlate with their ability to induce HO-1 rather than their directly antioxidant activity.

Stability of CAPE and FCAPE in rat plasma:

It was useful to obtain *in vivo* information of how CAPE and its most cytoprotective derivative FCAPE were distributed and eliminated as a function of time in animals following intravenous administration, which may provide some insight into their beneficial effects *in vivo*. Before pharmacokinetic characterization, however, the stability of CAPE and FCAPE in plasma needed to be addressed to prevent their further degradation in post-collection plasma samples as degradation of the compound could compromise the pharmacokinetic results. First-order hydrolysis kinetics of CAPE and FCAPE were observed in male Sprague Dawley rat plasma at 4, 25, and 37 °C. The activation energy for CAPE and FCAPE hydrolysis was estimated with Arrhenius equation and found to be 17.9 and 20.1 kcal/mol, respectively, suggesting that FCAPE is more stable than CAPE in rat plasma. The addition of the esterase inhibitor sodium fluoride (0.4%) and pH adjustment to 6 with 0.1 M acetate buffer retained the integrity of CAPE and FCAPE in rat plasma within the time period required.

Quantitative determination of CAPE and FCAPE in rat plasma:

An analytical method using ultra-performance liquid chromatography with electrospray ionization tandem mass spectrometry was developed for the quantitative determination of CAPE and FCAPE in rat plasma. This method was selective for the quantification of CAPE and FCAPE, and no endogenous interference was found in the area of interest. The method was validated over the calibration curve range of 1 to 1000 ng/ml CAPE or FCAPE, which was fitted using quadratic regression with 1/concentration weighting. Three-day validation results showed inter/intraday precision and accuracy for

CAPE and FCAPE were within 15 % variability. Stability and recovery studies were performed, and results were acceptable. This fast, sensitive, and reliable quantitative method was applied for the determination of pharmacokinetics of CAPE and FCAPE in rats.

Pharmacokinetic characterization of CAPE and FCAPE:

Pharmacokinetic (PK) profiles of CAPE and FCAPE was established following intravenous bolus administration of CAPE at 5, 10, and 20 mg/kg, and 20 mg/kg FCAPE to jugular vein catheterized male Sprague Dawley rats, respectively. Primary pharmacokinetic parameters of CAPE and FCAPE were estimated from non-compartmental analysis and bi-exponential fit. Relatively good agreement was observed for the PK parameters obtained from both analyses. At the doses used, dose proportionality of CAPE was not established. This was supported by the observed change of clearance and non-superimposable dose-normalized average plasma concentrations of CAPE. Statistically significant differences in total body clearance were observed between CAPE and FCAPE at the 20 mg/kg dose, which may be attributable to the differences in volume of distribution. It should be noted that the elimination half lives for CAPE and FCAPE were not statistically different.

In conclusion, the cytoprotective effect of CAPE against oxidative stress in human endothelial cells was attributed to its ability to alter transcriptional event of cells, especially the induction of cytoprotective gene heme oxygenase-1. The selective chemical modifications of CAPE provided insight into receptor binding for HO-1 induction, and further confirmed the importance of HO-1 induction for CAPE

cytoprotection. A direct antioxidant activity of CAPE for its cytoprotective effect was not supported by comparison to other derivatives that were not cytoprotective. One fluorinated derivative (FCAPE) with similar cytoprotective effect as CAPE in cell culture exhibited better stability in rat plasma. Pharmacokinetic results suggest that dose proportionality was not apparent for CAPE within the doses tested in Sprague Dawley rats. FCAPE may distribute more extensively into tissue than CAPE due to observed higher volume of distribution for FCAPE, which may indicate that FCAPE could exert its beneficial effect more extensively in tissues than CAPE.

Bibliography

1. The National Heart, Lung, and Blood Institute (NHLBI). 2004 [cited; Available from: http://grants.nih.gov/grants/guide/rfa-files/RFA-HL-04-016.html.

2. Ferrari, R., et al., *Role of oxygen free radicals in ischemic and reperfused myocardium.* Am J Clin Nutr, 1991. **53**(1 Suppl): p. 215S-222S.

3. Zweier, J.L. and M.A. Talukder, *The role of oxidants and free radicals in reperfusion injury.* Cardiovasc Res, 2006. **70**(2): p. 181-90.

4. Granger, D.N., M.E. Hollwarth, and D.A. Parks, *Ischemia-reperfusion injury: role of oxygen-derived free radicals.* Acta Physiol Scand Suppl, 1986. **548**: p. 47-63.

5. Carden, D.L. and D.N. Granger, *Pathophysiology of ischaemia-reperfusion injury.* J Pathol, 2000. **190**(3): p. 255-66.

6. McCord, J.M., *Oxygen-derived free radicals in postischemic tissue injury.* N Engl J Med, 1985. **312**(3): p. 159-63.

7. Hess, M.L. and N.H. Manson, *Molecular oxygen: friend and foe. The role of the oxygen free radical system in the calcium paradox, the oxygen paradox and ischemia/reperfusion injury.* J Mol Cell Cardiol, 1984. **16**(11): p. 969-85.

8. Hiraishi, H., et al., *Reactive oxygen metabolite-induced toxicity to cultured bovine endothelial cells: status of cellular iron in mediating injury.* J Cell Physiol, 1994. **160**(1): p. 132-4.

9. Dizdaroglu, M., et al., *Damage to the DNA bases in mammalian chromatin by hydrogen peroxide in the presence of ferric and cupric ions.* Arch Biochem Biophys, 1991. **285**(2): p. 317-24.

10. Mello Filho, A.C. and R. Meneghini, *In vivo formation of single-strand breaks in DNA by hydrogen peroxide is mediated by the Haber-Weiss reaction.* Biochim Biophys Acta, 1984. **781**(1-2): p. 56-63.

11. Emerit, J., C. Beaumont, and F. Trivin, *Iron metabolism, free radicals, and oxidative injury.* Biomed Pharmacother, 2001. **55**(6): p. 333-9.

12. Sepodes, B., et al., *Tempol, an intracelullar free radical scavenger, reduces liver injury in hepatic ischemia-reperfusion in the rat.* Transplant Proc, 2004. **36**(4): p. 849-53.

13. Rodriguez-Reynoso, S., et al., *Melatonin ameliorates renal ischemia/reperfusion injury.* J Surg Res, 2004. **116**(2): p. 242-7.

14. Portella, A.O., et al., *Effects of N-acetylcysteine in hepatic ischemia-reperfusion injury during hemorrhagic shock.* Transplant Proc, 2004. **36**(4): p. 846-8.

15. Buttemeyer, R., et al., *Epigallocatechin gallate can significantly decrease free oxygen radicals in the reperfusion injury in vivo.* Transplant Proc, 2003. **35**(8): p. 3116-20.

16. Facino, R.M., et al., *Diet enriched with procyanidins enhances antioxidant activity and reduces myocardial post-ischaemic damage in rats.* Life Sci, 1999. **64**(8): p. 627-42.

17. Ray, P.S., et al., *The red wine antioxidant resveratrol protects isolated rat hearts from ischemia reperfusion injury.* Free Radic Biol Med, 1999. **27**(1-2): p. 160-9.

18. Jiang, J., et al., *Neuroprotective effect of curcumin on focal cerebral ischemic rats by preventing blood-brain barrier damage.* Eur J Pharmacol, 2007. **561**(1-3): p. 54-62.

19. Hattori, R., et al., *Pharmacological preconditioning with resveratrol: role of nitric oxide.* Am J Physiol Heart Circ Physiol, 2002. **282**(6): p. H1988-95.

20. Imamura, G., et al., *Pharmacological preconditioning with resveratrol: an insight with iNOS knockout mice.* Am J Physiol Heart Circ Physiol, 2002. **282**(6): p. H1996-2003.

21. Potenza, M.A., et al., *EGCG, a green tea polyphenol, improves endothelial function and insulin sensitivity, reduces blood pressure, and protects against myocardial I/R injury in SHR.* Am J Physiol Endocrinol Metab, 2007. **292**(5): p. E1378-87.

22. Aneja, R., et al., *Epigallocatechin, a green tea polyphenol, attenuates myocardial ischemia reperfusion injury in rats.* Mol Med, 2004. **10**(1-6): p. 55-62.

23. Shen, S.Q., et al., *Protective effect of curcumin against liver warm ischemia/reperfusion injury in rat model is associated with regulation of heat shock protein and antioxidant enzymes.* World J Gastroenterol, 2007. **13**(13): p. 1953-61.

24. Koltuksuz, U., et al., *Caffeic acid phenethyl ester prevents intestinal reperfusion injury in rats.* J Pediatr Surg, 1999. **34**(10): p. 1458-62.

25. Ilhan, A., et al., *The effects of caffeic acid phenethyl ester (CAPE) on spinal cord ischemia/reperfusion injury in rabbits.* Eur J Cardiothorac Surg, 1999. **16**(4): p. 458-63.

26. Uz, E., et al., *The protective role of caffeic acid phenethyl ester (CAPE) on testicular tissue after testicular torsion and detorsion.* World J Urol, 2002. **20**(4): p. 264-70.

27. Celik, O., et al., *The protective effect of caffeic acid phenethyl ester on ischemia-reperfusion injury in rat ovary.* Eur J Obstet Gynecol Reprod Biol, 2004. **117**(2): p. 183-8.

28. Ozyurt, B., et al., *Protective effects of caffeic acid phenethyl ester on skeletal muscle ischemia-reperfusion injury in rats.* Mol Cell Biochem, 2006. **292**(1-2): p. 197-203.

29. Tsai, S.K., et al., *Caffeic acid phenethyl ester ameliorates cerebral infarction in rats subjected to focal cerebral ischemia.* Life Sci, 2006. **78**(23): p. 2758-62.

30. Khan, M., et al., *Caffeic acid phenethyl ester reduces neurovascular inflammation and protects rat brain following transient focal cerebral ischemia.* J Neurochem, 2007. **102**(2): p. 365-77.

31. Ozer, M.K., H. Parlakpinar, and A. Acet, *Reduction of ischemia--reperfusion induced myocardial infarct size in rats by caffeic acid phenethyl ester (CAPE).* Clin Biochem, 2004. **37**(8): p. 702-5.

32. Parlakpinar, H., et al., *Protective effect of caffeic acid phenethyl ester (CAPE) on myocardial ischemia-reperfusion-induced apoptotic cell death.* Toxicology, 2005. **209**(1): p. 1-14.

33. Ozer, M.K., et al., *Ischemia-reperfusion leads to depletion of glutathione content and augmentation of malondialdehyde production in the rat heart from overproduction of oxidants: can caffeic acid phenethyl ester (CAPE) protect the heart?* Mol Cell Biochem, 2005. **273**(1-2): p. 169-75.

34. Huang, S.S., et al., *Antiarrhythmic effect of caffeic acid phenethyl ester (CAPE) on myocardial ischemia/reperfusion injury in rats.* Clin Biochem, 2005. **38**(10): p. 943-7.

35. Tan, J., et al., *Caffeic acid phenethyl ester possesses potent cardioprotective effects in a rabbit model of acute myocardial ischemia-reperfusion injury.* Am J Physiol Heart Circ Physiol, 2005. **289**(5): p. H2265-71.

36. Esrefoglu, M., et al., *Effects of melatonin and caffeic acid phenethyl ester on testicular injury induced by myocardial ischemia/reperfusion in rats.* Fundam Clin Pharmacol, 2005. **19**(3): p. 365-72.

37. Ozer, M.K., et al., *Myocardial ischemia/reperfusion-induced oxidative renal damage in rats: protection by caffeic acid phenethyl ester (CAPE).* Shock, 2005. **24**(1): p. 97-100.

38. Irmak, M.K., et al., *The effect of caffeic acid phenethyl ester on ischemia-reperfusion injury in comparison with alpha-tocopherol in rat kidneys.* Urol Res, 2001. **29**(3): p. 190-3.

39. Irmak, M.K., et al., *Effects of caffeic acid phenethyl ester and alpha-tocopherol on reperfusion injury in rat brain.* Cell Biochem Funct, 2003. **21**(3): p. 283-9.

40. Banskota, A.H., Y. Tezuka, and S. Kadota, *Recent progress in pharmacological research of propolis.* Phytother Res, 2001. **15**(7): p. 561-71.

41. Nagaoka, T., et al., *Caffeic acid phenethyl ester (CAPE) analogues: potent nitric oxide inhibitors from the Netherlands propolis.* Biol Pharm Bull, 2003. **26**(4): p. 487-91.

42. Usia, T., et al., *Constituents of Chinese propolis and their antiproliferative activities.* J Nat Prod, 2002. **65**(5): p. 673-6.

43. Ahn, M.R., et al., *Antioxidant activity and constituents of propolis collected in various areas of Korea.* J Agric Food Chem, 2004. **52**(24): p. 7286-92.

44. Bankova, V., *Recent trends and important developments in propolis research.* Evid Based Complement Alternat Med, 2005. **2**(1): p. 29-32.

45. Kumazawa, S., T. Hamasaka, and T. Nakayama, *Antioxidant activity of propolis of various geographic origins.* Food Chemistry., 2004. **84**: p. 329-39.

46. Nakanishi, K., E.M. Oltz, and D. Grunberger, *U.S. Patent number 5008441.* 1991.

47. Chiao, C., et al., *Apoptosis and altered redox state induced by caffeic acid phenethyl ester (CAPE) in transformed rat fibroblast cells.* Cancer Res, 1995. **55**(16): p. 3576-83.

48. Liao, H.F., et al., *Inhibitory effect of caffeic acid phenethyl ester on angiogenesis, tumor invasion, and metastasis.* J Agric Food Chem, 2003. **51**(27): p. 7907-12.

49. Lee, Y.J., et al., *Involvement of tumor suppressor protein p53 and p38 MAPK in caffeic acid phenethyl ester-induced apoptosis of C6 glioma cells.* Biochem Pharmacol, 2003. **66**(12): p. 2281-9.

50. Chung, T.W., et al., *Novel and therapeutic effect of caffeic acid and caffeic acid phenyl ester on hepatocarcinoma cells: complete regression of hepatoma growth and metastasis by dual mechanism.* FASEB J, 2004. **18**(14): p. 1670-81.

51. Watabe, M., et al., *Caffeic acid phenethyl ester induces apoptosis by inhibition of NFkappaB and activation of Fas in human breast cancer MCF-7 cells.* J Biol Chem, 2004. **279**(7): p. 6017-26.

52. Orban, Z., et al., *Caffeic acid phenethyl ester induces leukocyte apoptosis, modulates nuclear factor-kappa B and suppresses acute inflammation.* Neuroimmunomodulation, 2000. **7**(2): p. 99-105.

53. Fitzpatrick, L.R., J. Wang, and T. Le, *Caffeic acid phenethyl ester, an inhibitor of nuclear factor-kappaB, attenuates bacterial peptidoglycan polysaccharide-induced colitis in rats.* J Pharmacol Exp Ther, 2001. **299**(3): p. 915-20.

54. Borrelli, F., et al., *Phytochemical compounds involved in the anti-inflammatory effect of propolis extract.* Fitoterapia, 2002. **73 Suppl 1**: p. S53-63.

55. Montpied, P., et al., *Caffeic acid phenethyl ester (CAPE) prevents inflammatory stress in organotypic hippocampal slice cultures.* Brain Res Mol Brain Res, 2003. **115**(2): p. 111-20.

56. Fesen, M.R., et al., *Inhibitors of human immunodeficiency virus integrase.* Proc Natl Acad Sci U S A, 1993. **90**(6): p. 2399-403.

57. Fesen, M.R., et al., *Inhibition of HIV-1 integrase by flavones, caffeic acid phenethyl ester (CAPE) and related compounds.* Biochem Pharmacol, 1994. **48**(3): p. 595-608.

58. Zhao, H., et al., *Arylamide inhibitors of HIV-1 integrase.* J Med Chem, 1997. **40**(8): p. 1186-94.

59. Sud'ina, G.F., et al., *Caffeic acid phenethyl ester as a lipoxygenase inhibitor with antioxidant properties.* FEBS Lett, 1993. **329**(1-2): p. 21-4.

60. Rezzani, R., et al., *The protective effect of caffeic acid phenethyl ester against cyclosporine A-induced cardiotoxicity in rats.* Toxicology, 2005. **212**(2-3): p. 155-64.

61. Aladag, M.A., et al., *Caffeic acid phenethyl ester (CAPE) attenuates cerebral vasospasm after experimental subarachnoidal haemorrhage by increasing brain nitric oxide levels.* Int J Dev Neurosci, 2006. **24**(1): p. 9-14.

62. Mohamadin, A.M., et al., *Attenuation of oxidative stress in plasma and tissues of rats with experimentally induced hyperthyroidism by caffeic acid phenylethyl ester.* Basic Clin Pharmacol Toxicol, 2007. **100**(2): p. 84-90.

63. Park, J.H., et al., *Immunomodulatory effect of caffeic acid phenethyl ester in Balb/c mice.* Int Immunopharmacol, 2004. **4**(3): p. 429-36.

64. Danthi, S., J.A. Enyeart, and J.J. Enyeart, *Caffeic acid esters activate TREK-1 potassium channels and inhibit depolarization-dependent secretion.* Mol Pharmacol, 2004. **65**(3): p. 599-610.

65. Parlakpinar, H., et al., *Protective effects of caffeic acid phenethyl ester (CAPE) on amikacin-induced nephrotoxicity in rats.* Cell Biochem Funct, 2006. **24**(4): p. 363-7.

66. Ocak, S., et al., *Protective effects of caffeic acid phenethyl ester, vitamin C, vitamin E and N-acetylcysteine on vancomycin-induced nephrotoxicity in rats.* Basic Clin Pharmacol Toxicol, 2007. **100**(5): p. 328-33.

67. Parlakpinar, H., et al., *Protective role of caffeic acid phenethyl ester (cape) on gentamicin-induced acute renal toxicity in rats.* Toxicology, 2005. **207**(2): p. 169-77.

68. Yagmurca, M., et al., *Caffeic acid phenethyl ester as a protective agent against doxorubicin nephrotoxicity in rats.* Clin Chim Acta, 2004. **348**(1-2): p. 27-34.

69. Fadillioglu, E., et al., *Protective effects of caffeic acid phenethyl ester on doxorubicin-induced cardiotoxicity in rats.* J Appl Toxicol, 2004. **24**(1): p. 47-52.

70. Uzar, E., et al., *The activity of adenosine deaminase and the level of nitric oxide in spinal cord of methotrexate administered rats: protective effect of caffeic acid phenethyl ester.* Toxicology, 2006. **218**(2-3): p. 125-33.

71. Uzar, E., et al., *The activities of antioxidant enzymes and the level of malondialdehyde in cerebellum of rats subjected to methotrexate: protective effect of caffeic acid phenethyl ester.* Mol Cell Biochem, 2006. **291**(1-2): p. 63-8.

72. Sahin, O., et al., *Lithium-induced lung toxicity in rats: the effect of caffeic acid phenethyl ester (CAPE).* Pathology, 2006. **38**(1): p. 58-62.

73. Oktem, F., et al., *Lithium-induced renal toxicity in rats: protection by a novel antioxidant caffeic acid phenethyl ester.* Mol Cell Biochem, 2005. **277**(1-2): p. 109-15.

74. Mollaoglu, H., et al., *Caffeic acid phenethyl ester prevents cadmium-induced cardiac impairment in rat.* Toxicology, 2006. **227**(1-2): p. 15-20.

75. Frenkel, K., et al., *Inhibition of tumor promoter-mediated processes in mouse skin and bovine lens by caffeic acid phenethyl ester.* Cancer Res, 1993. **53**(6): p. 1255-61.

76. Hwang, H.J., et al., *Inhibitory effects of caffeic acid phenethyl ester on cancer cell metastasis mediated by the down-regulation of matrix metalloproteinase expression in human HT1080 fibrosarcoma cells.* J Nutr Biochem, 2006. **17**(5): p. 356-62.

77. Xiang, D., et al., *Caffeic acid phenethyl ester induces growth arrest and apoptosis of colon cancer cells via the beta-catenin/T-cell factor signaling.* Anticancer Drugs, 2006. **17**(7): p. 753-62.

78. Mirzoeva, O.K. and P.C. Calder, *The effect of propolis and its components on eicosanoid production during the inflammatory response.* Prostaglandins Leukot Essent Fatty Acids, 1996. **55**(6): p. 441-9.

79. Michaluart, P., et al., *Inhibitory effects of caffeic acid phenethyl ester on the activity and expression of cyclooxygenase-2 in human oral epithelial cells and in a rat model of inflammation.* Cancer Res, 1999. **59**(10): p. 2347-52.

80. Sen, R. and D. Baltimore, *Inducibility of kappa immunoglobulin enhancer-binding protein Nf-kappa B by a posttranslational mechanism.* Cell, 1986. **47**(6): p. 921-8.

81. Han, Z., et al., *AP-1 and NF-kappaB regulation in rheumatoid arthritis and murine collagen-induced arthritis.* Autoimmunity, 1998. **28**(4): p. 197-208.

82. Neurath, M.F., et al., *Cytokine gene transcription by NF-kappa B family members in patients with inflammatory bowel disease.* Ann N Y Acad Sci, 1998. **859**: p. 149-59.

83. Natarajan, K., et al., *Caffeic acid phenethyl ester is a potent and specific inhibitor of activation of nuclear transcription factor NF-kappa B.* Proc Natl Acad Sci U S A, 1996. **93**(17): p. 9090-5.

84. Marquez, N., et al., *Caffeic acid phenethyl ester inhibits T-cell activation by targeting both nuclear factor of activated T-cells and NF-kappaB transcription factors.* J Pharmacol Exp Ther, 2004. **308**(3): p. 993-1001.

85. Abdel-Latif, M.M., et al., *Caffeic acid phenethyl ester modulates Helicobacter pylori-induced nuclear factor-kappa B and activator protein-1 expression in gastric epithelial cells.* Br J Pharmacol, 2005. **146**(8): p. 1139-47.

86. Mira, L., et al., *Interactions of flavonoids with iron and copper ions: a mechanism for their antioxidant activity.* Free Radic Res, 2002. **36**(11): p. 1199-208.

87. Lucarini, M., V. Mugnaini, and G.F. Pedulli, *Bond dissociation enthalpies of polyphenols: the importance of cooperative effects.* J Org Chem, 2002. **67**(3): p. 928-31.

88. Sestili, P., et al., *Plant-derived phenolic compounds prevent the DNA single-strand breakage and cytotoxicity induced by tert-butylhydroperoxide via an iron-chelating mechanism.* Biochem J, 2002. **364**(Pt 1): p. 121-8.

89. Chen, J.H. and C.T. Ho, *Antioxidant activities of caffeic acid and its related hydroxycinnamic acid compounds.* J Agric Food Chem, 1997. **45**(7): p. 2374-8.

90. Son, S. and B.A. Lewis, *Free radical scavenging and antioxidative activity of caffeic acid amide and ester analogues: structure-activity relationship.* J Agric Food Chem, 2002. **50**(3): p. 468-72.

91. Hsu, L.Y., et al., *Evaluation of polyphenolic acid esters as potential antioxidants.* Biol Pharm Bull, 2005. **28**(7): p. 1211-5.

92. Jaiswal, A.K., et al., *Caffeic acid phenethyl ester stimulates human antioxidant response element-mediated expression of the NAD(P)H:quinone oxidoreductase (NQO1) gene.* Cancer Res, 1997. **57**(3): p. 440-6.

93. Scapagnini, G., et al., *Caffeic acid phenethyl ester and curcumin: a novel class of heme oxygenase-1 inducers.* Mol Pharmacol, 2002. **61**(3): p. 554-61.

94. Balogun, E., et al., *Curcumin activates the haem oxygenase-1 gene via regulation of Nrf2 and the antioxidant-responsive element.* Biochem J, 2003. **371**(Pt 3): p. 887-95.

95. Manach, C., et al., *Polyphenols: food sources and bioavailability.* Am J Clin Nutr, 2004. **79**(5): p. 727-47.

96. Halliwell, B., J. Rafter, and A. Jenner, *Health promotion by flavonoids, tocopherols, tocotrienols, and other phenols: direct or indirect effects? Antioxidant or not?* Am J Clin Nutr, 2005. **81**(1 Suppl): p. 268S-276S.

97. Tsuchihashi, S., C. Fondevila, and J.W. Kupiec-Weglinski, *Heme oxygenase system in ischemia and reperfusion injury.* Ann Transplant, 2004. **9**(1): p. 84-7.

98. Schmidt, R., et al., *Heme oxygenase-1 induction by the clinically used anesthetic isoflurane protects rat livers from ischemia/reperfusion injury.* Ann Surg, 2007. **245**(6): p. 931-42.

99. Tenhunen, R., H.S. Marver, and R. Schmid, *The enzymatic conversion of heme to bilirubin by microsomal heme oxygenase.* Proc Natl Acad Sci U S A, 1968. **61**(2): p. 748-55.

100. Maines, M.D. and A. Kappas, *Cobalt induction of hepatic heme oxygenase; with evidence that cytochrome P-450 is not essential for this enzyme activity.* Proc Natl Acad Sci U S A, 1974. **71**(11): p. 4293-7.

101. Ponka, P., *Cell biology of heme.* Am J Med Sci, 1999. **318**(4): p. 241-56.

102. Ryter, S.W. and R.M. Tyrrell, *The heme synthesis and degradation pathways: role in oxidant sensitivity. Heme oxygenase has both pro- and antioxidant properties.* Free Radic Biol Med, 2000. **28**(2): p. 289-309.

103. Braggins, P.E., et al., *Characterization of two heme oxygenase isoforms in rat spleen: comparison with the hematin-induced and constitutive isoforms of the liver.* Biochem Biophys Res Commun, 1986. **141**(2): p. 528-33.

104. Trakshel, G.M., R.K. Kutty, and M.D. Maines, *Purification and characterization of the major constitutive form of testicular heme oxygenase. The noninducible isoform.* J Biol Chem, 1986. **261**(24): p. 11131-7.

105. Maines, M.D., G.M. Trakshel, and R.K. Kutty, *Characterization of two constitutive forms of rat liver microsomal heme oxygenase. Only one molecular species of the enzyme is inducible.* J Biol Chem, 1986. **261**(1): p. 411-9.

106. Trakshel, G.M., R.K. Kutty, and M.D. Maines, *Resolution of the rat brain heme oxygenase activity: absence of a detectable amount of the inducible form (HO-1).* Arch Biochem Biophys, 1988. **260**(2): p. 732-9.

107. Keyse, S.M. and R.M. Tyrrell, *Heme oxygenase is the major 32-kDa stress protein induced in human skin fibroblasts by UVA radiation, hydrogen peroxide, and sodium arsenite.* Proc Natl Acad Sci U S A, 1989. **86**(1): p. 99-103.

108. Maines, M.D., *The heme oxygenase system: a regulator of second messenger gases.* Annu Rev Pharmacol Toxicol, 1997. **37**: p. 517-54.

109. Ryter, S.W., J. Alam, and A.M. Choi, *Heme oxygenase-1/carbon monoxide: from basic science to therapeutic applications.* Physiol Rev, 2006. **86**(2): p. 583-650.

110. Wakabayashi, N., et al., *Protection against electrophile and oxidant stress by induction of the phase 2 response: fate of cysteines of the Keap1 sensor modified by inducers.* Proc Natl Acad Sci U S A, 2004. **101**(7): p. 2040-5.

111. Igarashi, K. and J. Sun, *The heme-Bach1 pathway in the regulation of oxidative stress response and erythroid differentiation.* Antioxid Redox Signal, 2006. **8**(1-2): p. 107-18.

112. Alam, J. and J.L. Cook, *How many transcription factors does it take to turn on the heme oxygenase-1 gene?* Am J Respir Cell Mol Biol, 2007. **36**(2): p. 166-74.

113. Willis, D., et al., *Heme oxygenase: a novel target for the modulation of the inflammatory response.* Nat Med, 1996. **2**(1): p. 87-90.

114. Nath, K.A., et al., *Induction of heme oxygenase is a rapid, protective response in rhabdomyolysis in the rat.* J Clin Invest, 1992. **90**(1): p. 267-70.

115. Lee, T.S., et al., *Simvastatin induces heme oxygenase-1: a novel mechanism of vessel protection.* Circulation, 2004. **110**(10): p. 1296-302.

116. Poss, K.D. and S. Tonegawa, *Heme oxygenase 1 is required for mammalian iron reutilization.* Proc Natl Acad Sci U S A, 1997. **94**(20): p. 10919-24.

117. Poss, K.D. and S. Tonegawa, *Reduced stress defense in heme oxygenase 1-deficient cells.* Proc Natl Acad Sci U S A, 1997. **94**(20): p. 10925-30.

118. Yachie, A., et al., *Oxidative stress causes enhanced endothelial cell injury in human heme oxygenase-1 deficiency.* J Clin Invest, 1999. **103**(1): p. 129-35.

119. Ryter, S.W. and L.E. Otterbein, *Carbon monoxide in biology and medicine.* Bioessays, 2004. **26**(3): p. 270-80.

120. Ostrow, J.D., J.H. Jandl, and R. Schmid, *The formation of bilirubin from hemoglobin in vivo.* J Clin Invest, 1962. **41**: p. 1628-37.

121. Kapitulnik, J., *Bilirubin: an endogenous product of heme degradation with both cytotoxic and cytoprotective properties.* Mol Pharmacol, 2004. **66**(4): p. 773-9.

122. Baranano, D.E., et al., *Biliverdin reductase: a major physiologic cytoprotectant.* Proc Natl Acad Sci U S A, 2002. **99**(25): p. 16093-8.

123. Ferris, C.D., et al., *Haem oxygenase-1 prevents cell death by regulating cellular iron.* Nat Cell Biol, 1999. **1**(3): p. 152-7.

124. Balla, G., et al., *Ferritin: a cytoprotective antioxidant strategem of endothelium.* J Biol Chem, 1992. **267**(25): p. 18148-53.

125. Attuwaybi, B.O., et al., *Heme oxygenase-1 induction by hemin protects against gut ischemia/reperfusion injury.* J Surg Res, 2004. **118**(1): p. 53-7.

126. Lai, I.R., et al., *The protective role of heme oxygenase-1 on the liver after hypoxic preconditioning in rats.* Transplantation, 2004. **77**(7): p. 1004-8.

127. Zhang, X., et al., *Small interfering RNA targeting heme oxygenase-1 enhances ischemia-reperfusion-induced lung apoptosis.* J Biol Chem, 2004. **279**(11): p. 10677-84.

128. Pachori, A.S., et al., *Hypoxia-regulated therapeutic gene as a preemptive treatment strategy against ischemia/reperfusion tissue injury.* Proc Natl Acad Sci U S A, 2004. **101**(33): p. 12282-7.

129. Pachori, A.S., et al., *Chronic recurrent myocardial ischemic injury is significantly attenuated by pre-emptive adeno-associated virus heme oxygenase-1 gene delivery.* J Am Coll Cardiol, 2006. **47**(3): p. 635-43.

130. Kato, Y., et al., *Bilirubin rinse: A simple protectant against the rat liver graft injury mimicking heme oxygenase-1 preconditioning.* Hepatology, 2003. **38**(2): p. 364-73.

131. Adin, C.A., B.P. Croker, and A. Agarwal, *Protective effects of exogenous bilirubin on ischemia-reperfusion injury in the isolated, perfused rat kidney.* Am J Physiol Renal Physiol, 2005. **288**(4): p. F778-84.

132. Fondevila, C., et al., *Biliverdin therapy protects rat livers from ischemia and reperfusion injury.* Hepatology, 2004. **40**(6): p. 1333-41.

133. Akamatsu, Y., et al., *Heme oxygenase-1-derived carbon monoxide protects hearts from transplant associated ischemia reperfusion injury.* Faseb J, 2004. **18**(6): p. 771-2.

134. Fujimoto, H., et al., *Carbon monoxide protects against cardiac ischemia--reperfusion injury in vivo via MAPK and Akt--eNOS pathways.* Arterioscler Thromb Vasc Biol, 2004. **24**(10): p. 1848-53.

135. Berberat, P.O., et al., *Heavy chain ferritin acts as an antiapoptotic gene that protects livers from ischemia reperfusion injury.* FASEB J, 2003. **17**(12): p. 1724-6.

136. Kvietys, P.R. and D.N. Granger, *Endothelial cell monolayers as a tool for studying microvascular pathophysiology.* Am J Physiol, 1997. **273**(6 Pt 1): p. G1189-99.

137. Ratych, R.E., R.S. Chuknyiska, and G.B. Bulkley, *The primary localization of free radical generation after anoxia/reoxygenation in isolated endothelial cells.* Surgery, 1987. **102**(2): p. 122-31.

138. Zweier, J.L., P. Kuppusamy, and G.A. Lutty, *Measurement of endothelial cell free radical generation: evidence for a central mechanism of free radical injury in postischemic tissues.* Proc Natl Acad Sci U S A, 1988. **85**(11): p. 4046-50.

139. Boyle, E.M., Jr., et al., *Endothelial cell injury in cardiovascular surgery: ischemia-reperfusion.* Ann Thorac Surg, 1996. **62**(6): p. 1868-75.

140. Mold, C. and C.A. Morris, *Complement activation by apoptotic endothelial cells following hypoxia/reoxygenation.* Immunology, 2001. **102**(3): p. 359-64.

141. Zhao, H., et al., *Anoxia and reoxygenation of human endothelial cells decrease ceramide glucosyltransferase expression and activates caspases.* FASEB J, 2003. **17**(6): p. 723-4.

142. Therade-Matharan, S., et al., *Reoxygenation after hypoxia and glucose depletion causes reactive oxygen species production by mitochondria in HUVEC.* Am J Physiol Regul Integr Comp Physiol, 2004. **287**(5): p. R1037-43.

143. Kossenjans, W., et al., *Menadione-induced oxidative stress in bovine heart microvascular endothelial cells.* Microcirculation, 1996. **3**(1): p. 39-47.

144. Warren, M.C., et al., *Oxidative stress-induced apoptosis of endothelial cells.* Free Radic Biol Med, 2000. **29**(6): p. 537-47.

145. Nagaoka, T., et al., *Inhibitory effects of caffeic acid phenethyl ester analogues on experimental lung metastasis of murine colon 26-L5 carcinoma cells.* Biol Pharm Bull, 2003. **26**(5): p. 638-41.

146. Etzenhouser, B., et al., *Mechanism of toxicity of esters of caffeic and dihydrocaffeic acids.* Bioorg Med Chem, 2001. **9**(1): p. 199-209.

147. Verma, R.P. and C. Hansch, *An Approach towards the quantitative structure-activity relationships of caffeic acid and its derivatives.* Chembiochem, 2004. **5**(9): p. 1188-95.

148. Bankova, V.S., *Synthesis of natural esters of substituted cinnamic acids.* J. Nat. Prod., 1990. **53**(4): p. 821-4.

149. Ho, C.C., et al., *Effects of CAPE-like compounds on HIV replication in vitro and modulation of cytokines in vivo.* J Antimicrob Chemother, 2005. **56**(2): p. 372-9.

150. Lee, Y.J., et al., *Preferential cytotoxicity of caffeic acid phenethyl ester analogues on oral cancer cells.* Cancer Lett, 2000. **153**(1-2): p. 51-6.

151. Kirk, K.L., et al., *Synthesis and adrenergic activity of ring-fluorinated phenylephrines.* J Med Chem, 1986. **29**(10): p. 1982-8.

152. Kirk, K.L., *Chemistry and pharmacology of ring-fluorinated catecholamines* J Fluorine Chem, 1995. **72**(2): p. 261-6.

153. Chirakal, R., et al., *The effect of aromatic fluorine substitution in l-DOPA on the in vivo behaviour of [^{18}F]2-, [^{18}F]5- and [^{18}F]6-fluoro-l-DOPA in the human brain.* J Fluorine Chem, 2002. **115**(1): p. 33-9.

154. Smart, B.E., *Fluorine substituent effects (on bioactivity).* J Fluorine Chem, 2001 **109**(1): p. 3-11.

155. Creveling, C.R. and K.L. Kirk, *The effect of ring-fluorination on the rate of O-methylation of dihydroxyphenylalanine (DOPA) by catechol-O-methyltransferase: significance in the development of 18F-PETT scanning agents.* Biochem Biophys Res Commun, 1985. **130**(3): p. 1123-31.

156. Vedejs, E., *The 1979 Nobel Prize for Chemistry.* Science, 1980. **207**(4426): p. 42-44.

157. Langer, O., et al., *Synthesis of high-specific-radioactivity 4- and 6-[18F]fluorometaraminol-PET tracers for the adrenergic nervous system of the heart.* Bioorg Med Chem, 2001. **9**(3): p. 677-94.

158. Scheidweiler, K.B., et al., *Stability of methylecgonidine and ecgonidine in sheep plasma in vitro.* Clin Chem, 2000. **46**(11): p. 1787-95.

159. Ceschel, G.C., et al., *In vitro permeation through porcine buccal mucosa of caffeic acid phenetyl ester (CAPE) from a topical mucoadhesive gel containing propolis.* Fitoterapia, 2002. **73 Suppl 1**: p. S44-52.

160. Del Boccio, P. and D. Rotilio, *Quantitative analysis of caffeic acid phenethyl ester in crude propolis by liquid chromatography-electrospray ionization mass spectrometry.* J Sep Sci, 2004. **27**(7-8): p. 619-23.

161. Celli, N., et al., *Development and validation of a liquid chromatographic-tandem mass spectrometric method for the determination of caffeic acid phenethyl ester in rat plasma and urine.* J Chromatogr B Analyt Technol Biomed Life Sci, 2004. **810**(1): p. 129-36.

162. Chen, C.Y., et al., *Resveratrol upregulates heme oxygenase-1 expression via activation of NF-E2-related factor 2 in PC12 cells.* Biochem Biophys Res Commun, 2005. **331**(4): p. 993-1000.

163. Motterlini, R., et al., *Curcumin, an antioxidant and anti-inflammatory agent, induces heme oxygenase-1 and protects endothelial cells against oxidative stress.* Free Radic Biol Med, 2000. **28**(8): p. 1303-12.

164. Zhao, B., et al., *Human endothelial cell response to gram-negative lipopolysaccharide assessed with cDNA microarrays.* Am J Physiol Cell Physiol, 2001. **281**(5): p. C1587-95.

165. Larson, E.M., et al., *A new, simple, nonradioactive, nontoxic in vitro assay to monitor corneal endothelial cell viability.* Investigative Ophthalmology & Visual Science, 1997. **38**(10): p. 1929-33.

166. Gao, X., A.T. Dinkova-Kostova, and P. Talalay, *Powerful and prolonged protection of human retinal pigment epithelial cells, keratinocytes, and mouse leukemia cells against oxidative damage: the indirect antioxidant effects of sulforaphane.* Proc Natl Acad Sci U S A, 2001. **98**(26): p. 15221-6.

167. Abuarqoub, H., et al., *Heme oxygenase-1 mediates the anti-inflammatory actions of 2'-hydroxychalcone in RAW 264.7 murine macrophages.* Am J Physiol Cell Physiol, 2006. **290**(4): p. C1092-9.

168. Katori, M., et al., *A novel strategy against ischemia and reperfusion injury: cytoprotection with heme oxygenase system.* Transpl Immunol, 2002. **9**(2-4): p. 227-33.

169. Fondevila, C., et al., *Biliverdin protects rat livers from ischemia/reperfusion injury.* Transplant Proc, 2003. **35**(5): p. 1798-9.

170. Hammerman, C., et al., *Protective effect of bilirubin in ischemia-reperfusion injury in the rat intestine.* J Pediatr Gastroenterol Nutr, 2002. **35**(3): p. 344-9.

171. Stocker, R., et al., *Bilirubin is an antioxidant of possible physiological importance.* Science, 1987. **235**(4792): p. 1043-6.

172. Brouard, S., et al., *Carbon monoxide generated by heme oxygenase 1 suppresses endothelial cell apoptosis.* J Exp Med, 2000. **192**(7): p. 1015-26.

173. Mishra, S., et al., *Carbon monoxide rescues ischemic lungs by interrupting MAPK-driven expression of early growth response 1 gene and its downstream target genes.* Proc Natl Acad Sci U S A, 2006. **103**(13): p. 5191-6.

174. Hori, R., et al., *Gene transfection of H25A mutant heme oxygenase-1 protects cells against hydroperoxide-induced cytotoxicity.* J Biol Chem, 2002. **277**(12): p. 10712-8.

175. Sheftel, A.D., S.F. Kim, and P. Ponka, *Non-heme induction of heme oxygenase-1 does not alter cellular iron metabolism.* J Biol Chem, 2007. **282**(14): p. 10480-6.

176. Lien, E.J., et al., *Quantitative structure-activity relationship analysis of phenolic antioxidants.* Free Radic Biol Med, 1999. **26**(3-4): p. 285-94.

177. Alanko, J., et al., *Modulation of arachidonic acid metabolism by phenols: relation to their structure and antioxidant/prooxidant properties.* Free Radic Biol Med, 1999. **26**(1-2): p. 193-201.

178. Kohn, M.C. and R.L. Melnick, *Biochemical origins of the non-monotonic receptor-mediated dose-response.* J Mol Endocrinol, 2002. **29**(1): p. 113-23.

179. Conolly, R.B. and W.K. Lutz, *Nonmonotonic dose-response relationships: mechanistic basis, kinetic modeling, and implications for risk assessment.* Toxicol Sci, 2004. **77**(1): p. 151-7.

180. Shigematsu, S., et al., *Resveratrol, a red wine constituent polyphenol, prevents superoxide-dependent inflammatory responses induced by ischemia/reperfusion, platelet-activating factor, or oxidants.* Free Radic Biol Med, 2003. **34**(7): p. 810-7.

181. Wang, Q., et al., *Neuroprotective mechanisms of curcumin against cerebral ischemia-induced neuronal apoptosis and behavioral deficits.* J Neurosci Res, 2005. **82**(1): p. 138-48.

182. Jones, W., et al., *Uptake, recycling, and antioxidant actions of alpha-lipoic acid in endothelial cells.* Free Radic Biol Med, 2002. **33**(1): p. 83-93.

183. Scapagnini, G., et al., *Ethyl ferulate, a lipophilic polyphenol, induces HO-1 and protects rat neurons against oxidative stress.* Antioxid Redox Signal, 2004. **6**(5): p. 811-8.

184. Samtani, M.N., et al., *Stabilization and HPLC analysis of betamethasone sodium phosphate in plasma.* J Pharm Sci, 2004. **93**(3): p. 726-32.

185. Samtani, M.N. and W.J. Jusko, *Stability of dexamethasone sodium phosphate in rat plasma.* Int J Pharm, 2005. **301**(1-2): p. 262-6.

186. Food and Drug Administration, *Guidance for Industry, Bioanalytical Method Validation.* 2001.

187. Bruins, A.P., *Mechanistic aspects of electrospray ionization.* J Chromatogr A, 1998. **794** (1-2): p. 345-57.

VITA

Xinyu Wang was born in Beijing, P.R. China on August 12, 1974, the son of Qiang Wang and Anqing Zou. After completing his work at High School of Peking University, Beijing, in 1993, he entered the School of Pharmaceutical Sciences at Beijing Medical University (now Peking University School of Pharmaceutical Sciences), Beijing, where he received the degree of Bachelor of Sciences in pharmacy in 1997. During the following years, Xinyu was employed in various research and teaching positions with Peking University School of Pharmaceutical Sciences in Beijing, China. In September 2001, he joined the interdisciplinary graduate program in Medical Sciences in Texas A&M University Health Science Center. In September 2002, Xinyu transferred to The University of Texas at Austin and entered the Ph.D. program in the pharmaceutics division of the College of Pharmacy. While earning his doctorate degree, he served as a teaching assistant for three semesters in basic pharmaceutical sciences. He has also served as a research assistant in the US Army Institute of Surgical Research under the supervision of Dr. Salomon Stavchansky and Dr. Phillip Bowman since January 2004. He has been awarded graduate fellowships from College of Pharmacy since 2003. Xinyu has presented his research at different regional and national conferences. His current and published work include:

Wang X, Pang J, Maffucci JA, Newman RA, Kerwin SM, Bowman PD, Stavchansky S. Pharmacokinetics of caffeic acid phenethyl ester and its fluorinated derivative in rats. In preparation.

Wang X, Stavchansky S, Kerwin SM, Bowman PD. Cytoprotection of fluorinated

derivatives of caffeic acid phenethyl ester (CAPE): effects on heme oxygenase-1 induction and antioxidant activities. In preparation.

Wang X, Stavchansky S, Zhao B, Bynum JA, Kerwin SM, Bowman PD. Cytoprotection of human endothelial cells from menadione cytotoxicity by caffeic acid phenethyl ester: The role of heme oxygenase-1. In submission.

Wang X, Pang J, Newman RA, Kerwin SM, Bowman PD, Stavchansky S. Quantitative determination of fluorinated caffeic acid phenethyl ester derivative from rat blood plasma by liquid chromatography-electrospray ionization tandem mass spectrometry. *Journal of Chromatography B*; submitted.

Wang X, Bowman PD, Kerwin SM, Stavchansky S. Stability of caffeic acid phenethyl ester and its fluorinated derivative in rat plasma. *Biomedical Chromatography* 2007; 21(4): 343-350.

Wang X, Stavchansky S, Bowman PD, Kerwin SM. Cytoprotective effect of caffeic acid phenethyl ester (CAPE) and catechol ring-fluorinated CAPE derivatives against menadione-induced oxidative stress in human endothelial cells. *Bioorganic & Medicinal Chemistry* 2006; 14(14): 4879-4887.

Permanent Address: 101 Arcadia Place, Apt# 312, San Antonio, TX 78209-5863.

This dissertation was typed by the author.